

SCUOLA DI INGEGNERIA E ARCHITETTURA
CORSO DI LAUREA MAGISTRALE IN INGEGNERIA ENERGETICA

TESI DI LAUREA

In

CENTRALI ELETTRICHE E GENERAZIONE DISTRIBUITA

MODELING AND VALIDATION OF THE THERMAL BEHAVIOR
OF BUILDINGS FOR THE DEVELOPMENT OF DEMAND
RESPONSE METHODS

CANDIDATO:

Alice Faccani

RELATORE:

Prof. Ing. Alberto Borghetti

CORRELATORE:

Dr. Gregor Verbič

Prof. Ing. Carlo Alberto Nucci

Anno Accademico 2015/2016

Sessione I

Abstract

The final aim of the project where this work is involved is to evaluate the relevance of phase change materials, PCM, for demand response purposes. In other words, the project aims are to incorporate the thermal behaviour of the building into home energy management optimization to minimize the energy costs while considering the addition of PCM into the building, which are expected to enhance the thermal inertia of the building enabling the HVAC system load shifting. The first step of the project, as well as goal of this thesis activity, is the development and validation of the thermal model of the building, it will then proceed with the PCM addition and the optimization problem solution.

The representation of the thermal behaviour of the building is achieved through a relatively simple dynamic model which takes into account the effects due to the thermal mass of the building components. The model of an intra-floor apartment has been built in the Matlab-Simulink environment and considers the heat transmission through the external envelope, wall and windows, the internal thermal masses, (i.e. furniture, internal wall and floor slabs) and the sun gain due to opaque and see-through surfaces of the external envelope. The simulation results for the entire year have been compared and the model validated, with the one obtained with the dynamic building simulation software Energyplus.

Abstract

L'obiettivo finale del progetto in cui coinvolto questo lavoro è la valutazione dei materiali a cambiamento di fase PCM per l'elaborazione di opportuni programmi di demand response. Ovvero, lo scopo del progetto è quello di introdurre il comportamento termico dell'edificio tenendo conto dei PCM nell'ottimizzazione energetica della casa, al fine di ridurre i costi energetici.

Obiettivo di questa tesi, lo sviluppo del modello termico dell'edificio e la relativa validazione. Successivamente il progetto procederà con l'introduzione dei PCM e alla soluzione del problema di ottimizzazione.

In questa tesi, la descrizione del modello termico dell'edificio è ottenuta tramite un modello relativamente semplice che tiene conto dei fenomeni dovuti all'inerzia termica dei componenti dell'edificio. Il modello di un appartamento inter piano è stato sviluppato grazie al software Matlab-Simulink e tiene conto della trasmissione di calore attraverso l'involucro esterno, muri e finestre, le masse termiche interne (arredi, muri interni e solai) e gli apporti solari attraverso le superfici opache e trasparenti dell'involucro esterno. Le simulazioni sono su base annuale e, al fine di validare il modello, i risultati sono stati confrontati con quelli ottenuti con il programma di simulazioni termiche dinamiche EnergyPlus.

Contents

1	Introduction	11
2	Heat transfer theory	13
2.1	Heat transfer theory	13
2.1.1	Conduction	13
2.1.2	Convection	14
2.1.3	Radiation	15
2.2	Heat transfer in building spaces	15
2.2.1	Heat transfer through fabric element	16
2.2.2	Solar gain	18
2.2.3	Air infiltration and ventilation	19
2.3	Schematic of the building	19
3	Wall parameter evaluation method	21
3.1	α - Method	21
3.2	Masy Correction	22
3.2.1	Wall Admittance Matrix	22
3.2.2	Boundary conditions	23
3.2.3	Wall network adjustment process	26
4	Matlab-Simulink model	28
4.1	Thermal model of the building	28
4.2	High mass and thermal mass component description	28
4.2.1	Imposed Temperature boundary condition:External wall	28
4.2.2	Imposed heat flow boundary condition surfaces	29
4.3	Low mass surfaces and infiltration loss	31
5	Ep model	32
5.1	Simulation parameter	32
5.2	Location and Climate	32
5.3	Surface construction element	33
5.4	Thermal zone and surfaces	33
5.5	Zone Airflow	33
6	Results comparison	34
6.1	All-in	34
6.2	Base	43
6.3	Infiltration	48
6.4	Windows	51

CONTENTS

6.5 Furniture	55
6.6 Sun	58
7 Conclusion	61

Lyst of Symbols

- $A_{c,k}$ Surface area of the k -th surface envelope component, (m^2)
- $A_{i,j}$ i,j -th surface area, (m^2)
- A_s Surface area, (m^2)
- A_{sol} k -th Effective solar capture area, (m^2)
- A_{total} Overall area of the element, (m^2)
- \tilde{A}_v Isothermal admittance, ($W/m^2 K$)
- \tilde{A}_{v_d} Adiabatic admittance, ($W/m^2 K$)
- $A_{w,k}$ Overall window surface (m^2)
- a_p Door area, $2.4 m^2$
- a_w Overall windows area, $10.5 m^2$
- C Overall thermal capacity, (J/K)
- $C_{1,2}$ Surface thermal capacity on side one and two of the surface, ($J/m^2 K$)
- C_i i -th Thermal capacity, (J/K)
- C_k Thermal capacity up to the k -th layer, ($J/ K m^2$)
- C_w Element thermal capacity, (J/ K)
- C_{we} Thermal capacity of the external wall, $3.891 MJ/ K$
- c Ceiling property,
- c Specific heat, ($J/kg K$)
- c_a Air capacity of the apartment, ($kJ/kg K$)
- c_i Specific heat of the i -th layer, ($J/ kg K$)
- c_p Specific heat, ($J/kg K$)
- c_{p_a} Air specific heat, $1.006 kJ/ kg K$
- c_{pl} Specific heat capacity up to the k -th layer, ($J/ m^2 K$)

- d_i Thickness of the i -th layer, (m)
- $-f$ Floor property,
- $-f_u$ Furniture property,
- F_f Frame fraction of the overall window surface
- $F_{sh,gl}$ Reduction factor due to mobile screenings
- f_d Dampening factor,
- f_i^{solar} Distribution factor of solar radiation,
- f_i i -th Distribution factor,
- g_{gl} Solar transmittance of the see-through part of th glazing component
- h Convection heat transfer coefficient, (W/m² K)
- h Radiation heat transfer coefficient, (W/m² K)
- i i -th layer-counting starts from the outer layer
- $-i_w$ Internal wall property,
- $I_{sol,k}$ Solar radiance averaged over the considered period on the k -th surface taking into account the tilt and azimuth surface angles, (W/m²)
- k Thermal conductivity, (W/ m k)
- k_l Thermal conductivity of the l -th layer, (W/ m K)
- m_a Air mass within the indoor environment, kg
- \tilde{K}_v Isothermal transmittance, (W/m² K)
- \dot{Q}_{cd} Conduction heat transfer rate, (W)
- \dot{Q}_{cv} Convection heat transfer rate, (W)
- \dot{Q}_{emit} Emission heat rate, (W)
- \dot{Q}_{lm} Low-mass heat transfer rate, (W)
- \dot{Q}_{rad} Radiation heat transfer rate rate, (W)
- \dot{Q}_{sol} Overall solar gain, (W)
- \dot{Q}_v Overall infiltration loss, (W)
- q Heat flux, (W/ m²)
- \dot{q} rate of internal heat gain/loss from source or sink within the material, (W)
- $q_{1,2}$ heat flow variations on the two sides of the surface, (W/m²)

- q_r Radiant source heat, (W)
- R Area-integrated overall thermal resistance, (m^2 K/W)
- $R_{1,2}$ Thermal resistance on side 1 and 2 of the surface, (m^2 K/ W)
- R_{cd} Overall conduction thermal resistance, (K/W)
- R_{cv} Overall convection thermal resistance, (K/W)
- R_{cv_i} Overall convection thermal resistance on i -th surface side, (K/W)
- R_c Ceiling thermal resistance, (K/W)
- R_f Floor thermal resistance, (K/W)
- R_{fu} Furniture thermal resistance, (K/W)
- R_i i -th Surface thermal resistance, K/W
- R_{in_e} External wall inside thermal resistance, (K/W)
- R_{in_i} Indoor wall thermal resistance, (K/W)
- R_{inf} Infiltration and low mass envelope components thermal resistance, K/W
- R_k Thermal resistance of the k -th layer, (K/ W)
- R_k^* Equivalent area-integrated thermal resistance up to the k -th layer, (K/ W)
- R_{i_n} Overall inside thermal resistance of the element, (K/W)
- R_{iv} Equivalent infiltration thermal resistance, (K/W)
- R_{lm} Overall low-mass envelope surfaces thermal resistance, (K/W)
- R_{out} Overall outside thermal resistance of the element, (K/W)
- R_{out_e} Outdoor side resistance of the external wall, 0.040 K/W
- r Thermal resistance, (m^2 K/ W)
- r_a Air gap thermal resistance, (m^2 K/ W)
- r_{si} Inside surface thermal resistance, (m^2 K/W)
- r_{se} Outdoor side surface thermal resistance, (m^2 K/ W)
- T Temperature, (K)
- T_∞ Fluid bulk temperature, (K)
- T_c Ceiling temperature, ($^\circ$ C)
- T_e External wall temperature, ($^\circ$ C)
- T_f Floor temperature, ($^\circ$ C)

- T_{fu} Furniture temperature, ($^{\circ}\text{C}$)
- T_i i -th Surface element temperature, ($^{\circ}\text{C}$)
- T_{in} Indoor temperature, (K)
- T_m Element temperature, (K)
- T_{out} Outdoor temperature, (K)
- T_s Surface temperature, (K)
- T_{s_i} i -th element surface temperature, (K)
- T_{wi} Internal wall temperature, ($^{\circ}\text{C}$)
- t Time, (s)
- $t_{1,2}$ Temperature variations on side one and two of the surface,(K)
- U Thermal conductance, ($\text{W} / \text{m}^2 \text{K}$)
- U_{-value} Thermal transmittance, ($\text{W} / \text{m}^2 \text{K}$)
- $U_{c,k}$ Transmittance of the k -th component, ($\text{W} / \text{m}^2 \text{K}$)
- U_d Door transmittance, $2.5 \text{ W} / \text{m}^2 \text{K}$
- U_w Window transmittance, $2.2 \text{ W} / \text{m}^2 \text{K}$
- vol_c Room volume air changes per time unit $0.3 / \text{h}$, [?]
- V Considered building space volume, (m^3)
- V_{air} Volume of the considered zone, (m^3)
- $\tilde{t}_{1,2}$ Temperature variations expressed as a complex quantity,(C)
- $\tilde{q}_{1,2}$ Heat flow variations expressed as a complex quantity, (W / m^2)
- ΔT Temperature difference between boundary surfaces, (K)
- Δx Distance between boundary surfaces, (m)
- $\Delta\theta_{er}$ Temperature difference between the outside air and the apparent temperature of the sky, 11 (K)
- $\Phi_{r,mn,k}$ Extraflux contribution from the k -th envelope component, (W)
- $\Phi_{sol_{we}}$ Solar contribution through the envelope opaque elements, (W)
- ∇T Temperature gradient, (K/m)
- α Thermal diffusivity of the material, (m^2 / s)
- α_i Thermal diffusivity of the i -th layer, (m^2 / s)

- $\alpha_{sol,i,j}$ solar absorptance of the i,j -th surface
- $\alpha_{sol,k}$ k -th element solar absorptance, (m^2 / s)
- ζ Position of the null heat flow plane respect to the inner side of the surface,
- ε Emissivity of the surface,
- θ Thermal resistance correction factor,
- $\theta_{\mu\nu}$ Thermal conductivity tensor
- λ_i Thermal conductivity of the i -th layer, ($W / m K$)
- ρ Density, (kg/m^3)
- ρ_a Air Density, $1.225 kg/m^3$, ISA conditions
- ρ_i Mass density, (kg/ m^3)
- σ Stephan-Boltzmann constant, $5.67 \cdot 10^{-8} W/m^2 K$
- ϕ Thermal capacity correction factor,
- ϕ_{sol_g} Glazing surfaces heat gain, (W)
- $\phi_{sol,k}$ solar heat gain on k -th surface, (W)
- ω Sinusoid pulsation, (rad/s)

Chapter 1

Introduction

The conventional way to manage the electric energy systems is a top-down oriented solution, where a limited number of large power plants feed the electricity network trying to satisfy the demand, [12] .

Two main issues are affecting the modern power systems. The first one is related to the raising penetration of renewable source power plants which are subject to a certain grade of volatility due to the fickle availability of the source. The second, concerns the steadily yearly increasing of energy consumption that may rise many worries about the grid capacity. These aspects are driving the evolution of the system management from the supply-following-demand to the demand-following-supply paradigm. The paradigm shift will require utilities and customers to master the full potential of the demand side management (DSM), believing that is much less expensive to intelligently reshape the load than to build new power plant or install electric storage devices.

The DSM aims deal with every action undertaken on the demand side of energy systems, ranging from users energy efficiency improving to managing the peak demand at the utility end. Demand response (DR) is one of the categories included in DSM actions. It refers to end-users changes from their normal electricity usage patterns in response to a dynamic price signal. Accordingly, the customers can shift their demand to the off-peak hours in order to minimise their electricity payment. Such shifting can be provided manually or automatically with the help of an home energy management system (EMS), whose main purpose is to minimise costs by scheduling and coordinating distributed energy resources (DER) while keeping suitable levels of comfort for the customers.

In smart homes, DER refer to distributed generation, thermal and battery storage. Another aspect when dealing with energy storage can be taken into account. Indeed, the thermal inertia of the building, which is defined as the capability of the thermal mass to resist temperature fluctuations provides a thermal energy buffer to enable HVAC system shifting without a remarkable change in the indoor temperature, can be considered as another DER in smart homes. In order to enhance this aspect, the phase change materials (PCM) can now be introduced. They are considered as a promising medium to be encapsulated in the building envelope to increase the thermal inertia [18], with the major advantages expected in lightweight building.

However in order to include the PCM in the optimization problem in EMS, an appropriate model of the building needs to be developed. The development of

the thermal model to be plugged into the optimization problem is the main aim of this work.

The work is divided the following part: the first one familiarizes with the environment of MATLAB-Simulink to solve ordinary differential equations and describes the implemented thermal model of the house. The second part validates the results with a inter-model comparison using the building thermal simulation tool EnergyPlus.

In the following chapters, at first the theory behind the thermal modelling of the building is introduced. Afterward the method to evaluate the thermal parameter of the modelled surfaces is presented. Chapter 4 and 5 are respectively dedicated to the Simulink and EnergyPlus model description. In the end the result of the simulations are reported, Chapter 6.

Chapter 2

Heat transfer theory

In order to understand how the building is modelled, the heat transfer theory and the relations between the building and the outside environment are first summarized in section 2.1 and 2.2 of this chapter. Afterwards, section 2.3, the schematic of the case study building is presented. In the end, section 2.4 the surfaces parameter evaluation methods will be explained. The theory description has been taken from [6], [8], [14] and [3].

2.1 Heat transfer theory

Heat transfer is energy transferred between physical systems because of a temperature difference. Energy flows from a higher-temperature region to a lower-temperature region by one or more of three modes: conduction, convection and radiation. In the following section each of the modes will be described.

2.1.1 Conduction

From a microscopic point of view, heat conduction is the transfer of energy from a more energetic particle to a less energetic one, where the energetic difference is based on their temperature. This can happen in gases or liquids due to random collisions between particles during their motion. In solids, it is due to the molecule vibrations in the lattice and the energy is transferred by free electrons. According to Fourier's law, the heat flux, q , through unit area per unit time can be written as:

$$q = -\vartheta_{\mu\nu}\nabla T \quad (2.1)$$

with the assumption of isotropic medium the thermal conductivity tensor $\vartheta_{\mu\nu}$ comes down to a constant value, κ [W / m K], 2.2.

$$q = -\kappa\nabla T \quad (2.2)$$

When assuming the problem one-dimensional in the x -direction, assumption usually made when dealing with the wall surfaces, and integrating over the material's cross sectional surface A_s ; 2.2 becomes:

$$\dot{Q}_{cd} = -kA_s \frac{\Delta T}{\Delta x} \quad (2.3)$$

where ΔT and Δx represent respectively the temperature difference and the distance between the two boundaries of the considered material. The thermal conductance of the material, U [$\text{W}/\text{m}^2 \text{K}$], can be now defined as:

$$U = \frac{\kappa}{\Delta x} \quad (2.4)$$

Equation 2.3 can be written as:

$$\dot{Q}_{cd} = UA_s(-\Delta T) \quad (2.5)$$

The reciprocal of conductance is *resistance*, r [$\text{m}^2 \text{K}/\text{W}$]. Resistance is additive when dealing with a multilayer element, so the following formula is usually used:

$$\dot{Q}_{cd} = \frac{A_s(-\Delta T)}{\frac{\Delta x_1}{\kappa_1} + \frac{\Delta x_2}{\kappa_2} + \frac{\Delta x_3}{\kappa_3} + \dots} \quad (2.6)$$

Defining the total resistance, R_{cd} [K/W], as:

$$R_{cd} = \frac{r_1 + r_2 + r_3 + \dots}{A_s} \quad (2.7)$$

the equation defining the heat conduction can be rewritten as:

$$\dot{Q}_{cd} = \frac{-\Delta T}{R_{cd}} \quad (2.8)$$

which means that the heat flow through a wall is proportional to the temperature difference at each side of the wall.

2.1.2 Convection

Convective heat transfer is the transfer of energy between a solid surface and a fluid in motion adjacent to the surface. Convection combines the effects of both the conduction within the air due to molecules motion and the overall motion of the air that removes the heated air near the wall to replaces it by a cooler one, this process is referred to as advection. Although convection is a complex process, the rate of convection heat transfer is proportional to the temperature difference between the surface and the bulk temperature of the fluid. This relationship is expressed by the Newton's law of cooling:

$$\dot{Q}_{cv} = hA_s(T_s - T_\infty) \quad (2.9)$$

where A_s , T_s and T_∞ are respectively the area and temperature of the considered surface and the bulk temperature of the fluid involved in the convection process. Equation 2.9 can be rewritten similar to 2.8 by defining the convective resistance $R_{cv} = 1/hA_s$, thus obtaining:

$$\dot{Q}_{cv} = \frac{T_s - T_\infty}{R_{cv}} \quad (2.10)$$

As explained above, both thermal conduction and convection can be explained considered as depending on the temperature difference and on the thermal resistance. When combining these two effects, thus the convection thermal resistances

on both sides of the surface and the surface conduction thermal resistance can be considered as a resistance series, the thermal transmittance, U_{-value} , of the element is obtained:

$$U_{-value} = \frac{1}{R_{cv_1} + R_{cd} + R_{cv_2}} \quad (2.11)$$

2.1.3 Radiation

From a microscopic point of view, thermal radiation is electromagnetic radiation due to inter-atomic collisions between particles which can bring to a charge particle kinetic energy change. This leads to a charge-acceleration and/or dipole oscillation which produces electromagnetic radiation. Since the thermal radiation is related to the kinetic energy, kinetic energy is related to temperature, thermal radiation takes place when a matter has a temperature greater than the absolute zero: always. Another feature of thermal radiation, which differs from conduction and convection, is that it does not require a medium to take place.

Dealing with solids, thermal radiation is usually considered a surface phenomenon and the rate of radiation that can be emitted from a body with a certain absolute surface temperature can be computed through the Stefan-Boltzmann law as follow:

$$\dot{Q}_{emit} = \varepsilon \sigma A_s T_s^4 \quad (2.12)$$

where $\sigma = 5.67 \cdot 10^{-8}$ [W/ m² K] is called Stephan-Boltzmann constant, ε is the emissivity of the surface, which values lays between 0 and 1. A_s and T_s are respectively, the surface area and temperature of the object considered. To find the thermal radiation heat transfer rate between two bodies, with surfaces temperatures T_{s_1} and T_{s_2} the following equation can be used:

$$\dot{Q}_{rad} = \varepsilon \sigma A_s (T_{s_1}^4 - T_{s_2}^4) \quad (2.13)$$

The most important radiation contribution to be taken into account while modelling the thermal behavior of the building, are the solar radiation, which is considered as a short-wave radiation, and the lightening contribution, which is usually considered a long-wave radiation. How solar gain is considered will be explained in the following.

Other contributions, like long-wave radiation between the internal surfaces, exists but for the aim of this work it will be neglected, as suggested by [5].

2.2 Heat transfer in building spaces

As shown is Fig. 2.1, for a simplified modelling of the indoor building space condition is connected with many different heat and mass transfer processes which can be summarized as follow:

- Heat transfer due to conduction through the fabric elements;
- Solar gain through glazing surfaces;
- Air infiltration from the outdoor environment and the adjoining rooms;
- Internal gain due to lighting, people, equipment and other inside the room;

- Air conditioning load and moisture control by the HVAC system.
- In the following each contribution considered in this work will be explained.

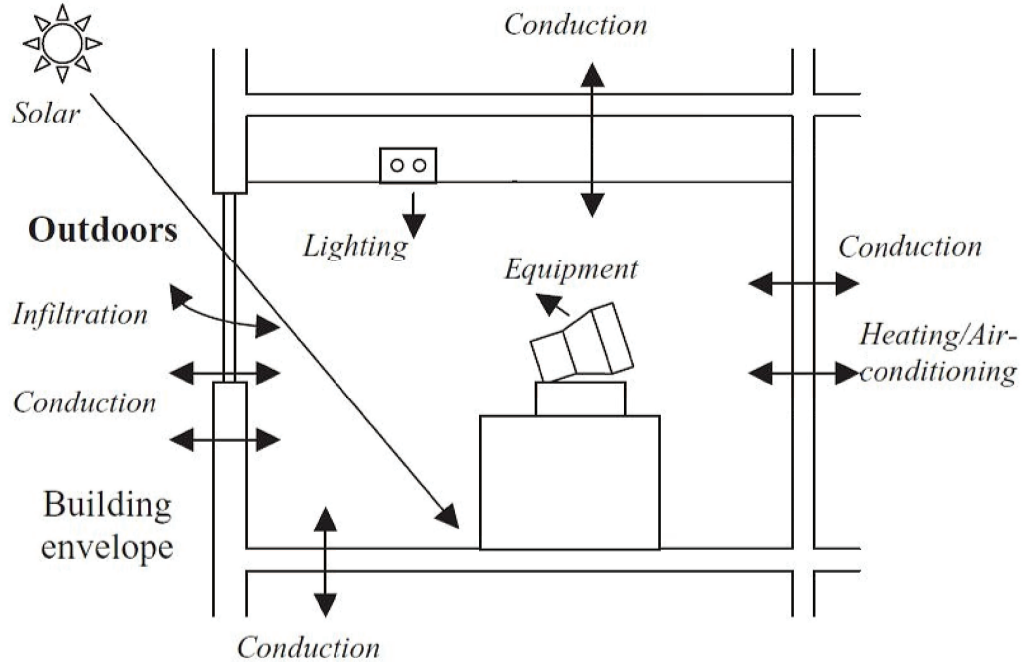


Figure 2.1: Heat transfer process involved in building energy modelling, [15].

2.2.1 Heat transfer through fabric element

The heat transfer through an homogeneous material can be described considering the following:

- the energy transferred per time unit across the boundary surfaces of an elemental volume is proportional to the temperature difference between the two surfaces;
- the heat generation or removal per time unit because of internal sources or sinks inside control volume;
- the temperature change of the material within the control volume due to the change in the internal energy.

The resulting governing equation is:

$$\rho c \frac{\delta T}{\delta t} - \nabla \cdot \kappa \nabla T - \dot{q} = 0 \quad (2.14)$$

which can be further more simplified assuming the following:

- the heat transfer problem is one-dimensional in the perpendicular direction, x of each surface delimiting the environment;
- isotropic heat transfer inside the material;
- thermophysical properties are temperature independent;

- no internal source or sink is presents inside the material.

The simplified governing equation is:

$$\frac{\delta T}{\delta t} = \alpha \frac{\delta^2 T}{\delta x^2} \quad (2.15)$$

The boundary conditions which combined with 2.15 lead to the solution of the conduction problem for the building element, could be:

- Imposed temperature, so that we know the temperature on each boundary surface;
- Imposed heat flow.

As will be explained in the following, different boundary conditions lead to a different way to model the respective component. Even though many accurate analytical method could be used to solve 2.15, such as the Analytical Time Response Analysis, the Laplace Transformation and the Response Factor Method; a simpler method to approach the solution of the equation is adopted. This approach is chosen considering the trade-off between accuracy and computational demand. It consists of treating each building element as a small number of lumped parameters, whence the name of the method *Lumped capacitance method*. According to the first-order lumped capacitance method, the wall can be modeled as a 2R1C circuit, as shown in Fig. 2.2.

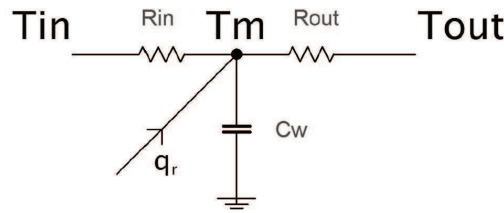


Figure 2.2: First-order lumped capacitance wall model

Thus, the resulting equation of heat transfer through the wall is:

$$C_w \frac{dT_m}{dt} = \frac{(T_{in} - T_m)}{R_{in}} + \frac{(T_{out} - T_m)}{R_{out}} + q_r \quad (2.16)$$

As reported by [15], two main problems affect the first-order model of the wall. The first one concerns the inadequate approximation describing the internal surface temperature of the element. The second one concerns the response of the surface to radiant inputs especially for high mass components. Anyway, for sake of simplicity, the first-order model is chosen and, in order to avoid the first problem, the evaluation of the wall parameters is carried out considering the frequency characteristic analysis of the wall instead of the method proposed by [15]. Both parameter evaluation method are described in Chapter 3.

Low thermal capacity external surfaces As sugested by [15], the thermal capacity of low-mass surfaces, like windows and doors, is negligible compared to the one of the high mass envelope surfaces. Thus, the resulting model of such

components, is a simply resistive path between the indoor temperature and the outdoor one.

$$\dot{Q}_{lm} = \frac{T_{in} - T_{out}}{R_{lm}} \quad (2.17)$$

Extraflux According to [4], an additional radiative contribution should be to considered which is due to the radiation exchange between the building envelope and the sky. Such contribution, called extraflux, is computed as follow:

$$\Phi_{r,mn,k} = r_{se} \cdot U_{c,k} \cdot A_{c,k} \cdot h_r \cdot \Delta\theta_{er} \quad (2.18)$$

Since that the extraflux contribution for the opaque surfaces is considered added to the external wall temperature node, only the the transmittance due to the outer part of the wall is considered.

The extraflux contribution due to the low-mass envelope surfaces is added directly into the inside-air temperature node.

2.2.2 Solar gain

Solar gain refers to the heat gain due to solar radiation on the outer surfaces of the building envelope. The solar gain has been considered as suggested by [4]. According to this method, assuming no un-conditioned spaces adjoining the considered space, the overall solar gain in the zone are:

$$Q_{sol} = \sum_k \phi_{sol,k} \cdot t$$

$$\phi_{sol,k} = F_{sh,ob,k} \cdot A_{sol,k} \cdot I_{sol,k}$$

Solar Radiation The solar radiation has been initially calculated according to [9], thus following the ASHRAE Clear Sky direct-beam radiation model. Further on, the same solar radiation values have been used in the Ep and Simulink model in order to minimize the difference of the results due to difference in the input values. In other word, the solar radiation input for the Simulink model has been derived from the Energy Plus spreadsheet output after enabling the Ep output variable "Surface Outside Face Incident Solar Radiation Rate per Area" to be reported.

Effective solar capture area calculation The effective solar capture area calculation depends on the type of surface considered, opaque or glazing one. For both type, it has been calculated for every orientation of the house in order to divide the different orientation solar contributions. In other words, the effective solar capture area in one direction will be subject to the solar radiance in the same direction. In the following the different approaches used for opaque and glazing surfaces are reported.

A_{sol} : **opaque surfaces** The effective solar capture area for opaque surfaces is calculated as follow:

$$A_{sol,k} = \alpha_{sol,k} \cdot r_{se} \cdot U_{c,k} \cdot A_{c,k} \quad (2.19)$$

Since that the model takes into account the external wall thermal capacity, the transmittance value considers only the outer part of the wall and the further calculated opaque solar gains are added to the external wall temperature node.

A_{sol} : **glazing surfaces** The effective solar capture area for glazing surfaces has been calculated as follow:

$$A_{sol,k} = F_{sh,gl} \cdot g_{gl} \cdot (1 - F_f) \cdot A_{w,k} \quad (2.20)$$

The solar gain due to radiation through the glazing surfaces are distributed among the interior surfaces according to the absorptance-weighted area ratio, as reported from [17] for short-wave radiation gains. According to this method, the radiative heat, $q_{radiative}$, received by a surface depend on the overall entering radiative heat, $Q_{radiative}$, through the distribution factor, f_i^{solar} , which is computed as follow:

$$f_i^{solar} = \frac{\alpha_{sol_i} \cdot A_i}{\sum_{surfaces} \alpha_{sol_j} \cdot A_j} \quad (2.21)$$

2.2.3 Air infiltration and ventilation

Air infiltration and ventilation losses are due to the air change of the indoor air for un-wanted and wanted contribution respectively. If the simple case of ventilation is assumed, as suggested by [4], we can combine both the losses and compute them as follow:

$$\dot{Q}_v = (T_{in} - T_{out}) / R_{iv} \quad (2.22)$$

$$R_{iv} = \frac{1}{vol_c \cdot c_{p_a} \cdot \rho_a \cdot V} \quad (2.23)$$

2.3 Schematic of the building

The case study building is a space whole conditioned which is supposed to have adjoining above and below spaces with similar indoor temperature path. In the following, data and schematic of the building will be reported.

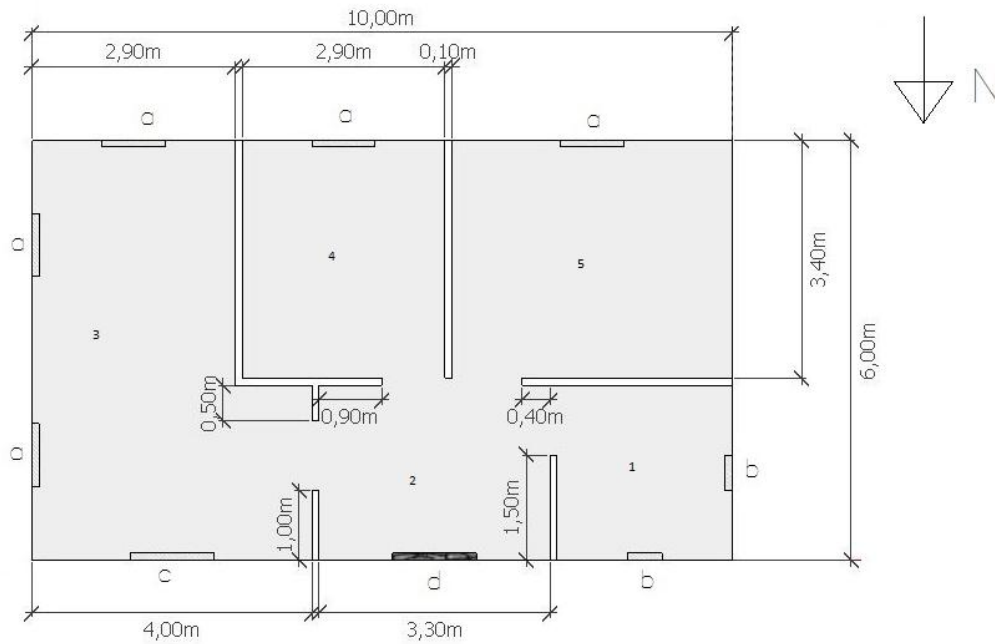


Figure 2.3: Schematic of the case study building

Table 2.1: Room height, windows and door data.

Roomheight		2.7 m
Window	type a	0.9 m × 1.5 m
	type b	0.5 m × 0.9 m
	type c	1.2 m × 2 m
	U_f	$2.2 \text{ W m}^{-2} \text{ K}^{-1}$
		low-e double pane window with air gap 4-8-4 mm and frame fraction, F_f , 0.3
Door	type d	1.2 m × 2 m
	U_d	$2.5 \text{ W m}^{-2} \text{ K}^{-1}$

All data are derived from the master course technical plant handout, [11].

Chapter 3

Wall parameter evaluation method

In order to evaluate the building wall parameters two different methods have been used. Initially, the model has been developed using the α -method reported by [3] to compute the wall inner and outer resistances as well as the capacity. Afterward, the method reported by [3] and [4] has been adopted. In the following, the calculation methods are reported.

3.1 α - Method

This method can be applied to any construction element consisting of L layers of material. Each element can be represented by two 'lumped' thermal resistances (R_{ins}, R_{out}), and one thermal capacity (C_{tot}). The evaluation of the two resistances depends on the total resistance of the element through the 'accessibility factor', α , which defines the position of the element capacity inside the element.

The parameters are calculated as follow:

$$R = (r_{si} + r_{se} + r_a + \sum_1^L \frac{x_l}{k_l}) / A_{total} \quad (3.1)$$

$$C = A_{total} \cdot (\sum_1^L x_l \cdot \rho_l \cdot c_{pl}) \quad (3.2)$$

$$R_{in} = \alpha \cdot R \quad (3.3)$$

$$R_{out} = (1 - \alpha) \cdot R \quad (3.4)$$

$$\alpha = 1 - \frac{\sum_1^L R_k^* \cdot C_k}{R \cdot C} \quad (3.5)$$

$$R_k^* = \sum_1^{k-1} R_i + \frac{R_k}{2} \quad (3.6)$$

When dealing with internal wall, the accessibility factor has been simply chose equal to 0.5, since both sides of the wall are subject to the same condition and the problem is symmetric.

3.2 Masy Correction

In this method two correction parameters for the capacity and resistances values of the component model are derived from the frequency characteristic analysis of the wall. This section comes from [10].

3.2.1 Wall Admittance Matrix

A n -layers wall is considered subject to a sinusoidal temperature or heat flow on both sides with the following assumptions:

- Homogeneous material;
- Heat transfer only across the wall;
- Isotropic heat transfer;
- No internal source or sink exists within the material;
- Thermophysical properties temperature independent;

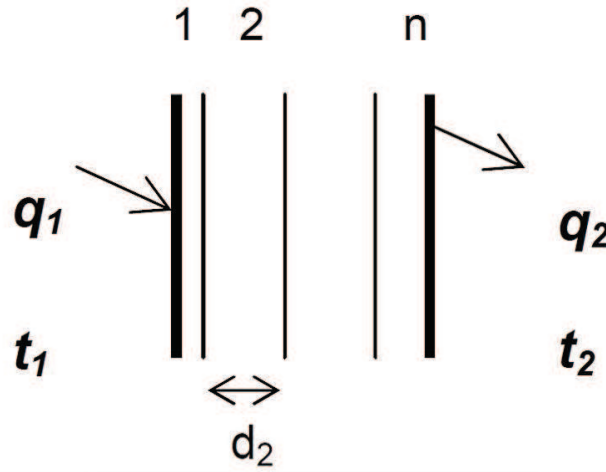


Figure 3.1: Temperature and heat flow variations on the two sides of a wall including n -layers

The relationship between the temperature and heat flow variations on the two sides of the wall can be defined as follow:

$$\begin{pmatrix} \tilde{t}_1 \\ \tilde{q}_1 \end{pmatrix} = \begin{pmatrix} A_1 & B_1 \\ C_1 & D_1 \end{pmatrix} \begin{pmatrix} A_2 & B_2 \\ C_2 & D_2 \end{pmatrix} \cdots \begin{pmatrix} A_n & B_n \\ C_n & D_n \end{pmatrix} \begin{pmatrix} \tilde{t}_2 \\ \tilde{q}_2 \end{pmatrix}$$

$$A_i = \cosh \sqrt{\tau_i \omega_i}$$

$$B_i = \frac{R_i}{\sqrt{\tau_i \omega_i}} \cosh \sqrt{\tau_i \omega_i}$$

$$C_i = \frac{\sqrt{\tau_i \omega_i}}{R_i} \sinh \sqrt{\tau_i \omega_i}$$

$$D_i = \cosh \sqrt{\tau_i \omega_i}$$

$$R_i = \frac{d_i}{\lambda_i}; \quad \tau_i = \frac{d_i^2}{\alpha_i}; \quad \alpha_i = \frac{\lambda_i}{\rho_i c_i}$$

The matrix product in the preceding relationship yields the *reverse transfer matrix*, \mathbf{Q} , whose determinant equals 1.

$$\begin{pmatrix} \tilde{t}_1 \\ \tilde{q}_1 \end{pmatrix} = \begin{pmatrix} Q_{11} & Q_{12} \\ Q_{21} & Q_{22} \end{pmatrix} \begin{pmatrix} \tilde{t}_2 \\ \tilde{q}_2 \end{pmatrix}$$

Expressing the heat flow variations as a function of the temperature, the *admittance matrix*, \mathbf{Y} , can be obtained:

$$\begin{pmatrix} \tilde{q}_1 \\ \tilde{q}_2 \end{pmatrix} = \begin{pmatrix} Y_{11} & Y_{12} \\ Y_{21} & Y_{22} \end{pmatrix} \begin{pmatrix} \tilde{t}_1 \\ \tilde{t}_2 \end{pmatrix}$$

where:

$$\begin{pmatrix} Y_{11} & Y_{12} \\ Y_{21} & Y_{22} \end{pmatrix} = \begin{pmatrix} \frac{Q_{22}}{Q_{12}} & \frac{-1}{Q_{12}} \\ \frac{1}{Q_{12}} & \frac{-Q_{11}}{Q_{12}} \end{pmatrix}$$

The *impedance transfer matrix*, \mathbf{Z} , is obtained expressing the temperature variations as a function of the heat flow variations on the two side of the element:

$$\begin{pmatrix} \tilde{t}_1 \\ \tilde{t}_2 \end{pmatrix} = \begin{pmatrix} Z_{11} & Z_{12} \\ Z_{21} & Z_{22} \end{pmatrix} \begin{pmatrix} \tilde{q}_1 \\ \tilde{q}_2 \end{pmatrix}$$

where:

$$\begin{pmatrix} Z_{11} & Z_{12} \\ Z_{21} & Z_{22} \end{pmatrix} = \begin{pmatrix} \frac{Q_{11}}{Q_{21}} & \frac{-1}{Q_{21}} \\ \frac{1}{Q_{21}} & \frac{-Q_{22}}{Q_{21}} \end{pmatrix}$$

3.2.2 Boundary conditions

In the building modelling environment, two types of thermal boundary condition can be set:

- Imposed temperature
- Imposed heat flow

Imposed Temperature

Walls like the external wall are submitted to the outdoor temperature on side 1. The heat flow on the indoor side can be computed according to the *admittance matrix*, \mathbf{Y} :

$$\tilde{q}_2 = \frac{1}{Q_{12}} \tilde{t}_1 - \frac{Q_{11}}{Q_{12}} \tilde{t}_2$$

The ratio of the indoor side heat flow variation to the imposed temperature on side one, outdoor temperature, for a constant indoor temperature and a given sinusoid frequency, defines the *isothermal transmittance*:

$$\tilde{K}_v = \left(\frac{\tilde{q}_2}{\tilde{t}_1} \right)_{\tilde{t}_2=0}$$

The ratio between the indoor side heat flow variation and the indoor side temperature variation, defines the *isothermal admittance*, for a constant outdoor temperature and a given frequency:

$$\tilde{A}_v = \left(\frac{\tilde{q}_2}{\tilde{t}_2} \right)_{\tilde{t}_1=0}$$

Thus:

$$\tilde{K}_v = \frac{1}{Q_{12}} \qquad \tilde{A}_v = -\frac{Q_{11}}{Q_{12}}$$

Imposed heat flow

The internal walls completely included in a zone are crossed by a null heat flow plane. The wall is then subdivided into two parts, each of them being analysed as a wall with an imposed null heat flow on the "outdoor" side 1. According to the *impedance matrix*, temperature variation on the indoor side 2, can be computed as:

$$\tilde{t}_2 = \frac{1}{Q_{21}} \tilde{q}_1 - \frac{Q_{22}}{Q_{21}} \tilde{q}_2$$

The ratio of the indoor side heat flow variation to the indoor side temperature variation, for a constant heat flow and for a given frequency, defines the *adiabatic admittance*:

$$\tilde{A}_{v_d} = \left(\frac{\tilde{q}_2}{\tilde{t}_2} \right)_{\tilde{q}_1=0}$$

Thus:

$$\tilde{A}_{v_d} = -\frac{Q_{21}}{Q_{22}}$$

Dealing with a homogeneous or symmetric internal wall, the null heat flow plane is symmetry plane; otherwise, the null heat flow plane position is defined by equalizing the dampening factors of two sinusoidal temperature solicitations acting separately on each wall side. The dampening factor, f_d , of a signal crossing n wall layers is defined as:

$$f_d = \prod_{i=1}^n \exp \left(-d_i \sqrt{\frac{\omega}{2\alpha_i}} \right)$$

Wall network model

The wall is modelled through a 2R1C model where resistances and capacity are chosen in order to reproduce the wall admittance and transmittance for a 24h period.

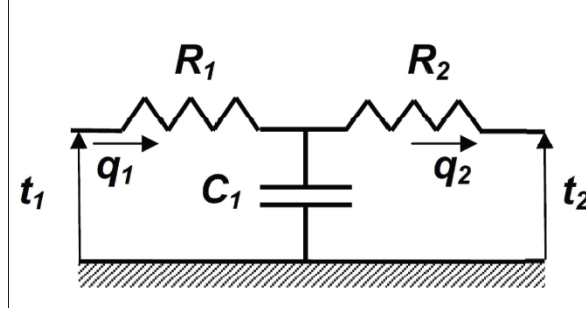


Figure 3.2: Wall 2R1C network

The reverse transfer matrix \mathbf{Q} of the 2R1C network is:

$$\begin{pmatrix} \tilde{t}_1 \\ \tilde{q}_1 \end{pmatrix} = \begin{pmatrix} Q_{11} & Q_{12} \\ Q_{21} & Q_{22} \end{pmatrix} \begin{pmatrix} \tilde{t}_2 \\ \tilde{q}_2 \end{pmatrix} = \begin{pmatrix} R_1 C_1 \omega j + 1 & R_1 R_2 C_1 \omega j + R_1 + R_2 \\ C_1 \omega j & R_2 C_1 \omega j + 1 \end{pmatrix} \begin{pmatrix} \tilde{t}_2 \\ \tilde{q}_2 \end{pmatrix}$$

- **Isothermal boundary condition** surfaces are modelled through a 2R1C network. The *isothermal transmittance* of the 2R1C network is given by:

$$\tilde{K}_v = \left(\frac{\tilde{q}_2}{\tilde{t}_1} \right)_{\tilde{t}_2=0} = -\frac{1}{R_1 + R_2 + R_1 R_2 C_1 \omega j}$$

The *isothermal admittance* of the 2R1C network is equal to:

$$\tilde{A}_v = \left(\frac{\tilde{q}_2}{\tilde{t}_2} \right)_{\tilde{t}_1=0} = -\frac{1 + R_1 C_1 \omega j}{R_1 + R_2 + R_1 R_2 C_1 \omega j}$$

- **Adiabatic Boundary condition** surfaces must be divided into two part sharing a null heat flow plane and each one associated to its related indoor zone. Each part is modelled though a 2R1C network, so that, actually, the adiabatic boundary condition wall is modeled through a 3R2C circuit. This type of model is applied to internals walls and partition walls in contact with neighbour zones which are supposed to be subject to a similar temperature pattern on both sides. The *adiabatic admittance* of each 2R1C network is computer from:

$$\tilde{A}_v = \left(\frac{\tilde{q}_2}{\tilde{t}_2} \right)_{\tilde{q}_1=0} = -\frac{C_1 \omega j}{1 + R_2 C_1 \omega j}$$

The resulting network for the adiabatic boundary condition walls can be observed in Fig.3.3.

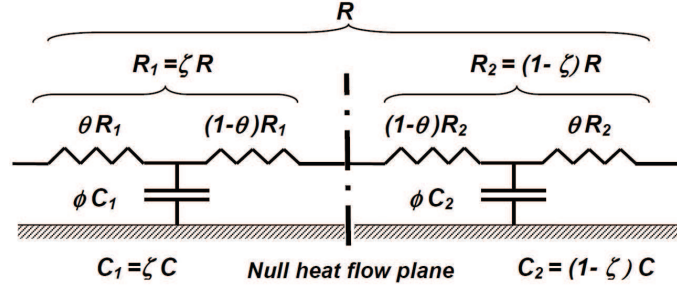


Figure 3.3: Adiabatic boundary condition element network model

3.2.3 Wall network adjustment process

The network adjustment process depends on the type of boundary condition to which the wall is subject to.

Isothermal boundary condition walls

For isothermal boundary condition walls, the adjustment process consists in equalizing the magnitudes of the wall isothermal admittance $|\tilde{A}_v|$ and transmittance $|\tilde{K}_v|$, computed for a 24 hours time period with the corresponding 2R1C network values. The adjustment process provides two resistances and one capacity (R_1, R_2, C_1) which can be expressed as fractions of the wall total resistance and capacity, through not dimensional factor θ and ϕ .

$$|\tilde{A}_v| = - \left| \frac{Q_{11}}{Q_{12}} \right| = - \left| \frac{1 + \phi(1 - \theta)RC\omega j}{R + \phi\theta(1 - \theta)R^2C\omega j} \right|$$

$$|\tilde{K}_v| = - \left| \frac{1}{Q_{12}} \right| = - \left| \frac{1}{R + \phi\theta(1 - \theta)R^2C\omega j} \right|$$

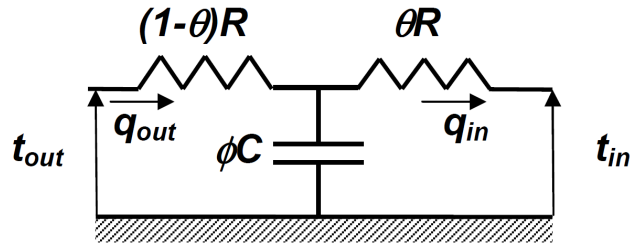


Figure 3.4: Adjusted 2R1C network for an isothermal boundary condition wall

The resulting equation for the correction parameters are:

$$\theta = \sqrt{\frac{U^2 - |\tilde{K}_v|^2}{|\tilde{A}_v|^2 - |\tilde{K}_v|^2}} \quad \phi = \frac{1}{(1 - \theta)\omega RC} \sqrt{\frac{|\tilde{A}_v|^2}{|\tilde{K}_v|^2} - 1} \quad U = \frac{1}{R}$$

where:

- factor ϕ defines the proportion of the whole wall capacity accessed by a 24h time period;
- factor θ , commonly called *accessibility*, gives the position of that capacity on the whole wall resistance.

Adiabatic boundary condition walls

For adiabatic boundary condition walls, the adjustment process concerns both parts of the wall shared by a null heat flow plane whose position is defined by equalizing the dampening factors of two sinusoidal temperature solicitations acting separately on each wall side. The adjustment consists in equalizing the magnitude and angle of the wall adiabatic admittance \tilde{A}_{v_d} computed for a 24 hours time period for the two part the wall is divided into. The adjustment process provides two resistances and one capacity (R_1, R_2, C_1) which can be expressed as fractions of the wall total resistance and capacity, through not dimensional factor θ and ϕ .

$$\tilde{A}_{v_d} = -\frac{Q_{21}}{Q_{22}} = -\frac{\phi C \omega j}{1 + \phi \theta R C \omega j}$$

The resistance $(1 - \theta)R$, outside resistance, is located on the null heat flow plane side and can be erased, as there is no heat flow passing through this network connection.

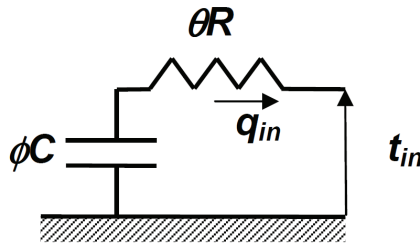


Figure 3.5: Adjusted 2R1C network for an adiabatic boundary condition wall

The correction parameters can be calculated as:

$$\theta = \frac{|R(\tilde{A}_{v_d})|}{R |\tilde{A}_{v_d}^2|} \quad \phi = \frac{|\tilde{A}_{v_d}^2|}{\omega C |I(\tilde{A}_{v_d})|}$$

Chapter 4

Matlab-Simulink model

In Matlab-Simulink environment, the building has been modelled through the differential equations of the system. In the following, the room model will be presented in order to obtain a general view of the model. Afterward, the details of how every component has been considered will be explained.

4.1 Thermal model of the building

The contribution to the thermal behaviour of the building which have been considered in this work can be summarized as:

- Heat flow through the external envelope;
- Infiltration losses;
- Solar gain;
- Internal heat storage due to furniture, internal walls and internal partitions;

The resulting equation of the room is the following:

$$m_a c_a \frac{dT_{in}}{dt} = \frac{T_{in} - T_e}{R_{in_e}} + \frac{T_{in} - T_c}{R_c} + \frac{T_{in} - T_f}{R_f} + \frac{T_{in} - T_{wi}}{R_{iw}} + \frac{T_{in} - T_{fu}}{R_{fu}} + \frac{T_{in} - T_{out}}{R_{inf}} \quad (4.1)$$

4.2 High mass and thermal mass component description

The thermal model of the high mass components depend on the boundary condition they are subject to. The Masy-correction method has been chosen to evaluate the model parameters. In the following the model of each considered surface will be explained.

4.2.1 Imposed Temperature boundary condition: External wall

The external wall is supposed to be in contact with the outdoor conditions on the external side, thus temperature and solar radiation; to the indoor conditions on

the internal side. The resulting model is:

$$C_{we} \frac{dT_e}{dt} = \frac{T_{in} - T_e}{R_{ine}} + \frac{T_{out} - T_m}{R_{oute}} + \Phi_{sol_{we}} \quad (4.2)$$

The calculation of the outside wall parameters through the frequency analysis of the wall leads to determine the following values of the correction parameters: $\theta_{we}=0.07$ and $\varphi_{we}=0.607$. The values of the inner and outer thermal resistances are then increased by 15 % in order to consider the thermal bridges, [4].

Table 4.1: External wall data

Layers	κ [W/m K]	d [m]	ρ [kg/m ³]	c_p [J/kg K]	r [m ² K/W]
Indoor surface resistance	-	-	-	-	0.13
Gypsum plasterboard	0.35	0.005	1200	960	-
Perforated brick blocks	0.25	0.08	600	900	-
Air gap	-	-	-	-	0.18
Asbestos cementos	0.6	0.025	1200	990	-
Outdoor surface resistance	-	-	-	-	0.04

Data for the wall structure are derived from [11] and refer to a building lightweight envelope

4.2.2 Imposed heat flow boundary condition surfaces

This type of surfaces are modelled as containing a null heat flow plane, which is derived from the assumption of similar conditions on the two sides of the element. The position of the null heat flow plane is defined from the frequency analysis of the element. The surfaces heat exchange considered are with the indoor air and the solar gain through the glazing surfaces which are shared among these surfaces according to the solar absorptance-weighted method [17].

The resulting model, with slightly different parameter calculations, is:

$$C_i \frac{dT_i}{dt} = \frac{T_{in} - T_i}{R_i} + f_i \Phi_{sol_g} \quad (4.3)$$

$i = \text{internal wall, floor slabs, furniture}$

Internal wall The internal wall structure is symmetric, thus the null heat flow plane overlaps the symmetry plane of the wall.

Table 4.2: Internal wall data

Layers	κ [W/m K]	d [m]	ρ [kg / m ³]	c_p [J/kg K]	r [m ² K/ W]
Indoor surface resistance	-	-	-	-	0.13
Gypsum plasterboard	0.9	0.01	1800	910	-
Perforated brick blocks	0.25	0.08	600	900	-
Gypsum plasterboard	0.9	0.01	1800	910	-
Indoor surface resistance	-	-	-	-	0.13

Data for the internal wall structure are derived from [11]

Parameter calculation In order to apply the Masy-correction method, only half-wall is considered for the specific parameter calculation. The 'outside' layer is the null heat flow plane which overlap the symmetry plane of the wall. The 'inside' layer is the one related to the inner surface resistance. The resulting correction parameter values for the internal wall surface are: $\theta_{iw}=0.512$ and $\varphi_{iw}=0.997$. The final overall parameter values introduced in 4.3 are:

$$\begin{aligned} C_{iw} & 3.238 \text{ MJ/K}; \\ R_{iw} & 0.0018 \text{ K/W}; \\ f_{iw} & 0.1747; \end{aligned}$$

floor slabs Data related to the floor slabs are taken from [10], annex 2. A light structure has been chosen and is described as follow:

- finishing flooring;
- mortar;
- insulation between joists;
- gypsum board;
- overall slab transmittance, U_{slab} , equals $0.699 \text{ W/m}^2\text{K}$;
- overall slab surface specific capacity, C_{slab} , equals $84\,041 \text{ J/m}^2\text{K}$;
- the portion of floor slab accessed by a 24h time period, ζ_{floor} , equals 0.21;
- the portion of ceiling slab accessed by a 24h time period, $\zeta_{ceiling}$, equals $(1-\zeta_{floor})$ thus 0.79;

Parameter calculation This description comes from a list of wall typology drafted by the author of [10]. The resulting parameter values introduced in 4.3, for ceiling and floor respectively, are:

$$\begin{aligned} C_c & 3.984 \text{ MJ/K}; \\ R_c & 0.0019 \text{ K/W}; \\ f_c & 0.1651; \\ \\ C_f & 1.059 \text{ MJ/K}; \\ R_f & 0.0009 \text{ K/W}; \\ f_f & 0.4181; \end{aligned}$$

Furniture The main highlighted furniture aspect emerged from literature concerns both the importance of considering more than a empty room in order to better describe the thermal behaviour of the building, [16], and the lack of guidance for selecting reasonable furniture parameter values, [13]. 'How to model' and 'how much' furniture are the two main challenges of this topic.

The first one is solved considering a one-side adiabatic wooden surface which exchange heat with the room environment. The prevention of the heat exchange between the room environment and both the internal wall and the floor is considered through sharing equally the overall furniture surface between the floor and the internal wall. In other words, the heat exchanging surface between the floor and the indoor environment is diminished by the half of the furniture overall surface considered; the same happens to the internal wall heat exchanging surface. Anyway the overall thermal capacity of these two element is not affected by the furniture.

The second concern is solved merging what reported in [7] and [13]. Furniture data can be found in the following table.

Table 4.3: Furniture data

Amount of internal mass	80	kg/m ² _{floor}
Density	540	kg/m ³
Average thickness	0.2	m

The resulting overall surface is 44 m², and the thermophysical properties to compute the furniture thermal resistance and capacity are the spruce-pine-fir (SPF) ones, [1].

Table 4.4: SPF data

Thermal conductivity	0.12	W/m ² K
Specific heat capacity	1380	J/kgK

The resulting parameters values to be introduced in 4.3 are:

$$\begin{aligned}
 C_{fu} & 2.17 \text{ MJ/K}; \\
 R_{fu} & 0.0093 \text{ K/W}; \\
 f_{fu} & 0.2421;
 \end{aligned}$$

4.3 Low mass surfaces and infiltration loss

Low mass and infiltration loss contributions have been considered as a direct heat exchange with the outdoor environment as follow:

$$\begin{aligned}
 \dot{Q}_{inf} &= \frac{T_{in} - T_{out}}{R_{inf}} \\
 R_{inf} &= \frac{1}{\frac{vol_c \cdot V_{air} \cdot \rho_{air} \cdot c_{p_{air}}}{3600} + U_w \cdot a_w + U_p \cdot a_p}
 \end{aligned}$$

The air specific heat capacity value is derived from [2].

Chapter 5

Ep model

EnergyPlus is an energy and thermal load simulation tool which is used when dealing with building energy environment, from sizing plant to retrofit studies as well as optimizing energy performances. EnergyPlus has been chosen to validate the model through a inter-model results comparison in order to provide a consistent baseline, [18]. In the following some of the features chosen to implement the Ep model are listed and commented. They are reported in the same order they are found in the Ep IDF Class List.

5.1 Simulation parameter

Building In this section, the model chosen for the solar is the FullExterior. With this model, the program calculates the amount of beam radiation through glazing surfaces which is supposed to fall on the floor and absorbed according to the floor solar absorptance. Any reflected contribution is added to the diffuse radiation which is uniformly distributed on all interior surfaces.

Surface convection algorithm chosen for the Ep model are Simple and Simple-Combined respectively for the Inside and Outside environment. These options consider a constant heat transfer coefficient which depend on the surface orientation for the Inside environment and on the surface roughness and wind speed for the Outside environment. Moreover, for the outer side, also the radiation exchange with sky, ground and air is considered.

Heat balance algorithm Conduction transfer algorithm has been chosen. This selection considers only the sensible heat solution and does not take into account moisture storage or diffusion in the construction elements.

5.2 Location and Climate

Site location Bologna, 44,5 N 11,33 E

Run period Simulation for the all year. The only option deselected is the Apply Weekend and Holiday Rule.

5.3 Surface construction element

Material All materials are described according to the data presented in the previous chapters. Exception is the description of the floor and ceiling slabs because the only data available were the transmittance and the surface specific capacity of the slab. The trick adopted is to consider an homogeneous layer which thickness is 0.4 [m] and density of 1800 [kg/m³] in order to obtain the same overall values given by [10]. The portion of slab considered for the ceiling and floor respectively is the same as in the Simulink model. In other words, not the overall slab is considered for both the horizontal layers, but only the portion between the indoor environment and the null heat flow plane. The position of the null heat flow plane, thus the portion of slab considered, is the same of the Simulink model.

5.4 Thermal zone and surfaces

Internal wall surfaces The internal wall overall surface is modelled as through the internal mass object.

Windows Glazing surfaces are modelled per orientation. On each different oriented outside wall the glazing surface in the Ep model is equal to the sum of the glazing surfaces located on the respective outside wall.

5.5 Zone Airflow

Zone Infiltration:Design flow rate The infiltration contribution is modelled through the AirChanges/Hour method. The Air changes per Hour value is set to 0.3 and the associated schedule makes it constant during the all run period, thus during the year.

Chapter 6

Results comparison

In this chapter the results of the comparison between the Simulink model and the Ep one are summarized. The comparison between the whole model will be firstly presented, following with relevant results of the investigation carried out in order to get a better understanding of the mismatch between the two models. The results reported can be summarized as the absolute value and difference between the Matlab-Simulink and the Ep value of the following variables:

- Indoor air temperature;
- Surfaces temperature;
- Heat flux exchanged between the surfaces and the environment;
- Difference between the overall indoor heat flux of the two models.

When dealing with a surface heat flux, positive value is considered when entering the surface; negative otherwise. Dealing with the overall indoor heat flux, instead, is positive when entering the indoor air; negative otherwise.

Except for the first and second section, where all the results are shown, in the following only the indoor temperature and the section specific result will be presented. The others are reported in the appendix.

In order to observe more clearly the behaviour of the model during the different seasons, a zoom of the indoor temperature path during a reference winter, spring (middle season) and summer week will be done. The reference weeks chosen are the ones starting on the 21st of January and July respectively for the winter and summer conditions. For the middle season, the weeks starting on the 21st of April and October presents a similar path, but the spring condition has been chosen because of the less predictable path of the temperature during the week.

6.1 All-in

As the name suggests, this model takes into account all the aspects described in Chapter 2. The outdoor air temperature and solar radiation input values are taken from the following output variables in the Ep model, for an yearly simulation period:

- Site Outdoor Air Dry Bulb Temperature;
- Surface Outside Face Solar Radiation Rate per Area;

The Ep output variables used to compare the results between the models are:

- Zone air temperature;

- Surface Inside Face Temperature;
- Surface Inside and Outside Convection Heat Gain Energy. The last one only for the external wall;
- Zone Infiltration Sensible Heat Gain Energy.

The Ep heat gain variables are hourly given, so that they are compared with the hourly sampled heat flux from the Matlab-Simulin model.

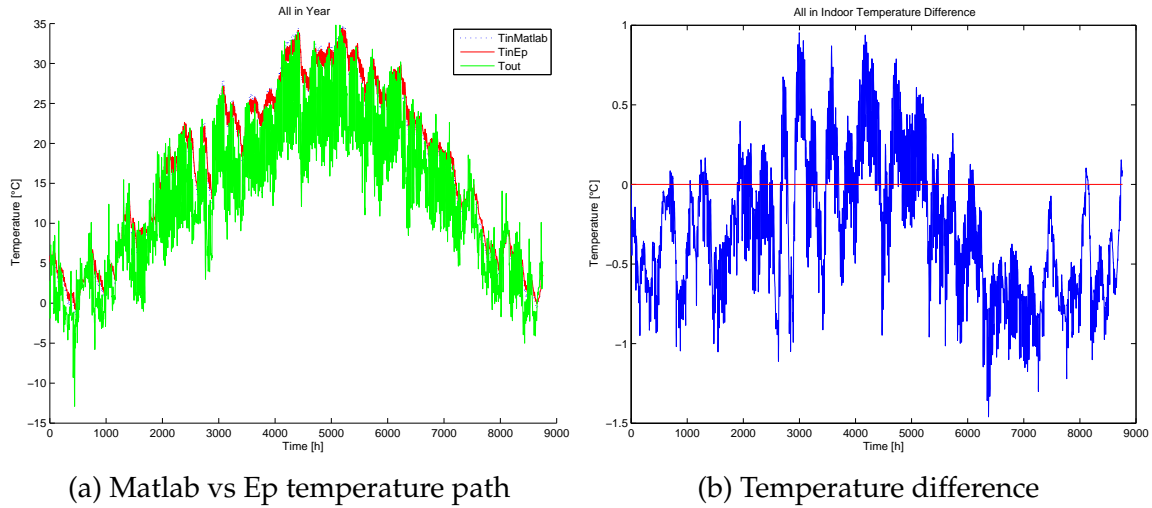


Figure 6.1: All-in indoor temperature

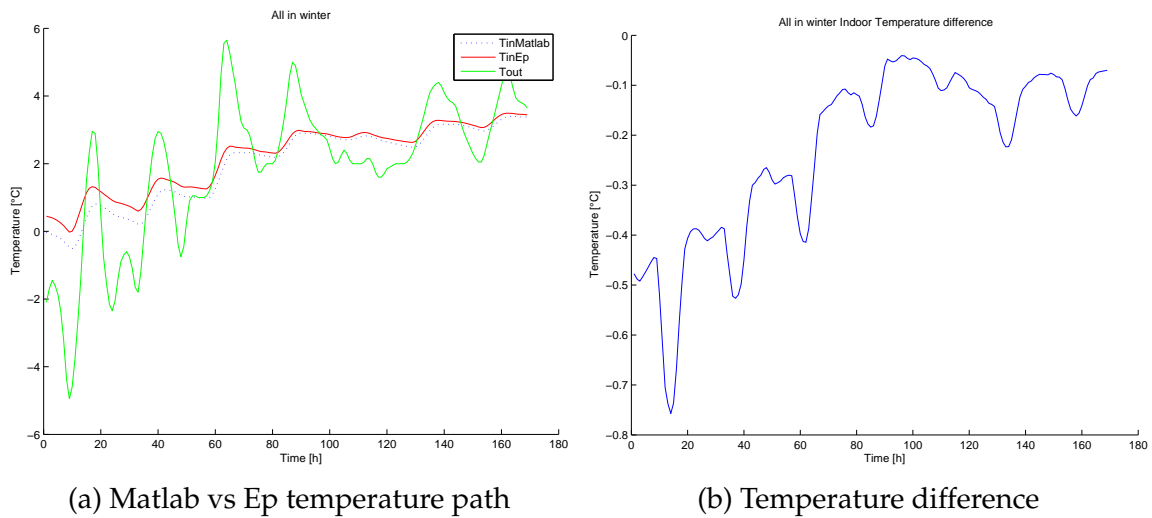


Figure 6.2: All-in winter indoor temperature

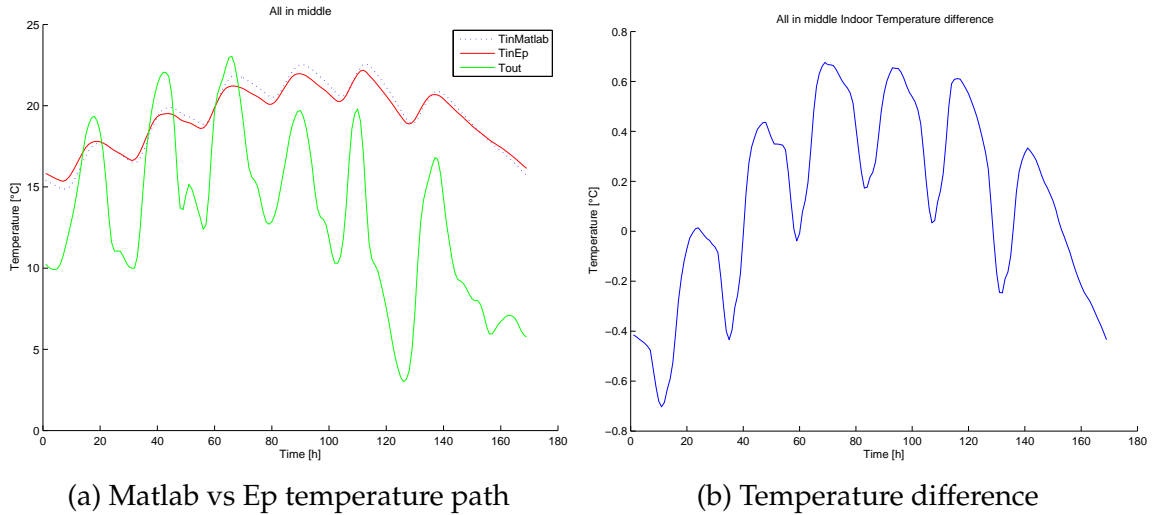


Figure 6.3: All-in spring indoor temperature

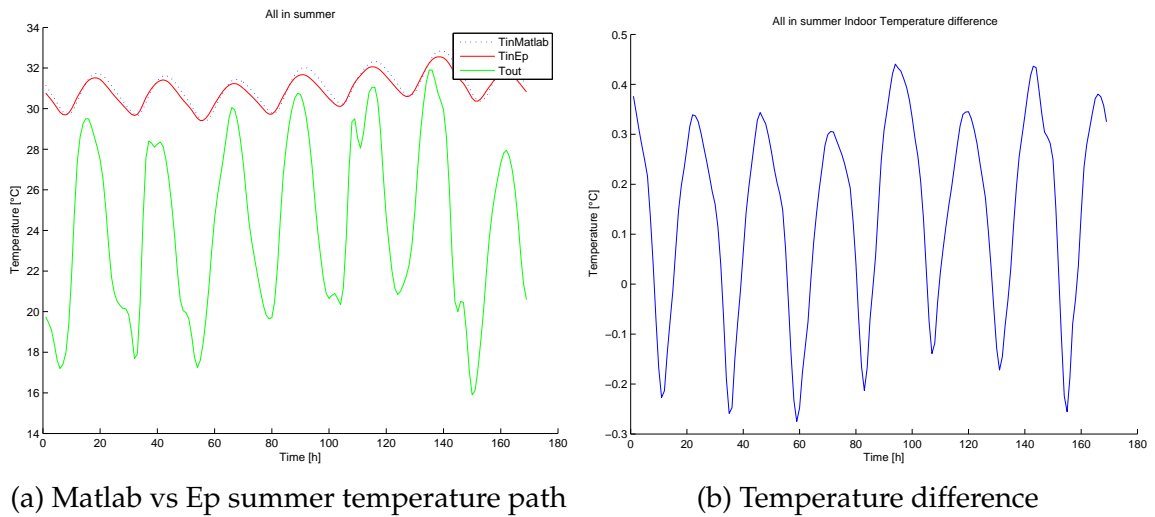


Figure 6.4: All-in summer indoor temperature

From Fig. 6.5, for the external wall temperature a similar path can be observed in the two models. The same cannot be stated for the heat fluxes of the outdoor and indoor side. As it will be seen from the following figures, a difference between the heat fluxes of the two models can always be observed which can be probably addressed to the different surface model of in the Ep environment. Here, the surfaces are model through a 3R2C circuit. However, dealing with the external wall, a greater difference results can be observed in Fig.6.6 and Fig. 6.7 which show respectively the outdoor and indoor side convection heat fluxes. The following evaluations can be stated:

- The 2R1C circuit and the respective way to compute the wall parameters, make the surface 'more accessible' from the inner side. In other words, the outer resistance value is much greater compared to the inner one. Thus, the external wall temperature trend in the Matlab-Simulink model has is similar to the Ep one since that the Inner Surface Temperature is reported;

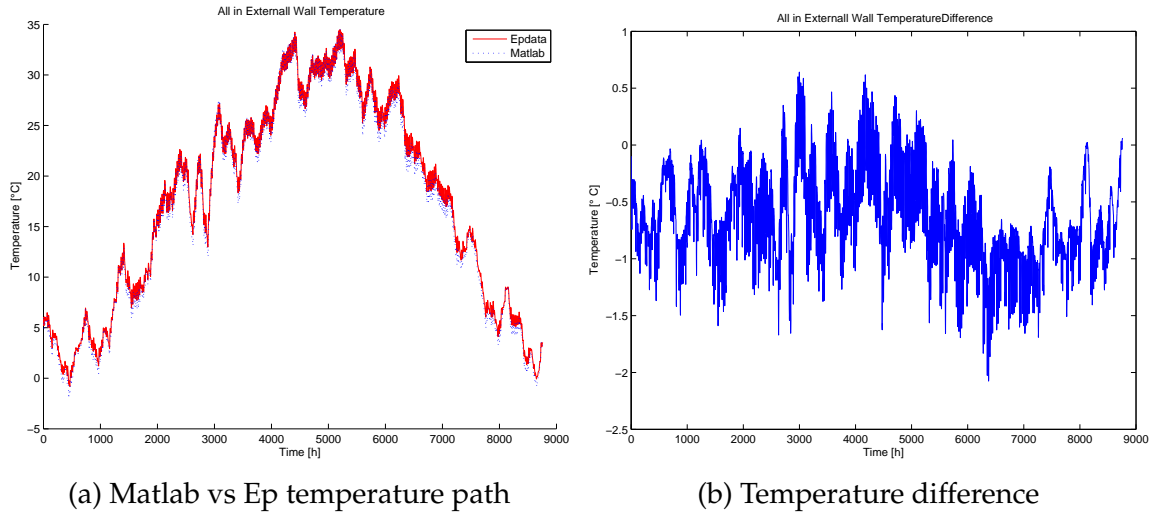


Figure 6.5: All-in external-wall temperature

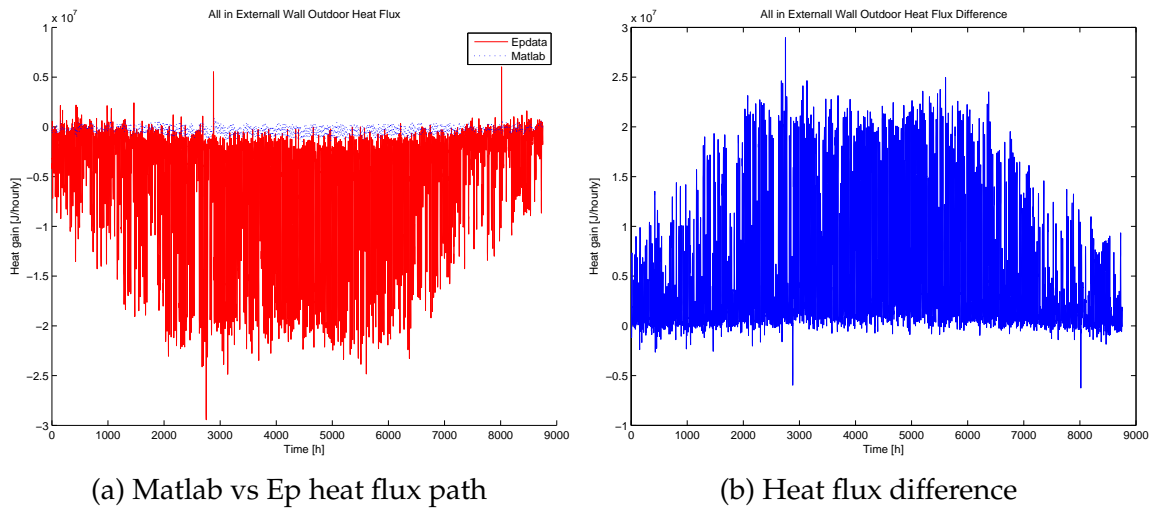


Figure 6.6: All-in external-wall outdoor side heat flux

- Due to the wall parameter computation in the Matlab-Simulink environment, the resistances of the wall take into account also the conduction resistance through the surface, so the heat flux value is calculated through the outer resistance value. In the Ep case, instead, the heat flux considers only the convective heat flux, e.g. only the resistance due to convection, on the outer surface.

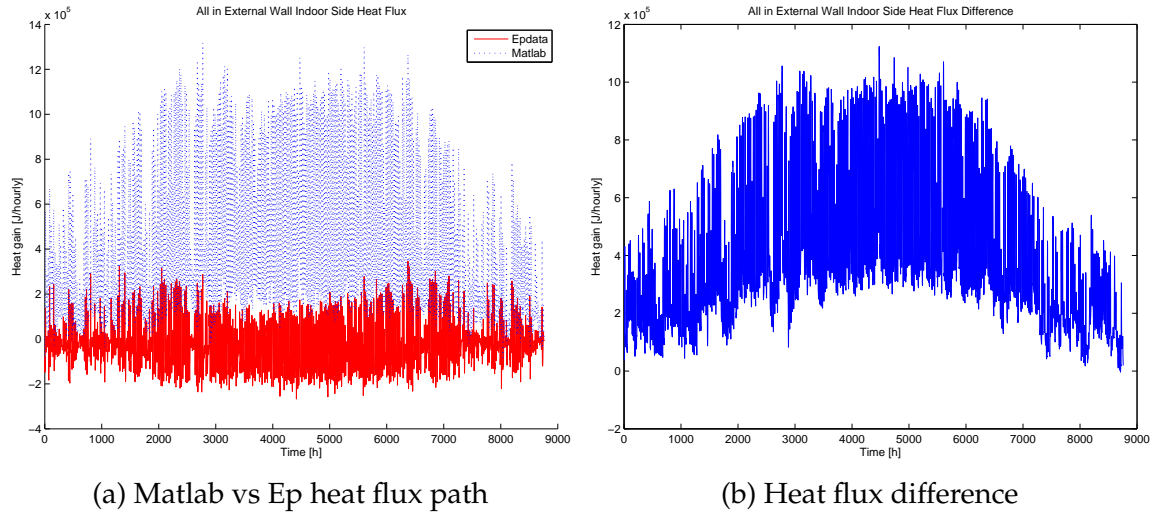


Figure 6.7: All-in external-wall indoor side heat flux

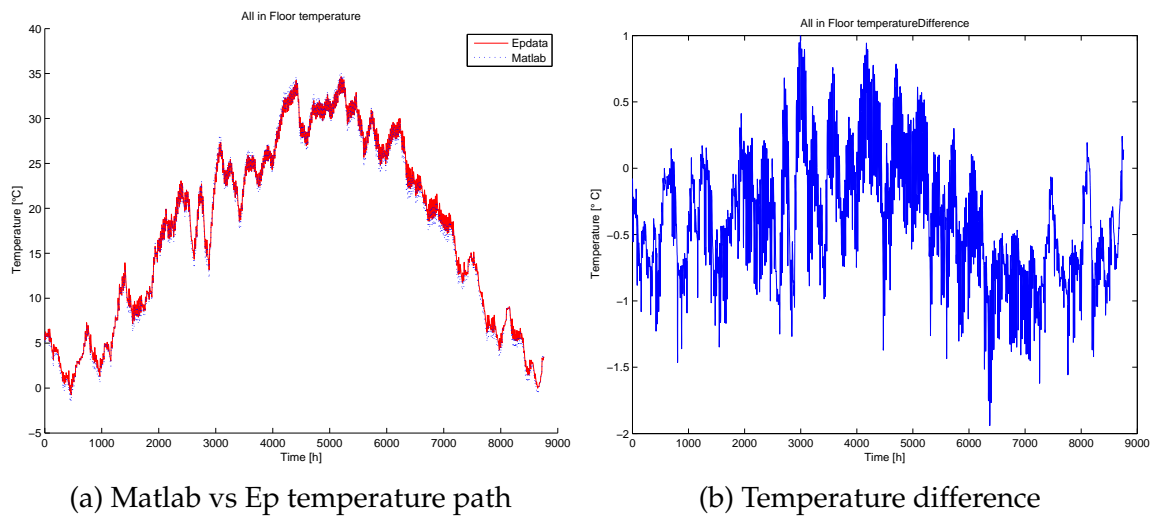


Figure 6.8: All-in floor temperature

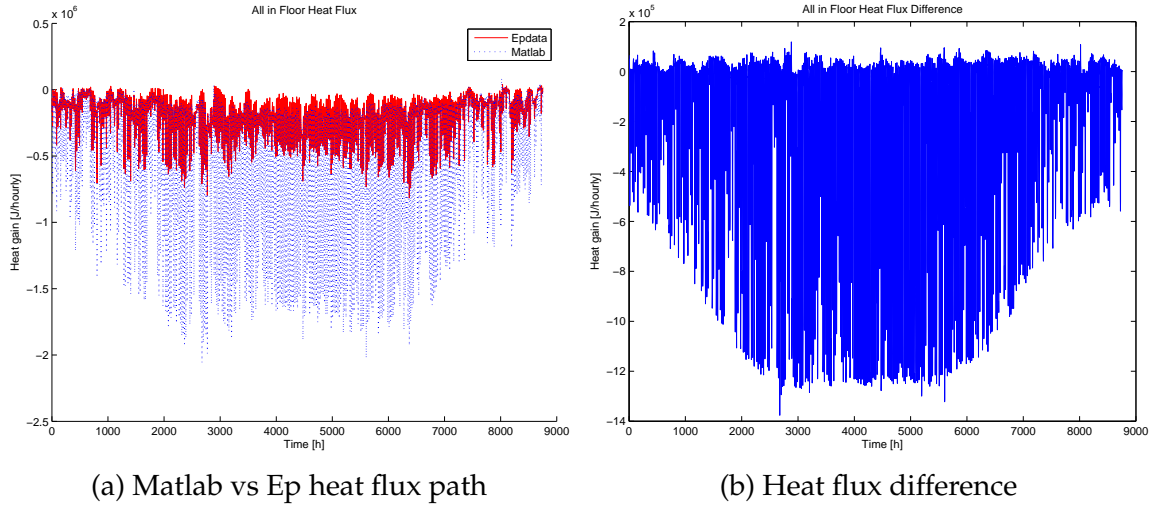


Figure 6.9: All-in floor heat flux

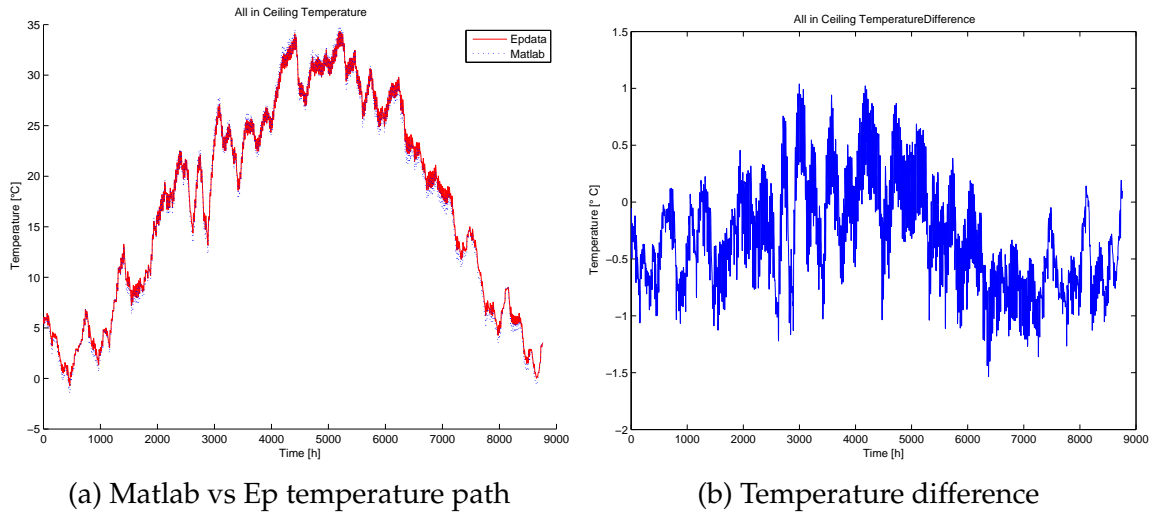


Figure 6.10: All-in ceiling temperature

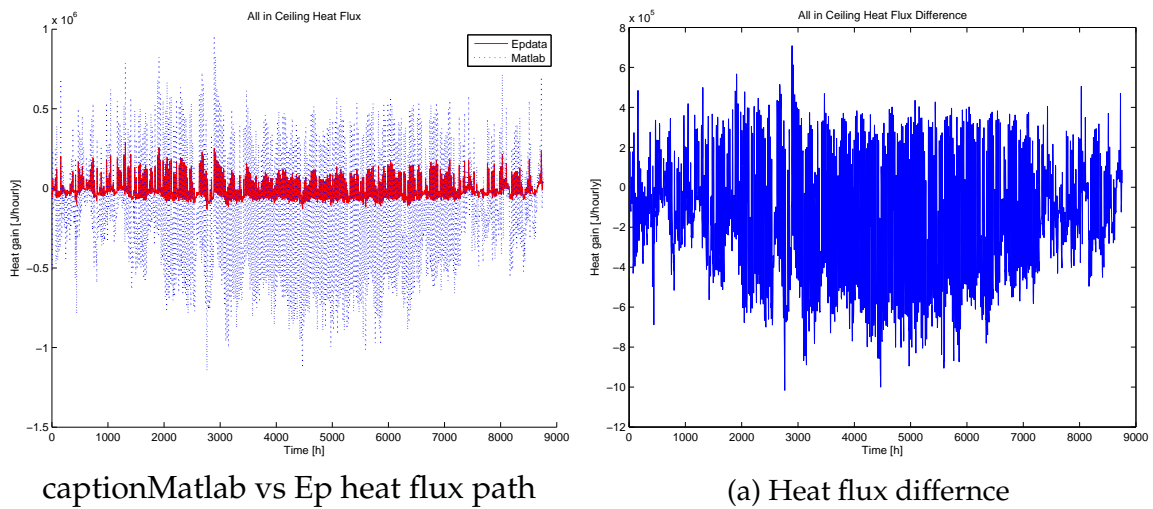
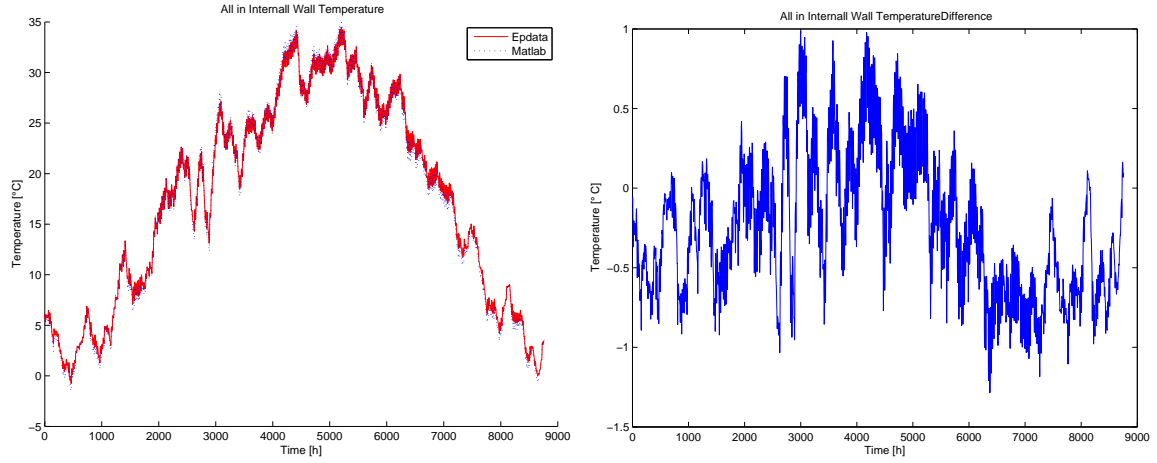


Figure 6.11: All-in ceiling heat flux



(a) Matlab vs Ep temperature path

(b) Yearly temperature difference

Figure 6.12: All-in internal wall temperature

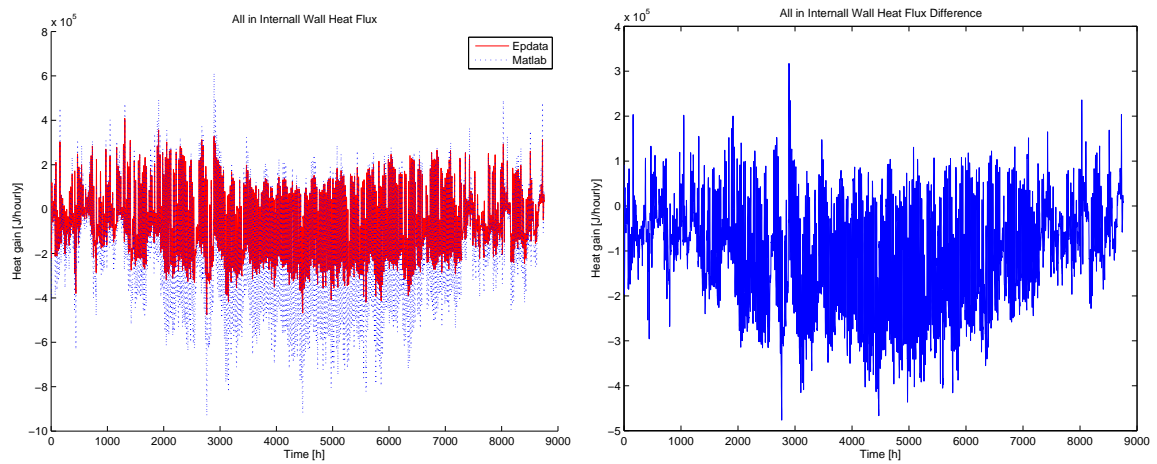


Figure 6.13: Internal wall heat flux

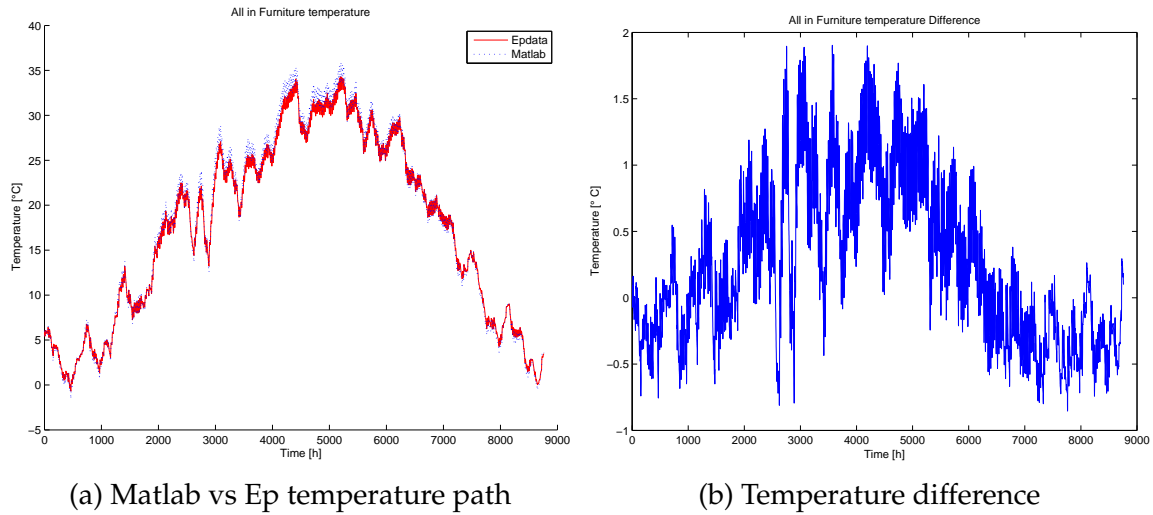


Figure 6.14: All-in furniture temperature

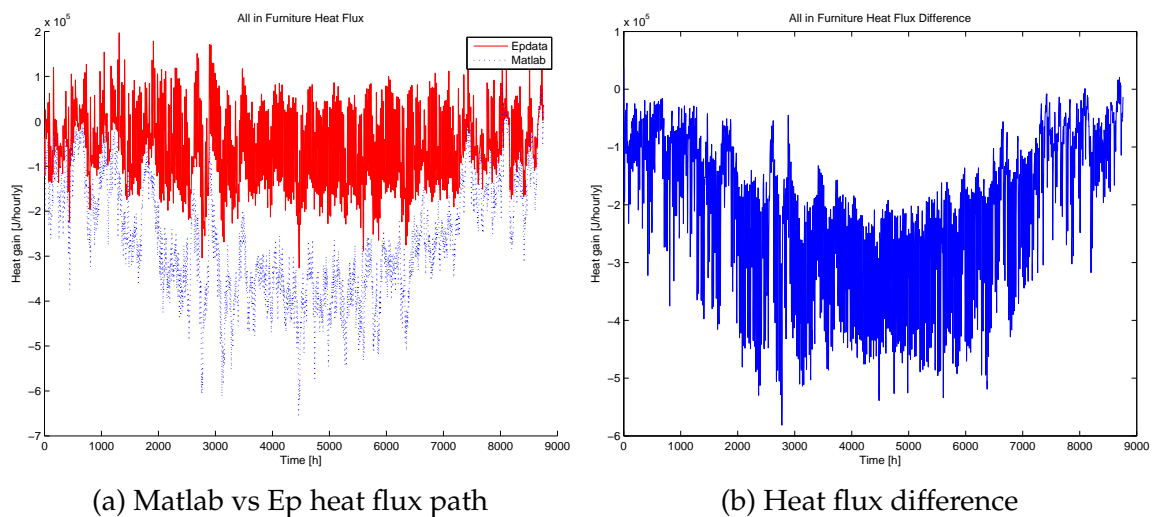


Figure 6.15: All-in furniture heat flux

As Fig.6.15 shows, a difference can be observed in the furniture heat flux. This is to be addressed to the way the beam solar radiation is spread inside the considered space. While in the Ep it is considered as falling on the floor, in the Matlab-Simulink environment it is considered as shared among the internal surfaces (i.e internal wall, furniture, floor and ceiling) through the solar absorptance-weighted method. The sun effect can be observed, in the Matlab-Simulink results, in all the internal surfaces since the heat flux from each indoor surface to the indoor environment present an increasing trend during the major radiation period, i.e. the central part of the simulation which represents the middle season and summer time. This effect is more evident for the floor and furniture surfaces because, depending on their distribution factor, they receive respectively the 42 % and 24 % of the solar radiation entering the environment.

Fig. 6.16 show the accordance between the infiltration trends, where the difference is likely due to the temperature difference between the two models.

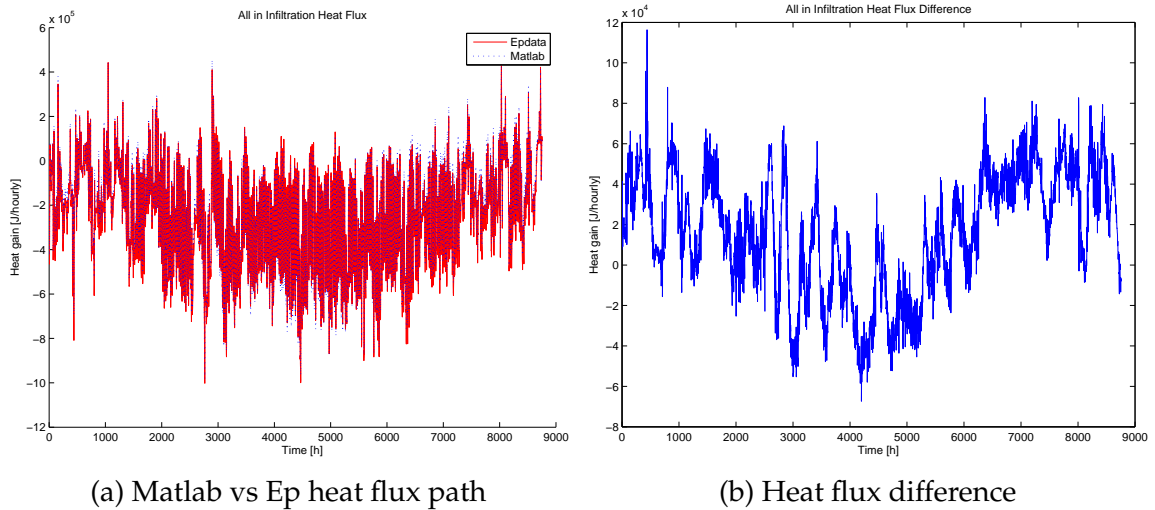


Figure 6.16: All-in infiltration heat flux

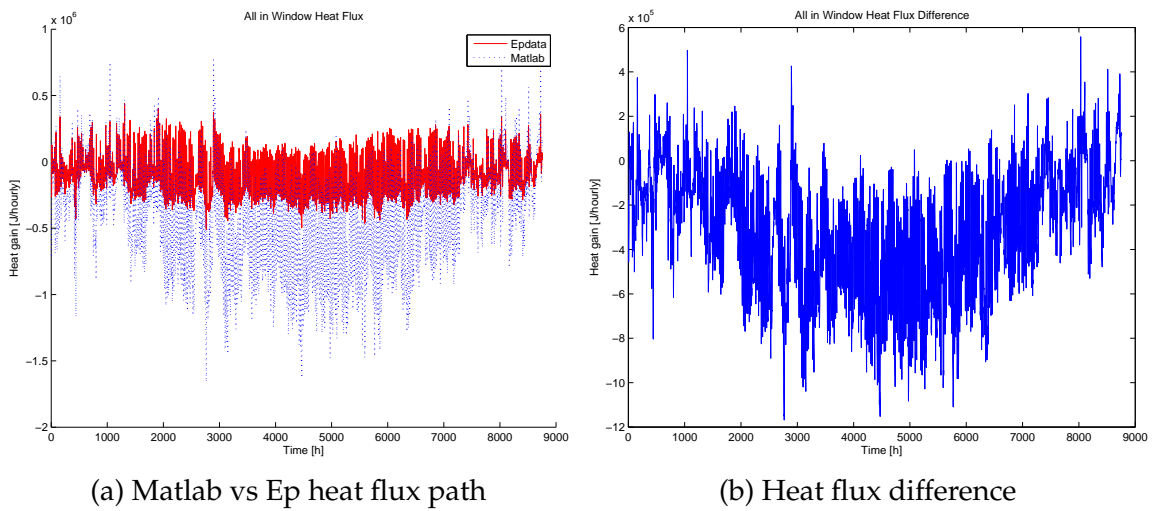


Figure 6.17: All-in window heat flux

The same cannot be stated for the window heat flux, Fig. 6.17. This probably because the Ep data refers to the inside face convection heat flux, making us assume the window model is a component with thermal mass even if the way it has been modeled, i.e. Simple Glazing System, should not be considered this way, [?]. In the Matlab-Simulink environment, instead, it is assumed as a simple resistive component, neglecting the window thermal mass.

Fig. 6.18 shows the accordance between the Overall Indoor Heat Flux of the two models. It can be stated that the difference between the two trends is related to the temperature difference of the two models.

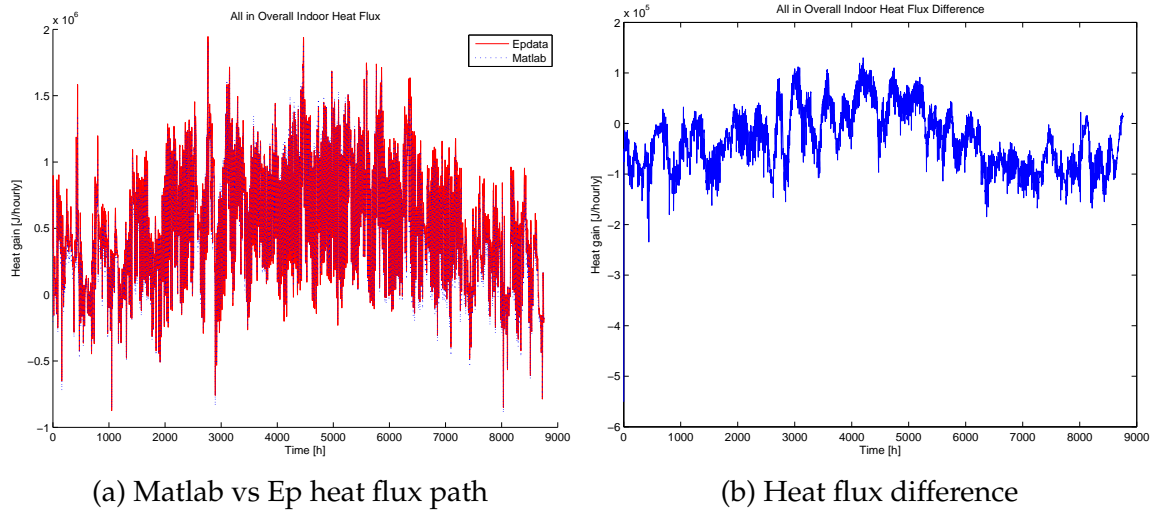


Figure 6.18: Overall indoor heat flux

6.2 Base

The Base model is comprehensive of external wall, floor slabs and internal walls. This 'bunker' choice has been made because is the simpler model that can be compared in the Ep.

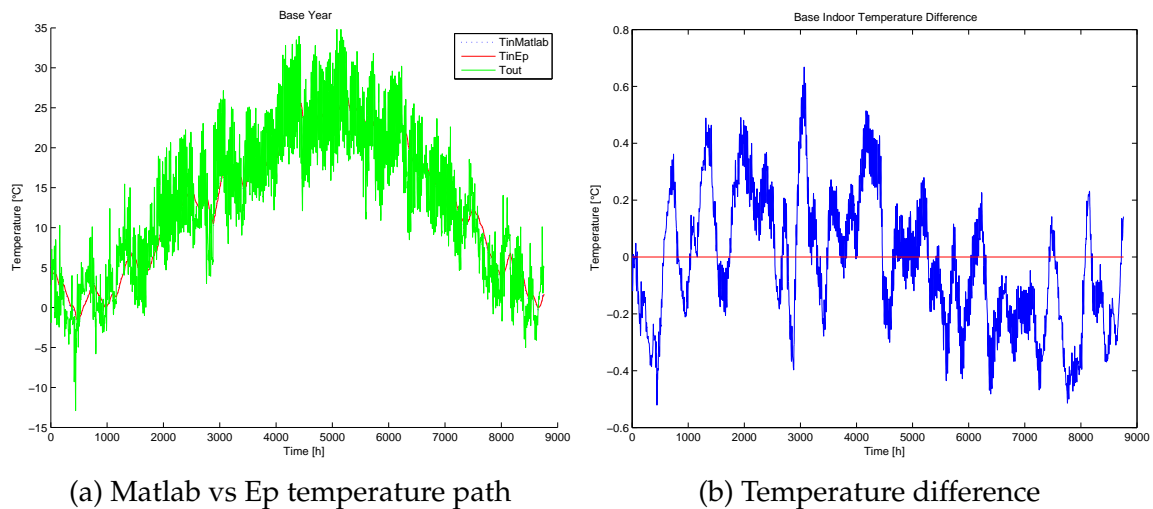


Figure 6.19: Base indoor temperature

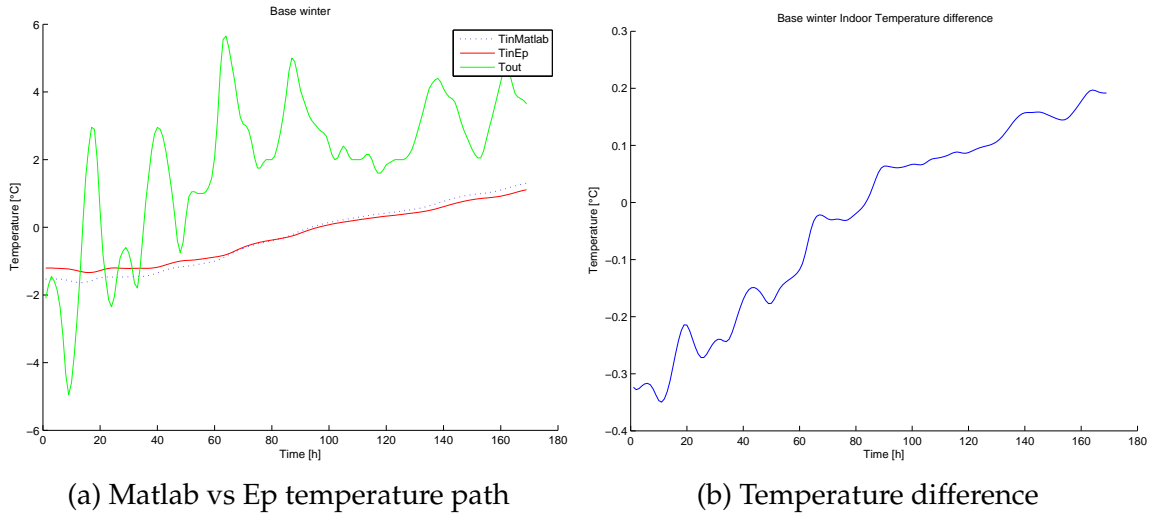


Figure 6.20: Base winter indoor temperature

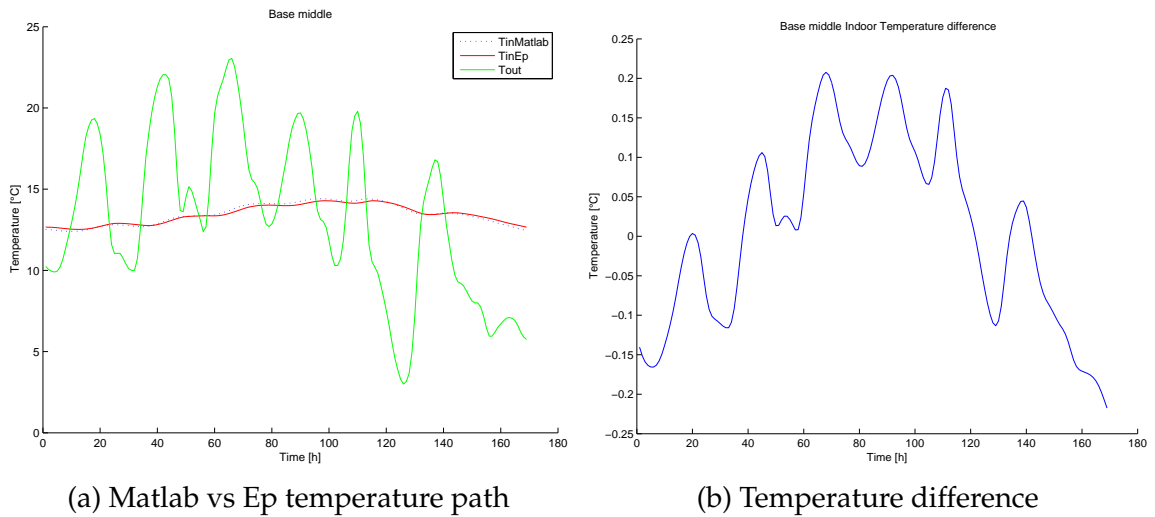


Figure 6.21: Base spring indoor temperature

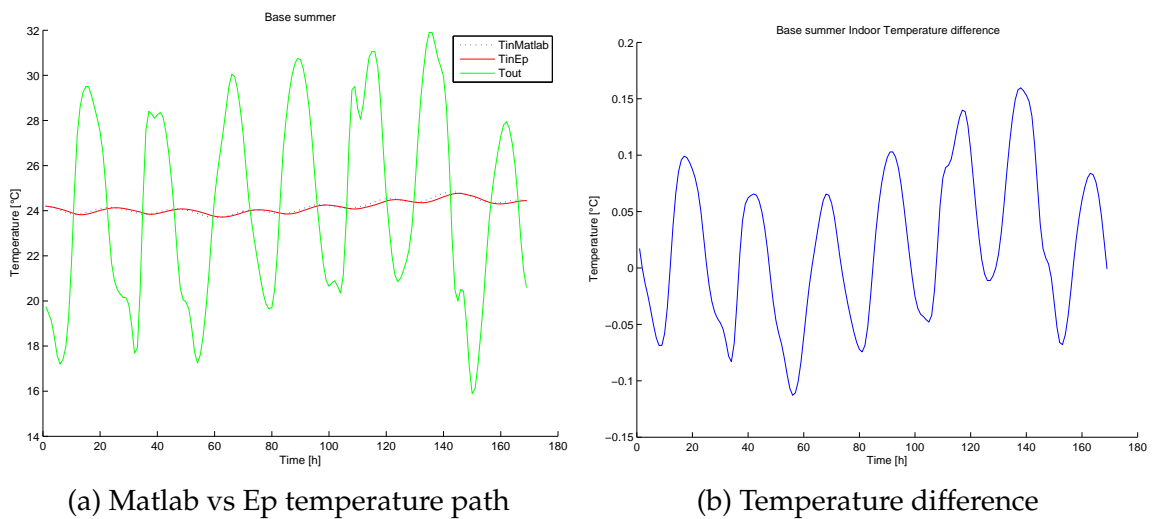


Figure 6.22: Base summer indoor temperature

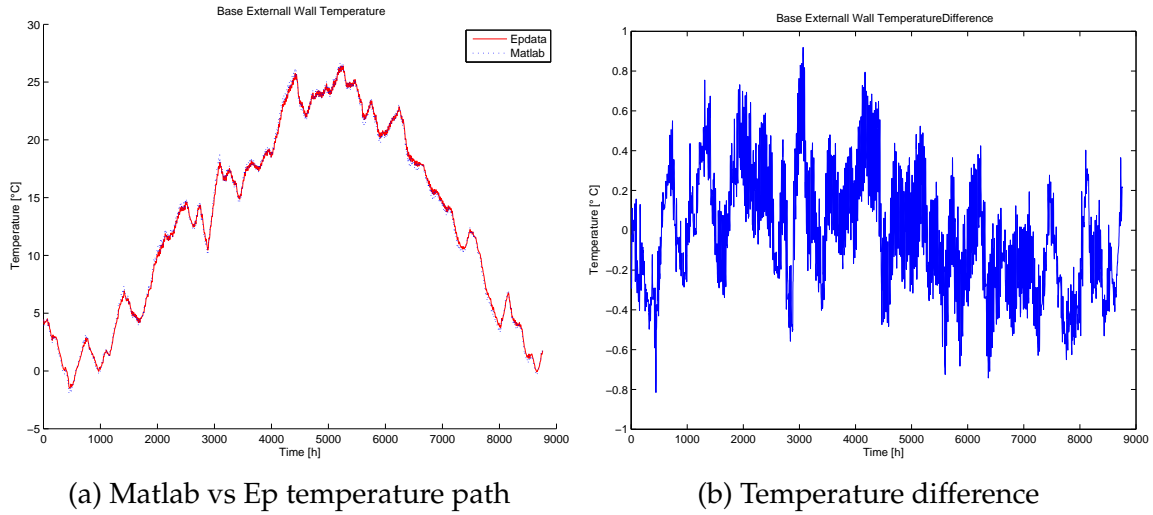


Figure 6.23: Base external-wall temperature

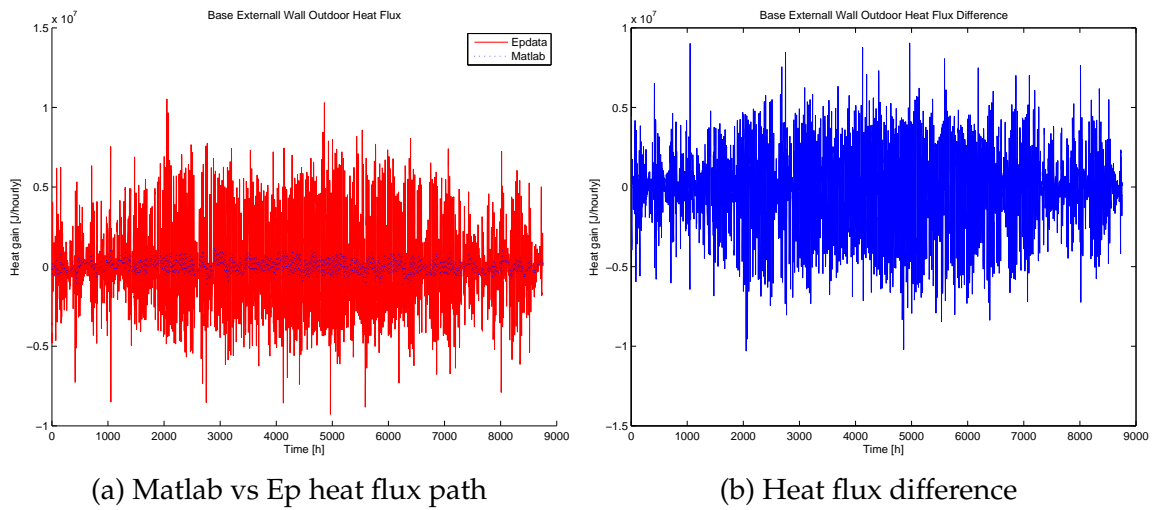


Figure 6.24: Base external-wall outdoor side heat flux

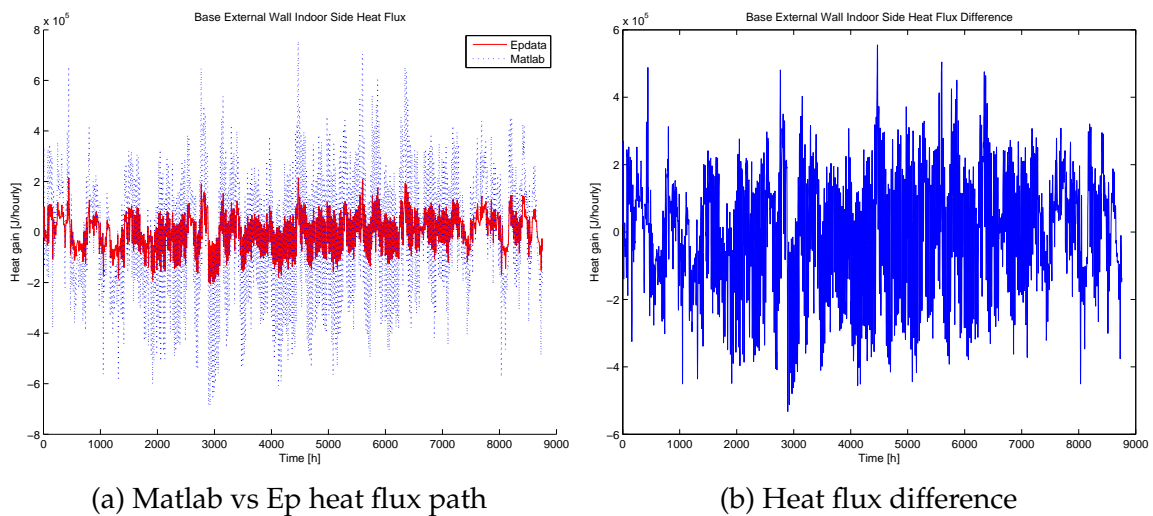
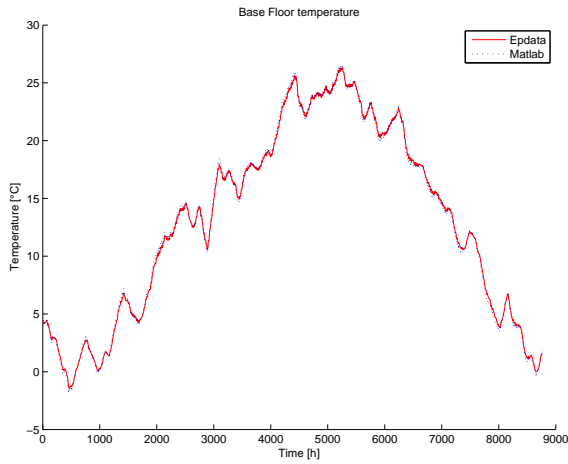
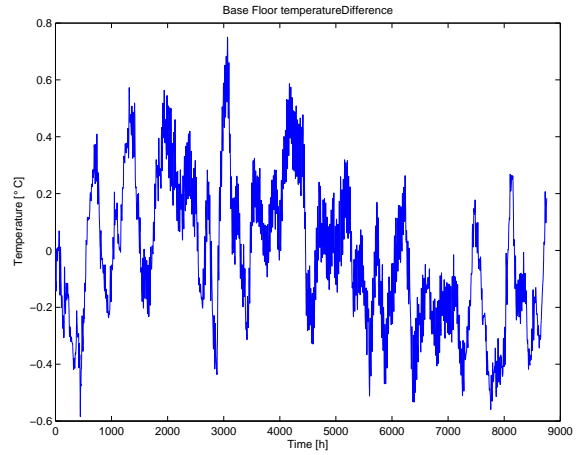


Figure 6.25: Base external-wall indoor side heat flux

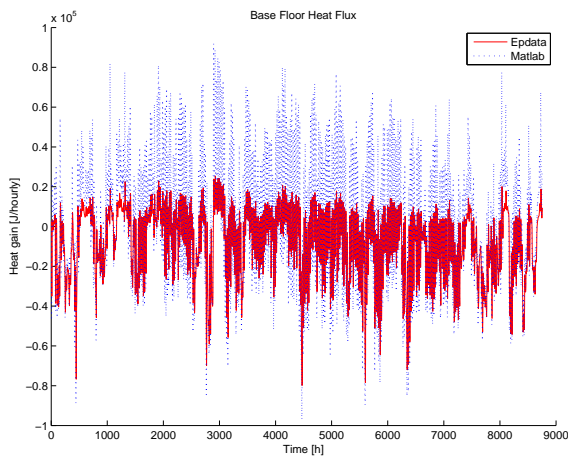


(a) Matlab vs Ep temperature path

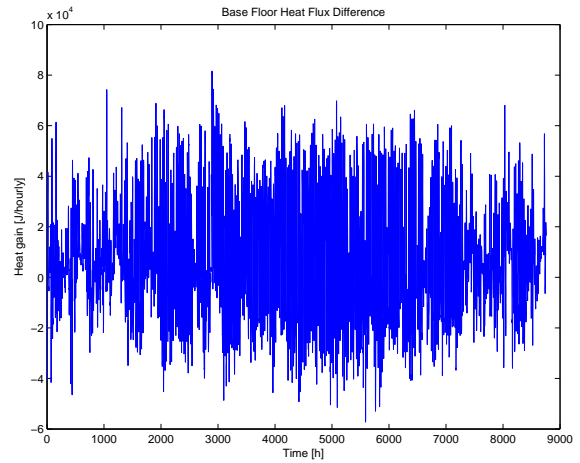


(b) Temperature difference

Figure 6.26: Base floor temperature

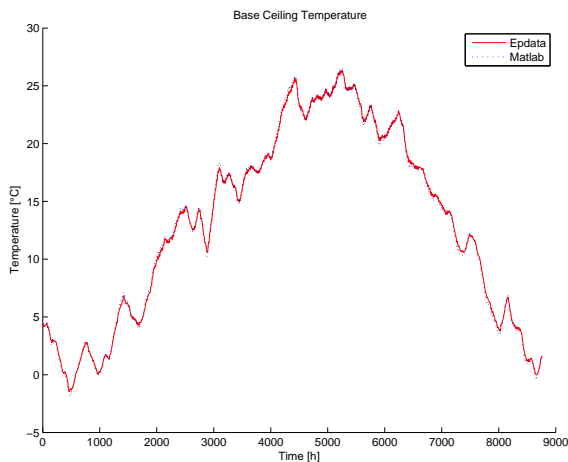


(a) Matlab vs Ep heat flux path

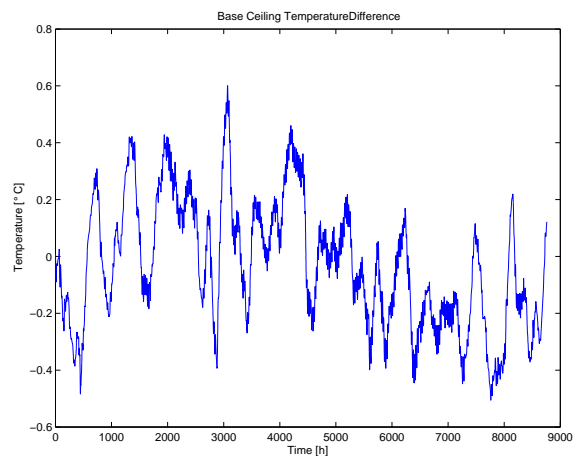


(b) Heat flux difference

Figure 6.27: Base floor heat flux



(a) Matlab vs Ep temperature path



(b) Temperature difference

Figure 6.28: Base ceiling temperature

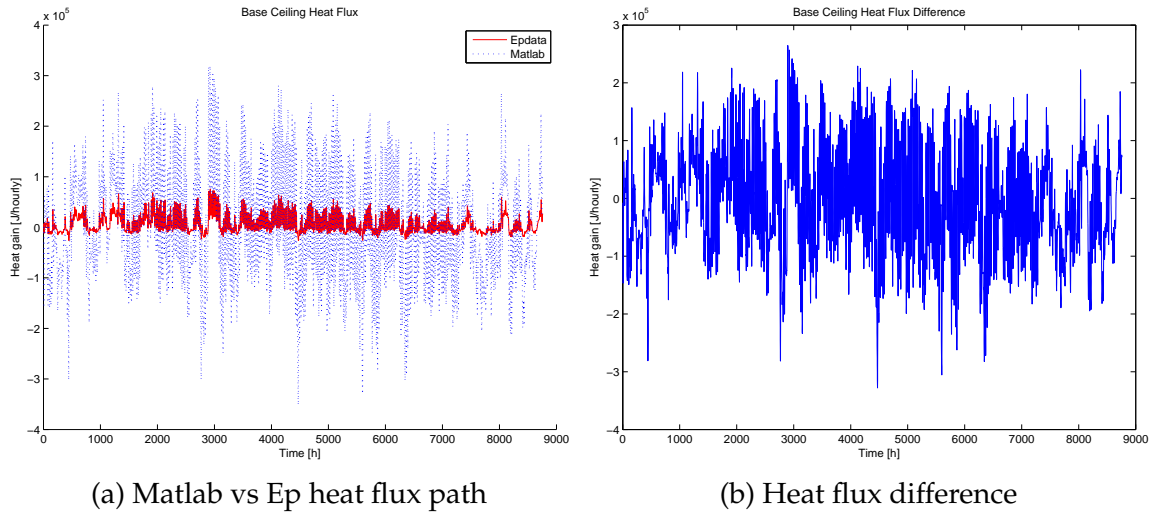


Figure 6.29: Base ceiling heat flux

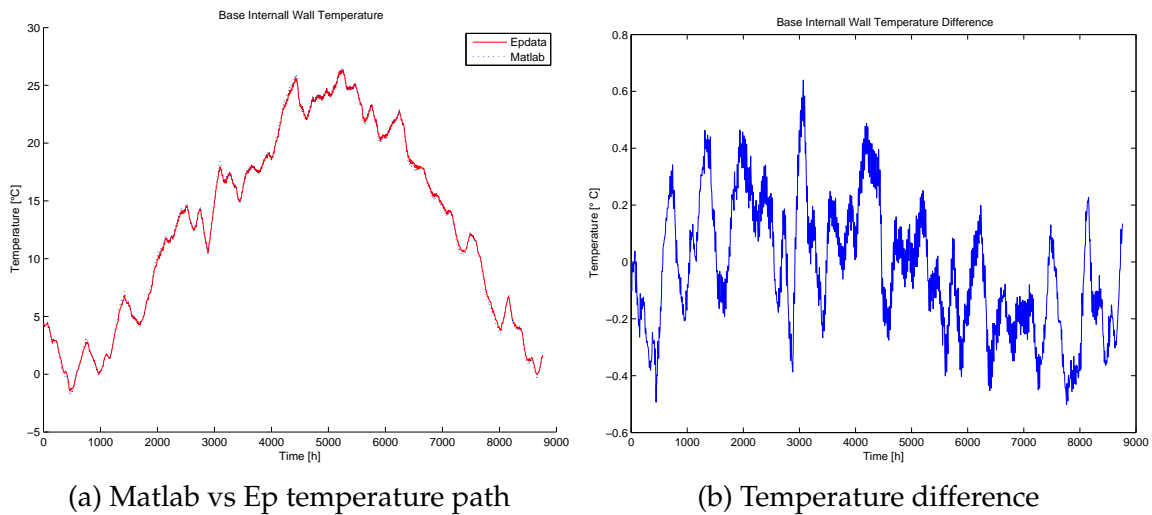


Figure 6.30: Base internal wall temperature

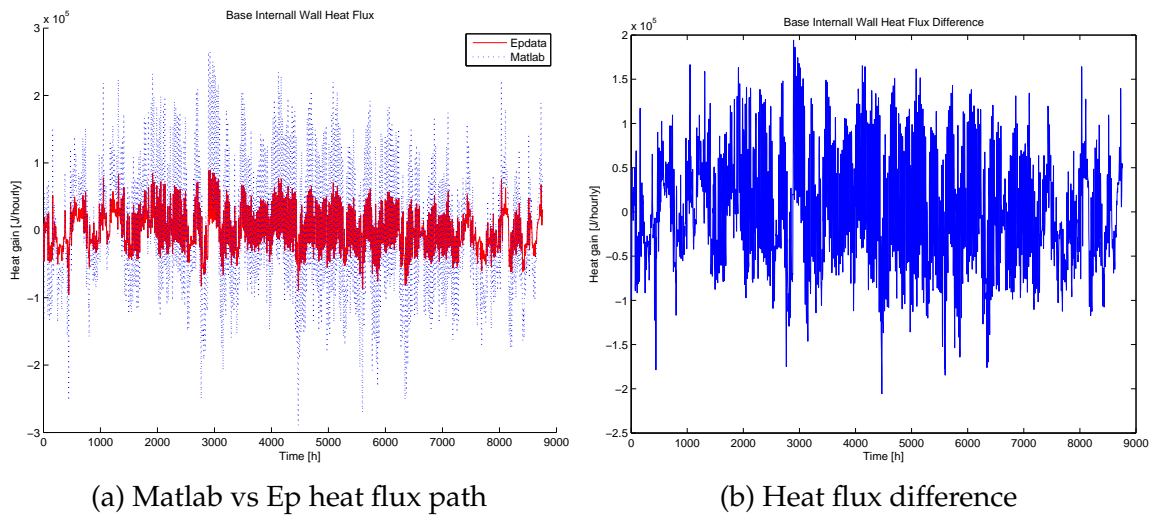


Figure 6.31: Internal wall heat flux

Figs. 6.19-6.20-6.21-6.22 show the temperature trends of the indoor temperature between the two models. The Matlab-Simulink temperature trend slightly leads, 3 hours, the Ep model one.

Figs. 6.23-6.26 - 6.28 -6.30 show the surface temperature paths accordance between the two models of the external wall, floor, ceiling and internal wall respectively. The indoor surfaces temperature difference trend between the two models is similar to the indoor temperature one.

Figs. 6.24-6.25 show the external wall heat flux respectively on the outer and inner side, with the notes of the previous section.

Figs. 6.27-6.29-6.31 show the heat flux comparison of the floor, ceiling and internal wall respectively. The Matlab-Simulink result value is quite different from the Ep one in very case.

6.3 Infiltration

The Infiltration model is obtained from the Base case by adding the effect of infiltration and ventilation as reporter in Chapter 4. Fig. 6.36 shows the accordance between the infiltration heat flux in the two model. The difference can be addressed to the temperature difference between the two models, which can be observed in Fig. 6.32-6.33-6.34-6.35.

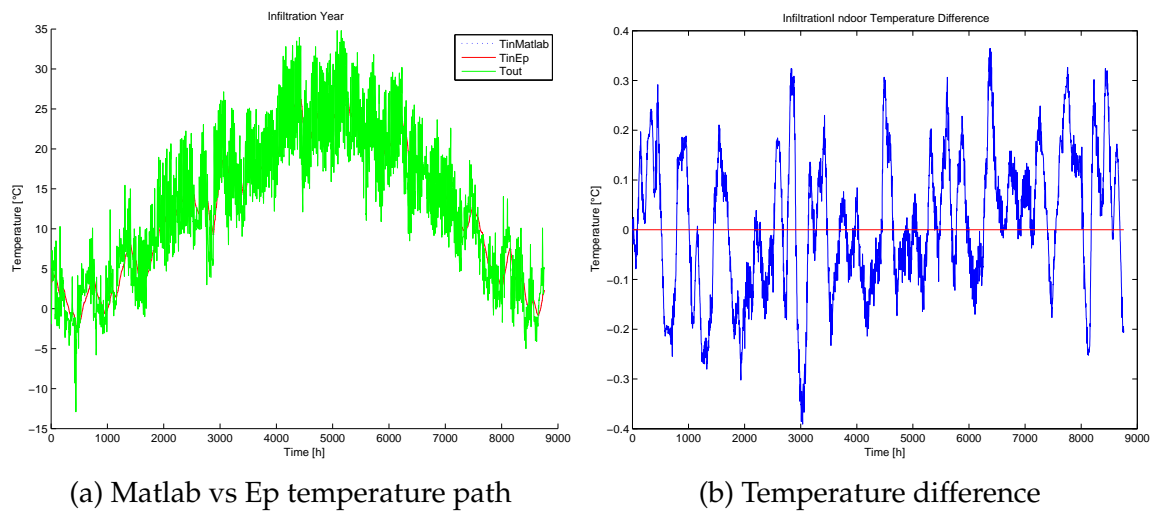


Figure 6.32: Infiltration indoor temperature

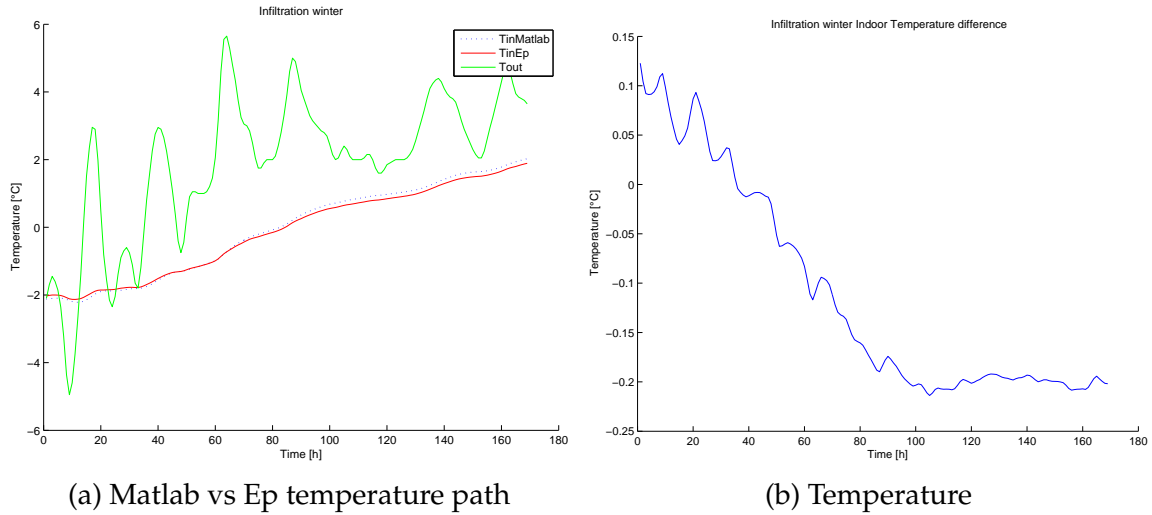


Figure 6.33: Infiltration winter indoor temperature

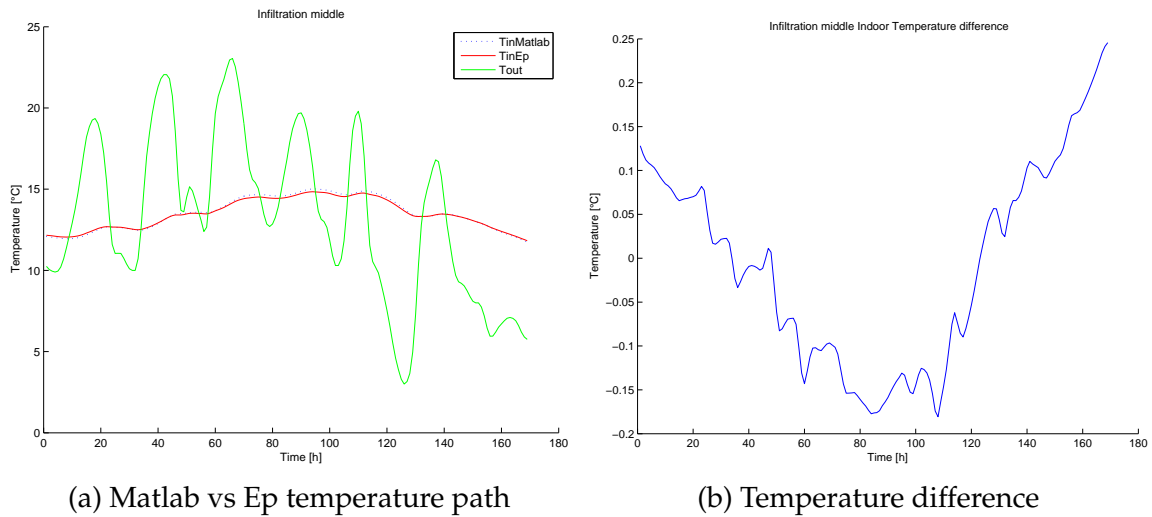


Figure 6.34: Infiltration spring indoor temperature

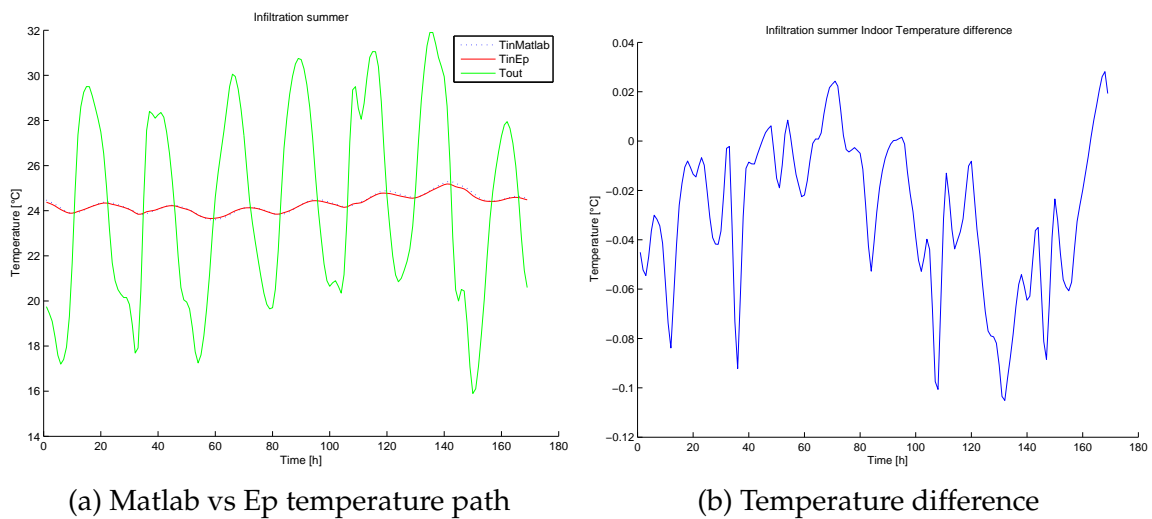
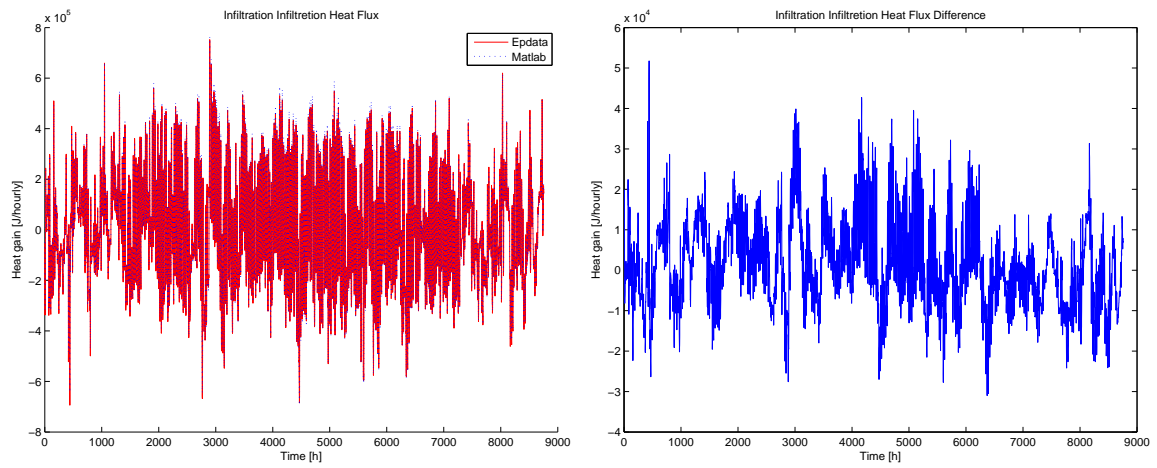


Figure 6.35: Infiltration summer indoor temperature



(a) Matlab vs Ep heat flux path

(b) Heat flux difference

Figure 6.36: Infiltration heat flux

6.4 Windows

In this section the heat conduction through the low mass envelope surfaces, i.e. windows and door, is inspected.

As showed clearly from Fig. 6.37, a positive difference between the Matlab-Simulink temperature and the Ep one stands during the all year.

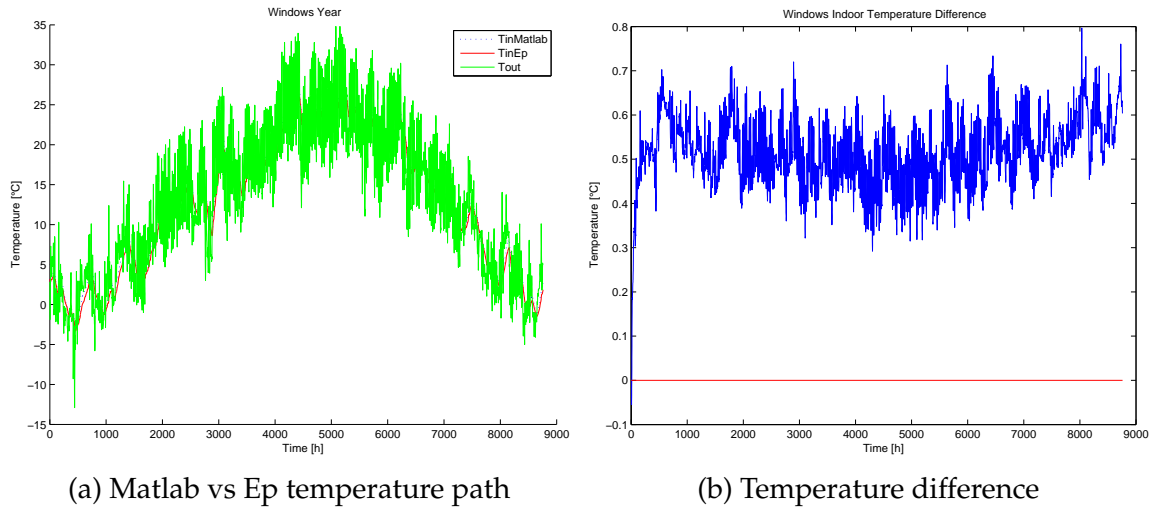


Figure 6.37: Windows indoor temperature

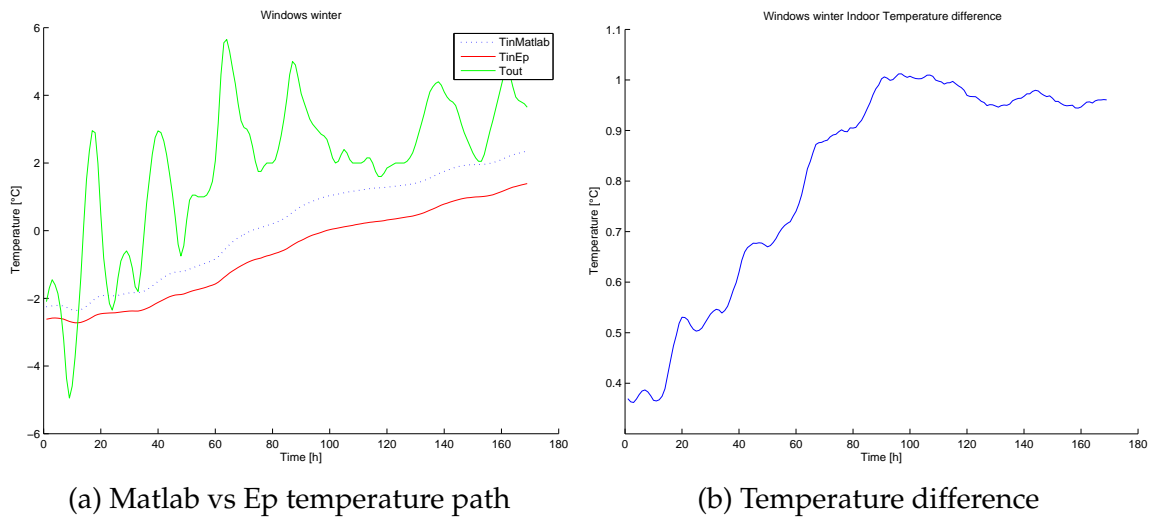


Figure 6.38: Windows winter indoor temperature

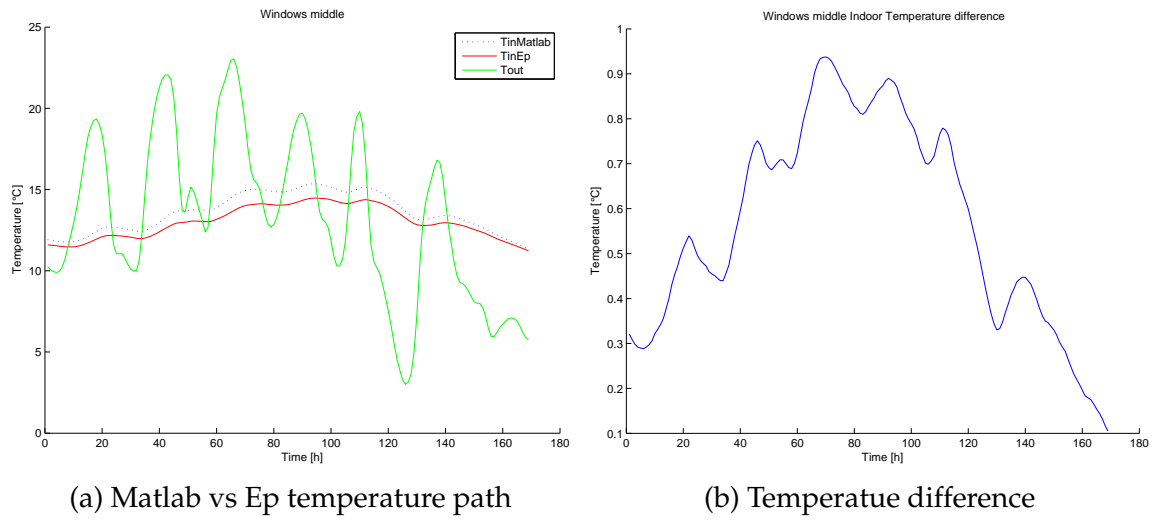


Figure 6.39: Windows spring indoor temperature

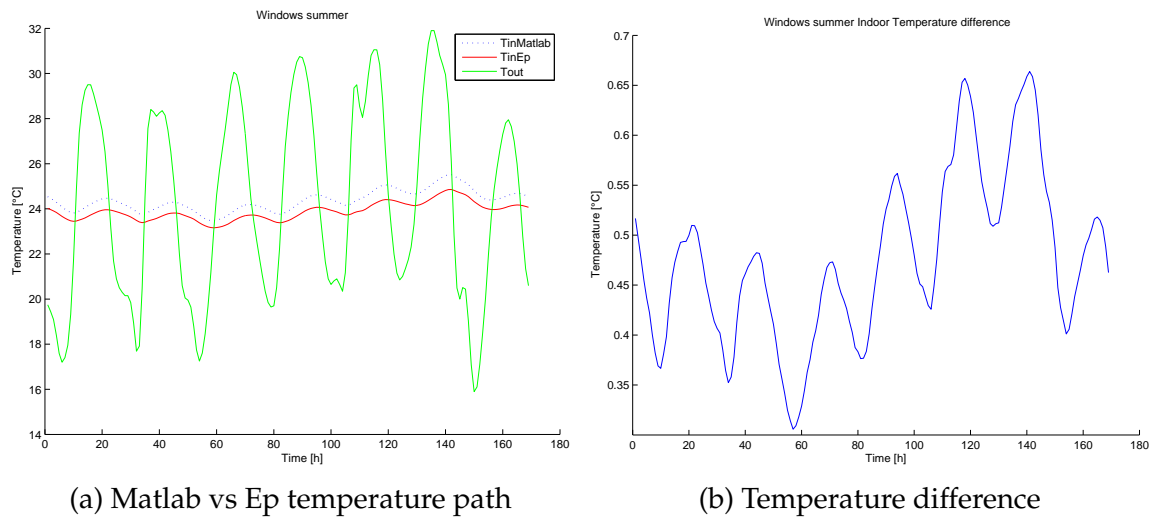
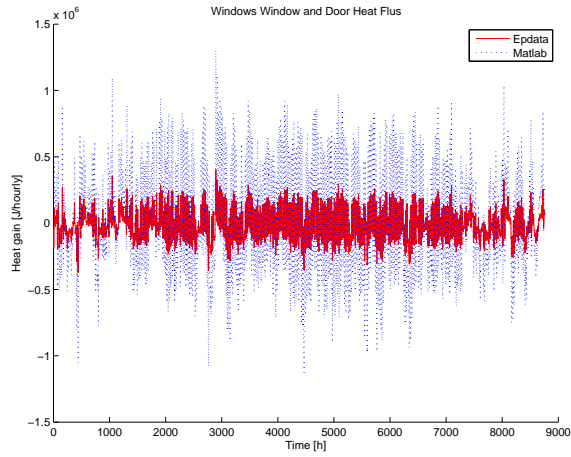
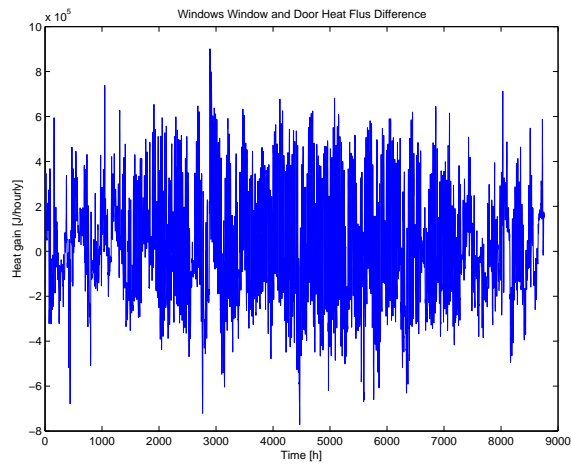


Figure 6.40: Windows summer indoor temperature



(a) Matlab vs Ep heat flux path



(b) Heat flux difference

Figure 6.41: Windows low-mass surfaces heat flux

title

In order to better understand why some discrepancies rise between the two models while adding the low mass envelope surfaces contributions, the evolution of the indoor temperature from the Base model to the Window model for both the Energy Plus and the Simulink model has been inspected. It can be observed respectively in Fig. 6.42 and fig. 6.43.

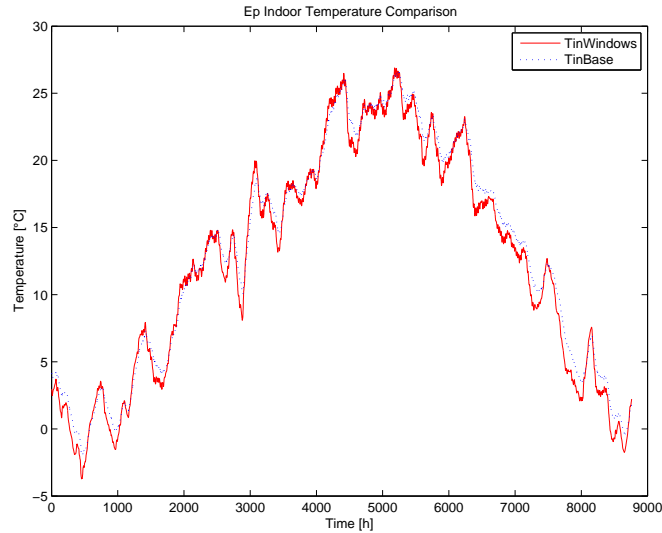


Figure 6.42: Ep Base-Window indoor temperature

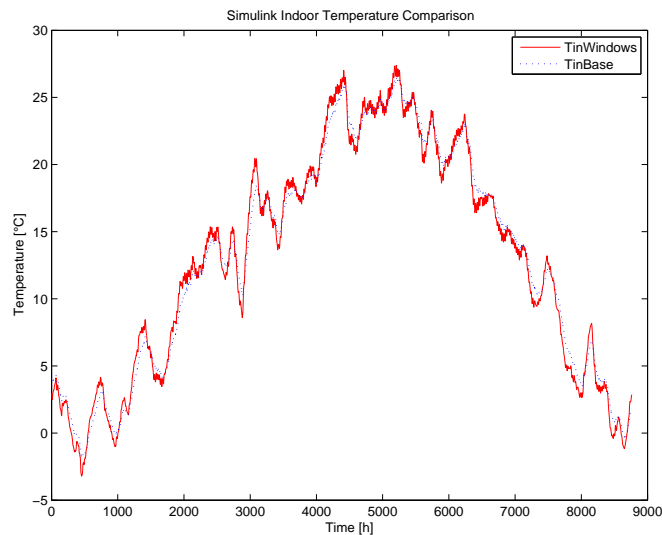


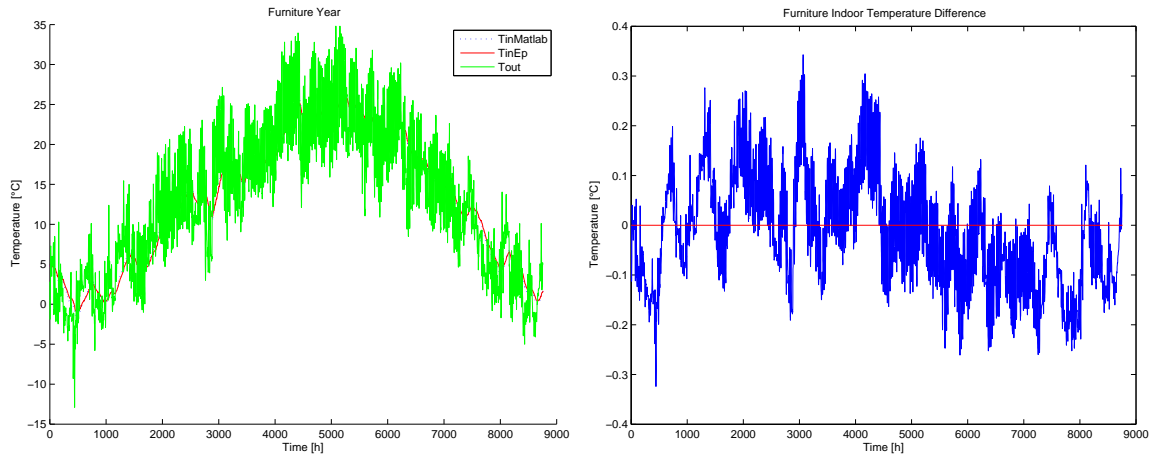
Figure 6.43: Simulink Base-Window indoor temperature

It can be observed that in Simulink case the introduction of the Low-mass envelope surfaces leads to a greater temperature variation. In the Ep plus case, instead, the Window model indoor temperature value stands at a lower value compared to the Base model one. Meanwhile for the Simulink model the explanation could be the thermal losses increase due to the direct connection between the inside and the outside environment; the Ep evolution is not yet explained.

6.5 Furniture

In the Furniture model the effect of furniture is checked by adding to the Base case the furniture contribution.

As Fig. 6.44-6.45-6.46-6.47 show, the furniture addition does not change the Base case trend significantly and the indoor temperature paths accordance between the models in the Matlab-Simulink and Ep is maintained.

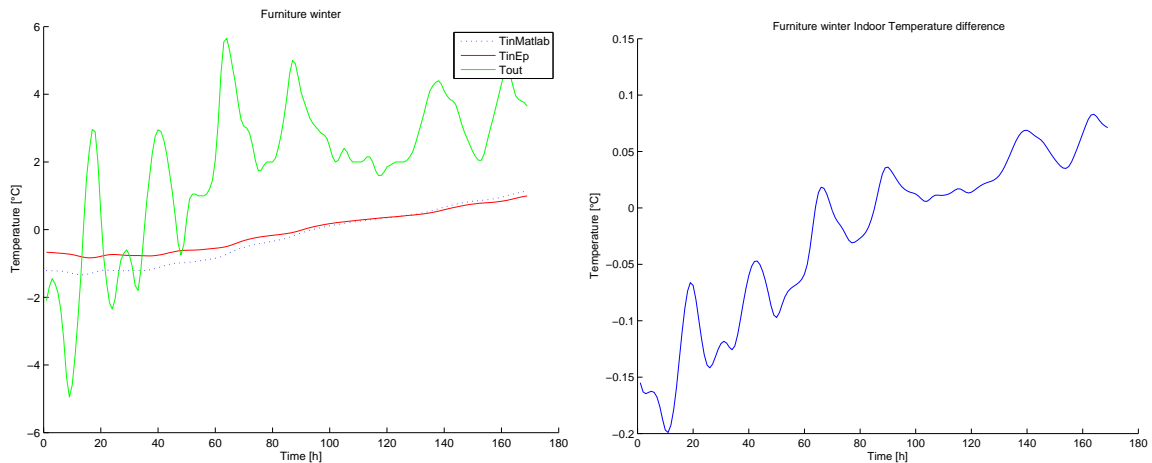


(a) Matlab vs Ep yearly indoor temperature path

(c) Temperature difference

(b) Matlab vs Ep temperature path

Figure 6.44: Furniture indoor temperature



(a) Matlab vs Ep temperature path

(b) Temperature difference

Figure 6.45: Furniture winter indoor temperature

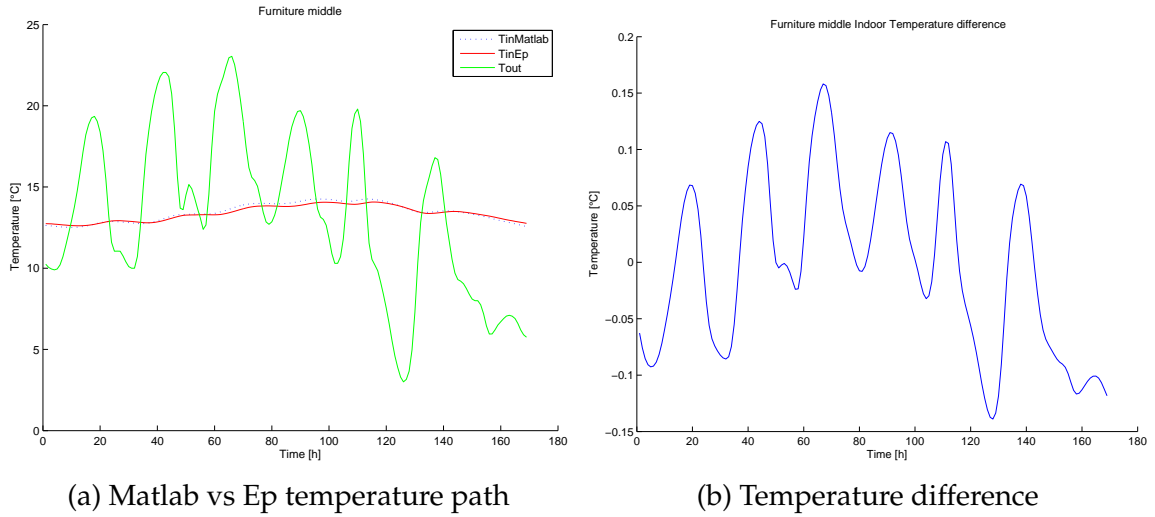


Figure 6.46: Furniture spring indoor temperature

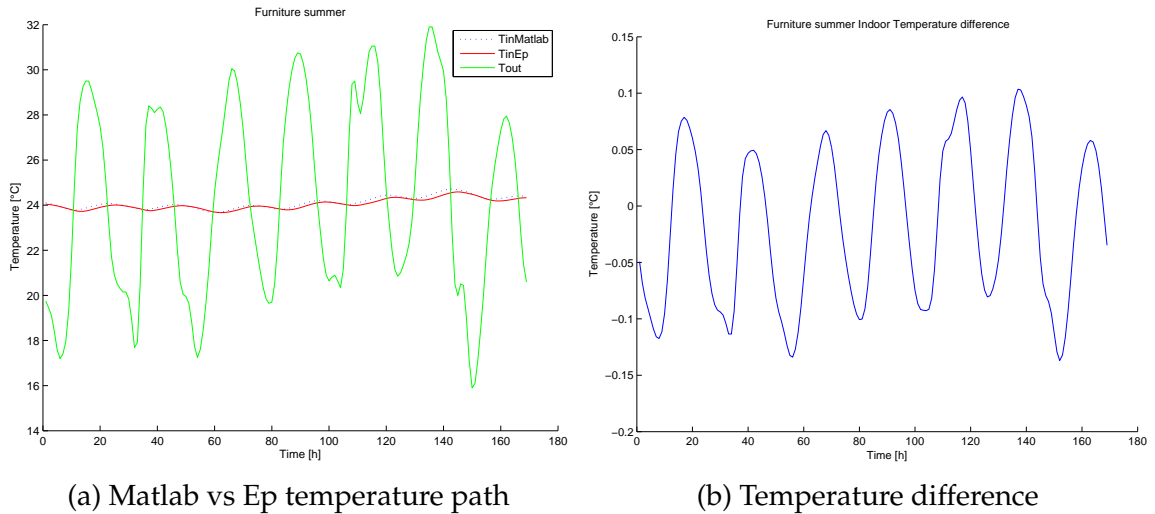


Figure 6.47: Furniture summer indoor temperature

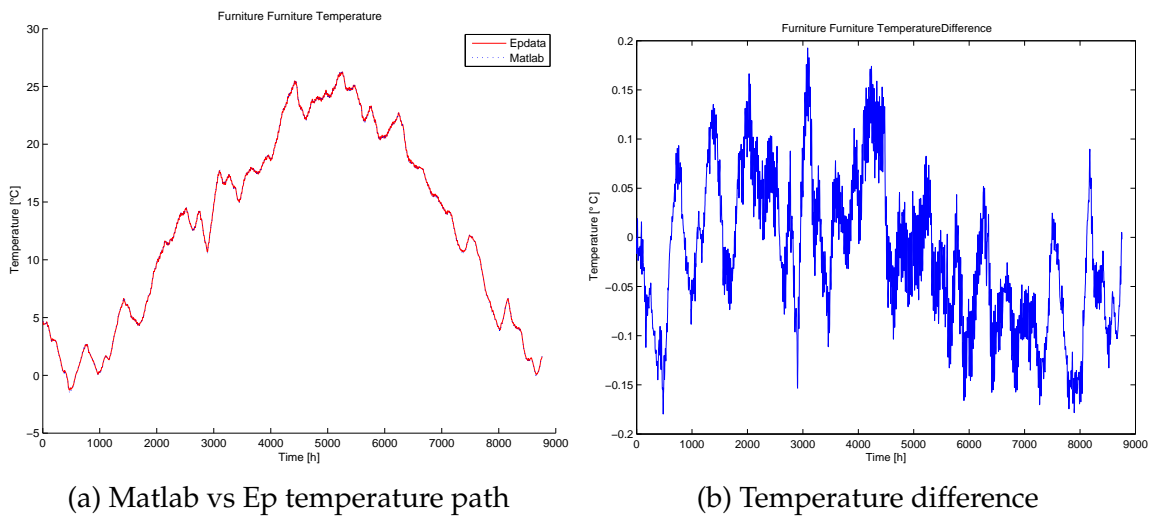
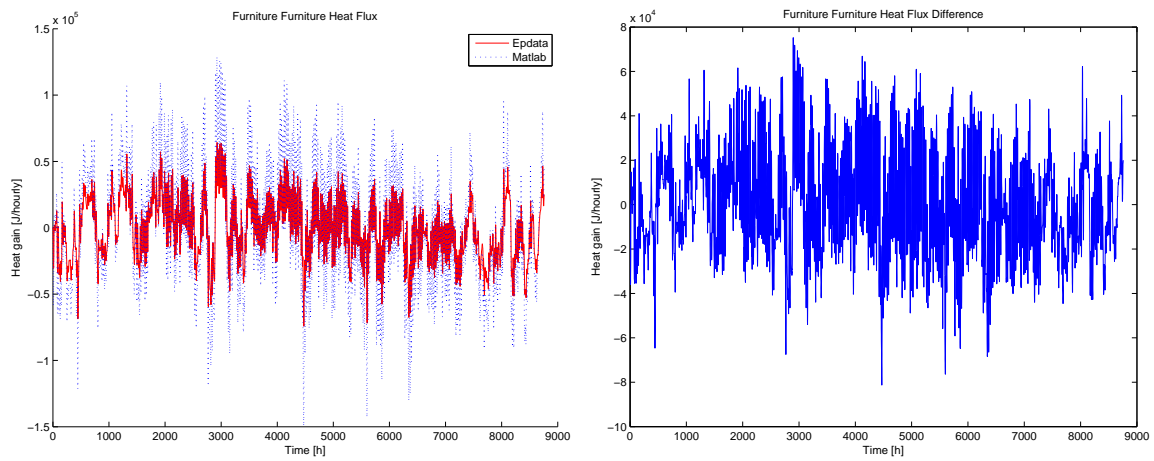


Figure 6.48: Furniture temperature



(a) Matlab vs Ep heat flux path

(b) Temperature difference

Figure 6.49: Furniture heat flux

6.6 Sun

The Sun models consider the addition of the sun effect on the opaque surfaces, i.e. the external wall, of the Base case.

Fig. 6.50 show a significant difference between the Matlab-Simulink model and the Ep one, which can be appreciated also in the seasonal reference week, Fig. 6.51-6.52-6.53. The indoor temperature of the Matlab-Simulink model is always lower than the Ep one during the year. Particularly, the difference trend shows the lowest value, i.e. highest difference, during the summer period when the solar radiation is higher. This suggests that the sun effect due to opaque surface is underestimated. However, the most important solar contribution is through the glazing surfaces and not through the opaque surfaces. Indeed, the All-in indoor temperature error trend and magnitude are different from the Sun case. Particularly, during the minor radiation period the indoor temperature is lower than the Ep one. The opposite during the higher radiation period. Overall the model gives good results.

In Fig. 6.54 the external wall temperature is reported. As explained in the All-in section, the wall capacity is more accessible from the indoor side; thus the wall temperature path and difference, trend and magnitude, are similar to the indoor temperature.

Fig. 6.55 and Fig. 6.56 show the external wall outdoor side heat flux and indoor side heat flux respectively. While the indoor side heat flux path and difference are similar to the Base case, or both the Matlab-Simulink and Ep models. The same cannot be stated for the outdoor side one. The different outdoor side heat flux is the Ep case is due to the higher temperature of the outer surface of the wall which leads to an higher convection heat flux.

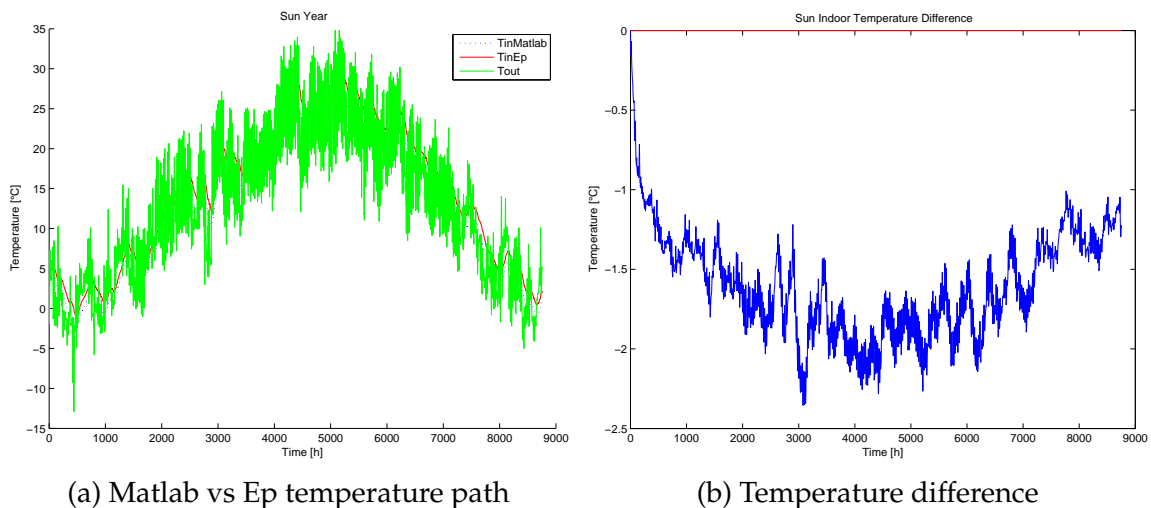


Figure 6.50: Sun indoor temperature

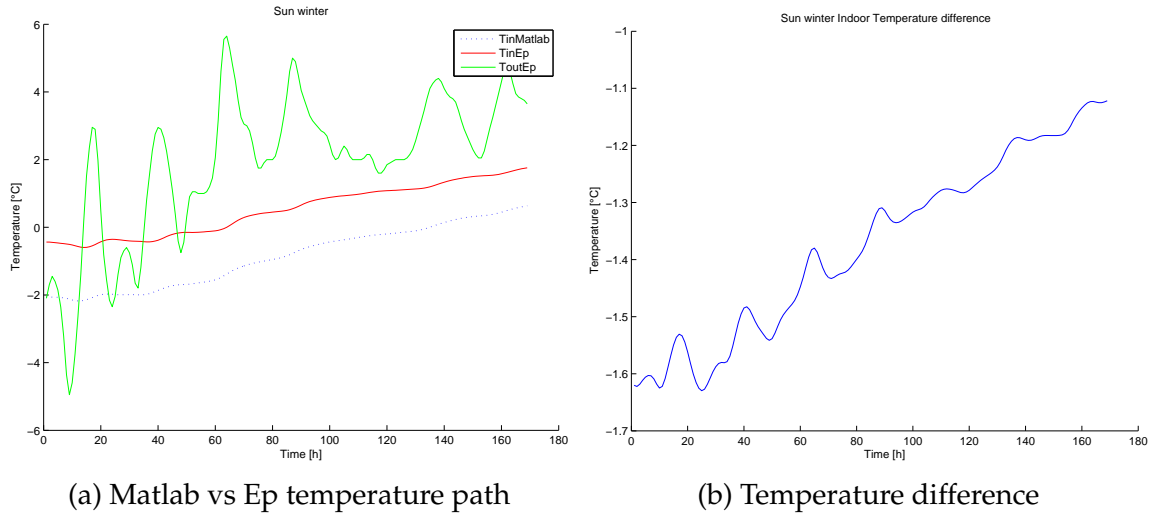


Figure 6.51: Sun winter indoor temperature

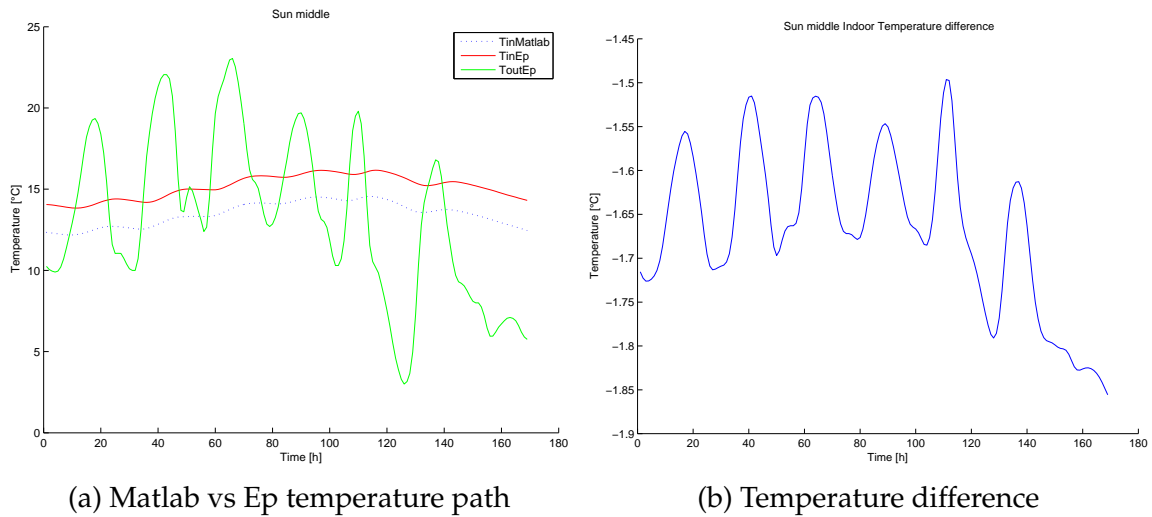


Figure 6.52: Sun spring indoor temperature

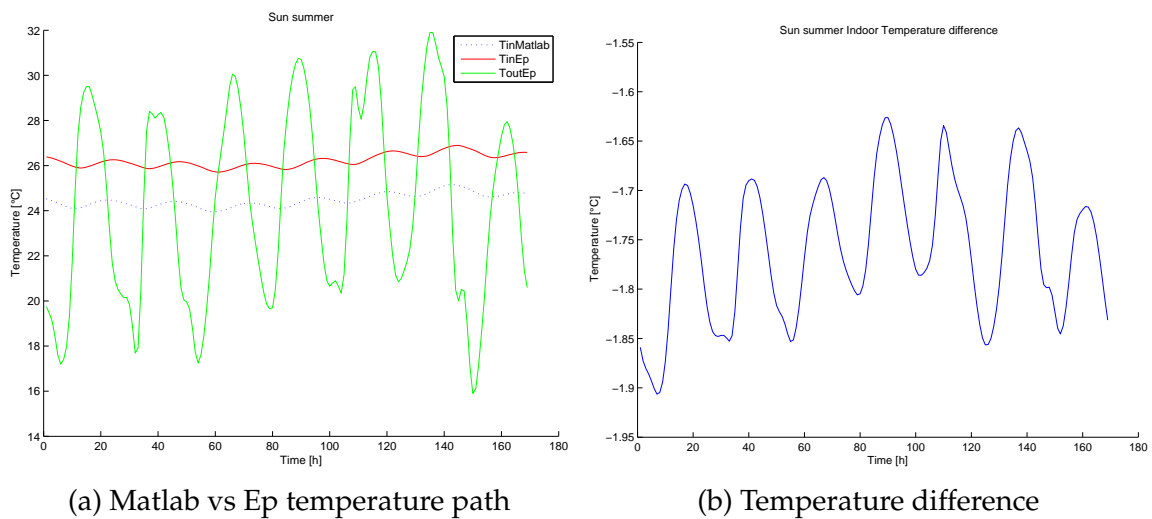
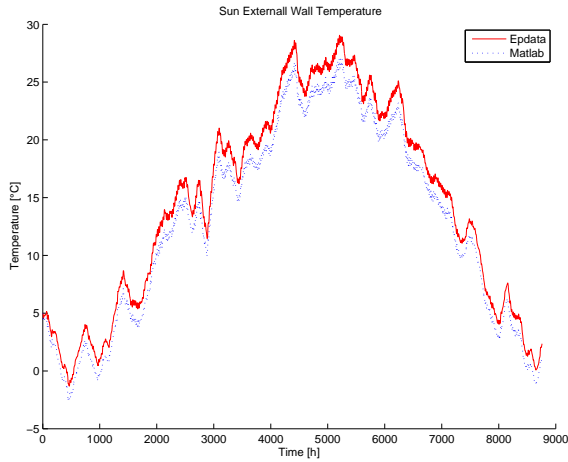
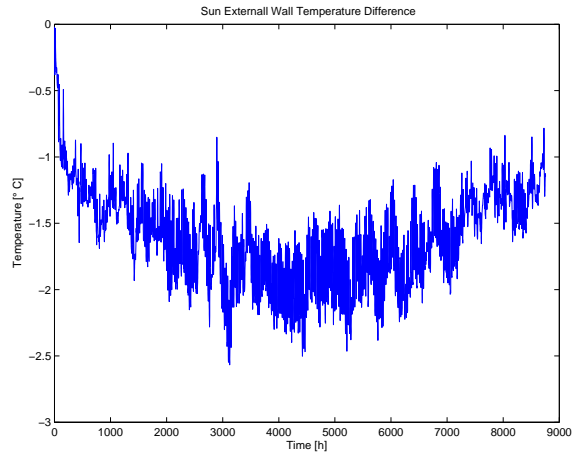


Figure 6.53: Sun summer indoor temperature

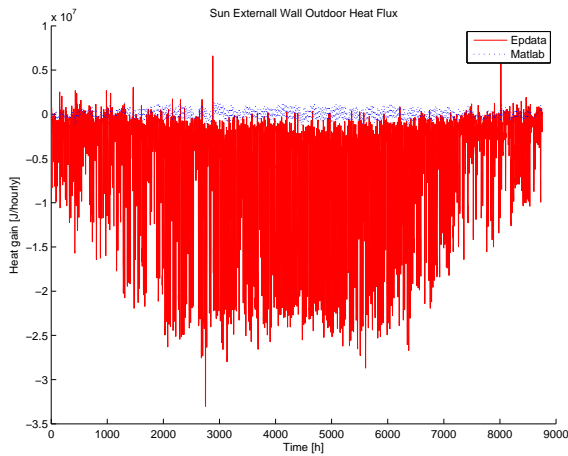


(a) Matlab vs Ep temperature path

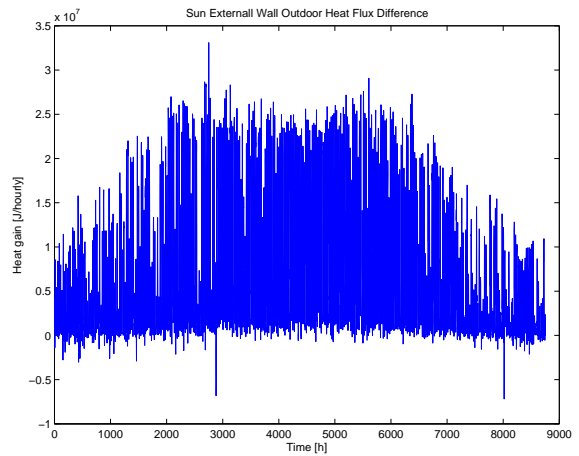


(b) Temperature difference

Figure 6.54: Sun external-wall temperature

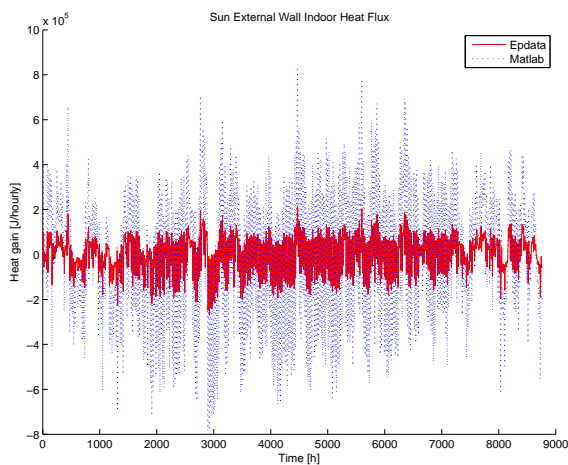


(a) Matlab vs Ep heat flux path

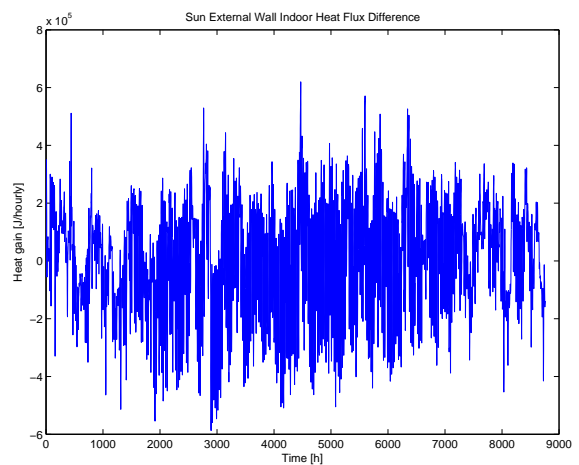


(b) Heat flux difference

Figure 6.55: Sun external-wall outdoor side heat flux



(a) Matlab vs Ep heat flux path



(b) Heat flux difference

Figure 6.56: Sun external-wall indoor side heat flux

Chapter 7

Conclusion

The thermal model of the building which considers the fabric elements, internal masses due to furniture and internal wall, solar gain through opaque and glazing surfaces and heat transmission through the low-mass envelope surfaces has been implemented in the Simulink environment.

In order to validate the model, the comparison has been carried out with the Ep software, which is used as reference tool for benchmarking the performance of the thermal model of the building.

Even though the indoor temperature pattern of the Simulink model quite match the Ep one, an investigation has been done in order to identify which modelled aspects affects the model accuracy. Two possible reasons of the difference between the two models are the following. The first one is the heat transmission through the windows, which leads the Ep model to a standing 0.5°C lower temperature compared to the Simulink one. The second one, is the solar gain through opaque surfaces which leads to a Simulink standing lower temperature compared to the Ep one. Another highlight is the difference of the surfaces heat fluxes between the two models. Even though intuitively it can be assigned to the different way to model the surfaces, a better understanding of the result is needed.

To further evaluate the impact of PCM material in order to increase the thermal inertia of lightweight building for DR purposes, many other aspects need to be modelled and validated, e.g. HVAC system and internal gains. How different climates affect the benefit of the introduction of PCM also deserves to be investigated. In the end, the optimization of the house energy management has to be carried out.

This means: a challenging trip to go!

Appendix

In this section the additional results related to the indoor surfaces temperature and heat flux of each model will be reported.

Infiltration

In this case, the Base model has been added of the infiltration and ventilation contribution.

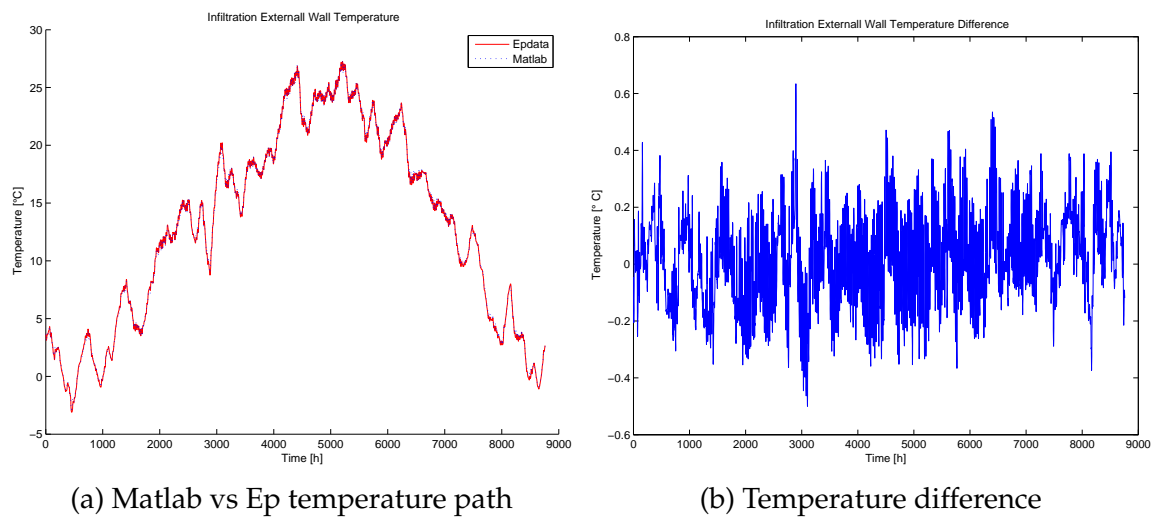
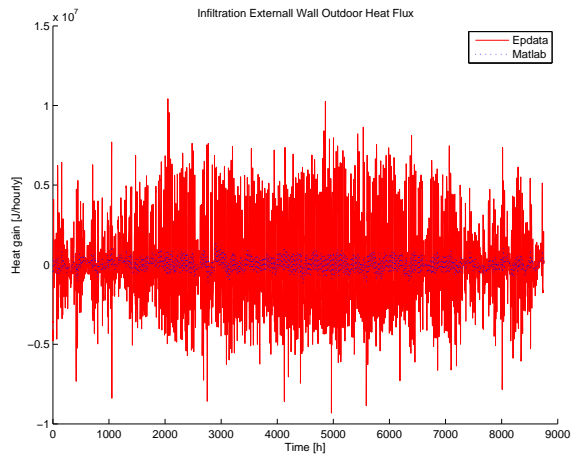
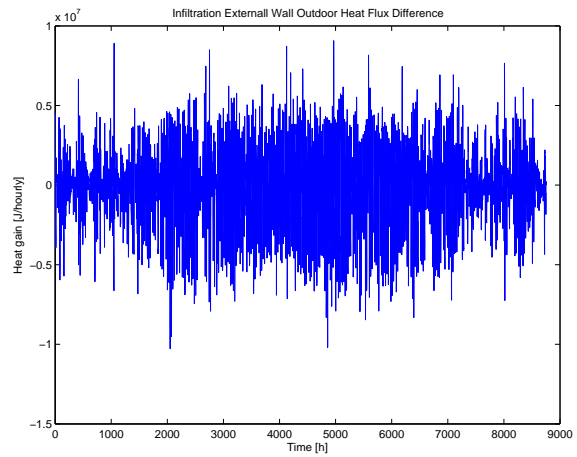


Figure 7.1: Infiltration external-wall temperature

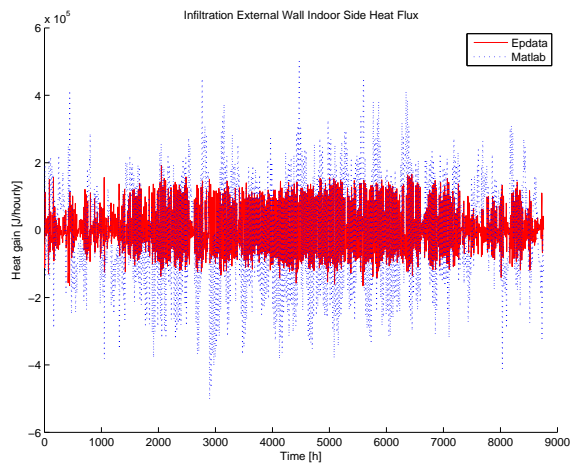


(a) Matlab vs Ep heat flux path

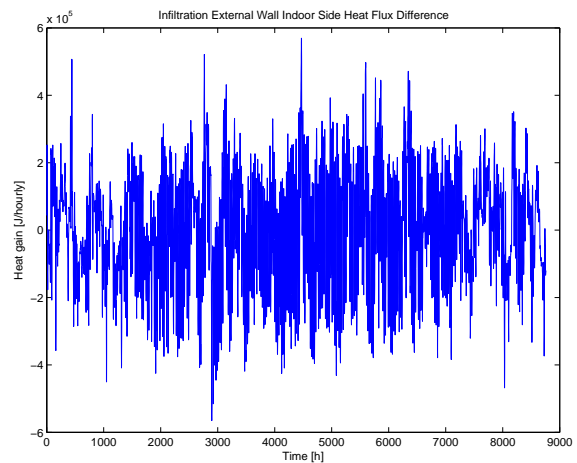


(b) Heat flux difference

Figure 7.2: Infiltration external-wall outdoor side heat flux

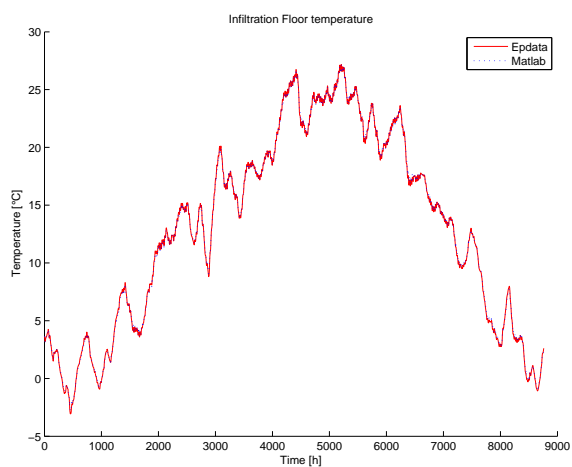


(a) Matlab vs Ep heat flux path

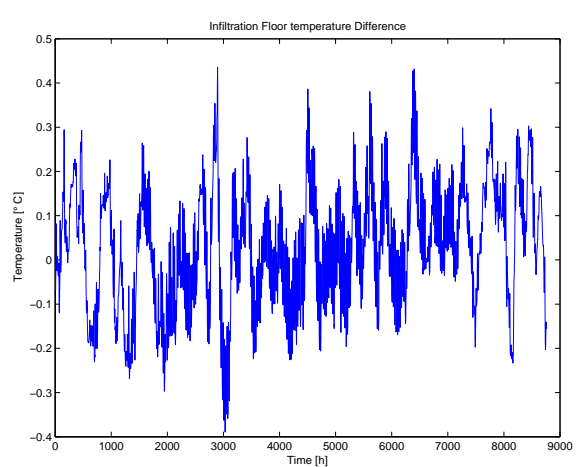


(b) Heat flux difference

Figure 7.3: Infiltration external-wall indoor side heat flux

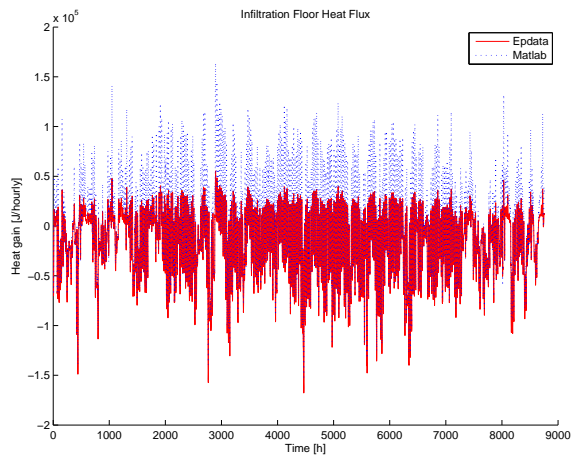


(a) Matlab vs Ep temperature path

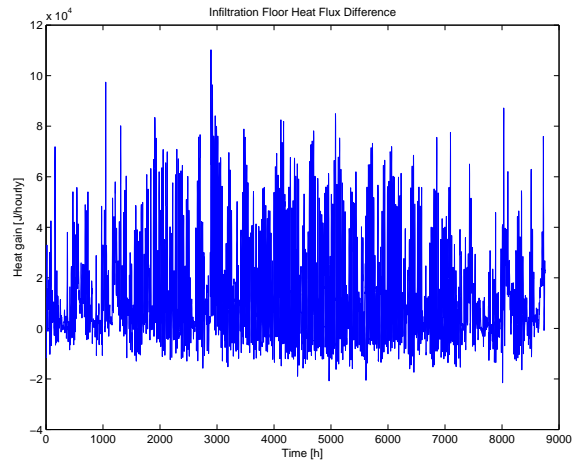


(b) Temperature difference

Figure 7.4: Infiltration floor temperature

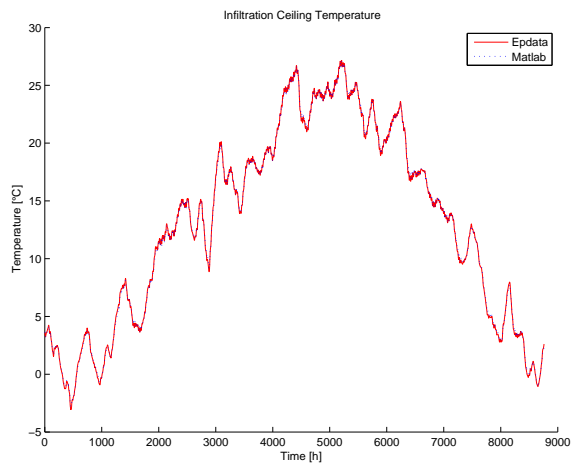


(a) Matlab vs Ep heat flux path

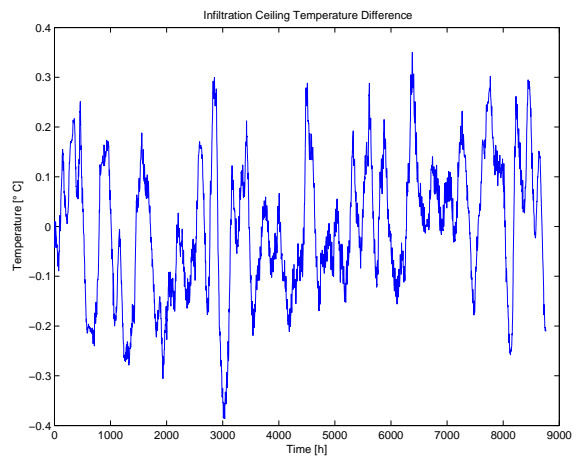


(b) Heat flux difference

Figure 7.5: Infiltration floor heat flux

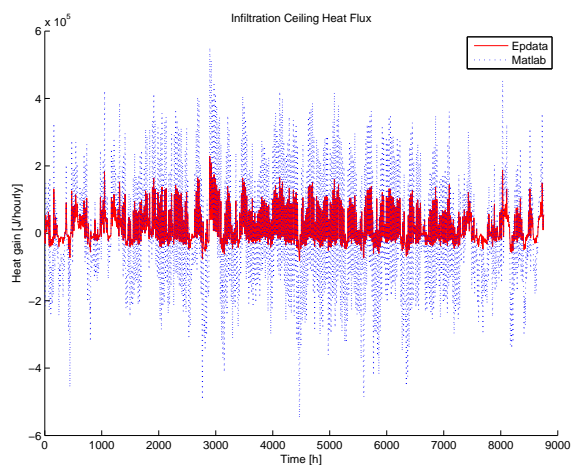


(a) Matlab vs Ep temperature path

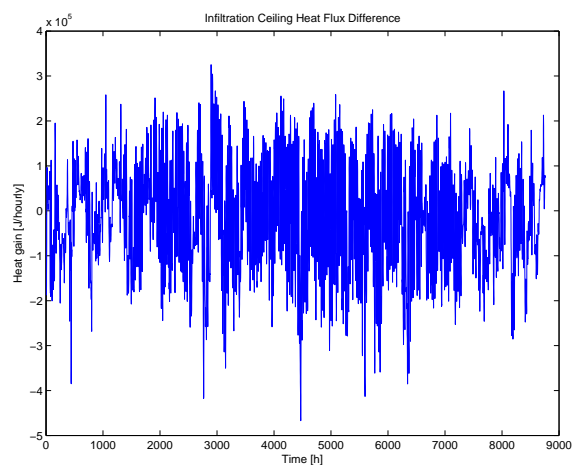


(b) Temperature difference

Figure 7.6: Infiltration ceiling temperature

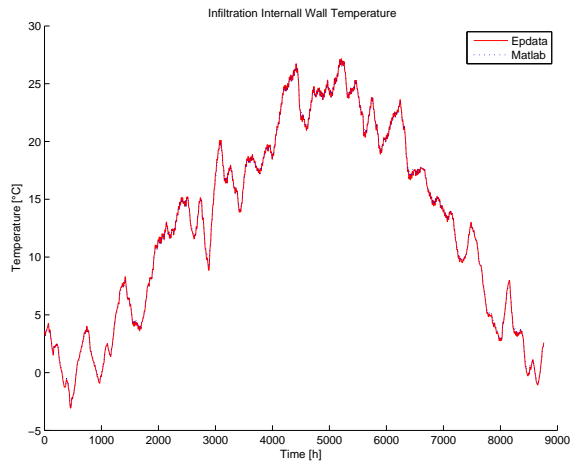


(a) Matlab vs Ep heat flux path

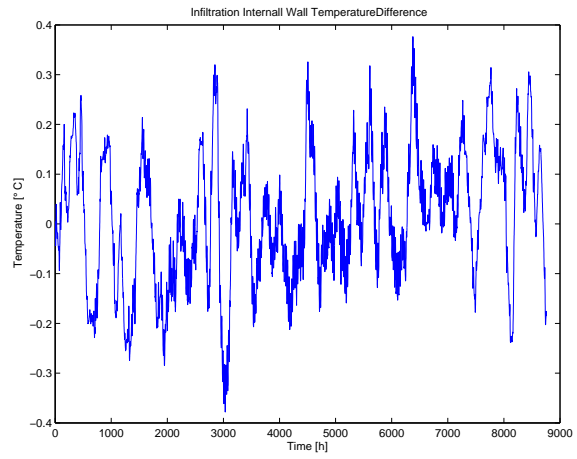


(b) Heat flux difference

Figure 7.7: Infiltration ceiling heat flux

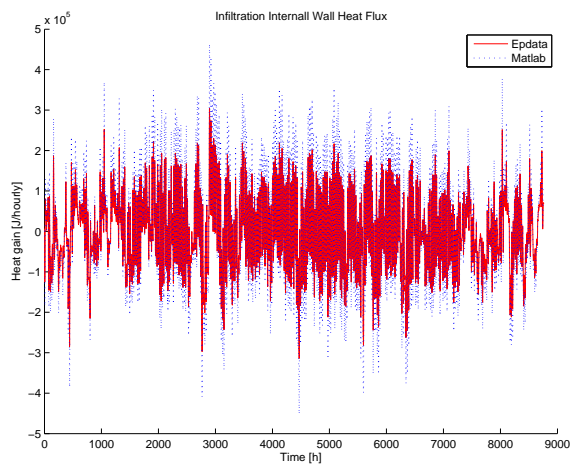


(a) Matlab vs Ep temperature path

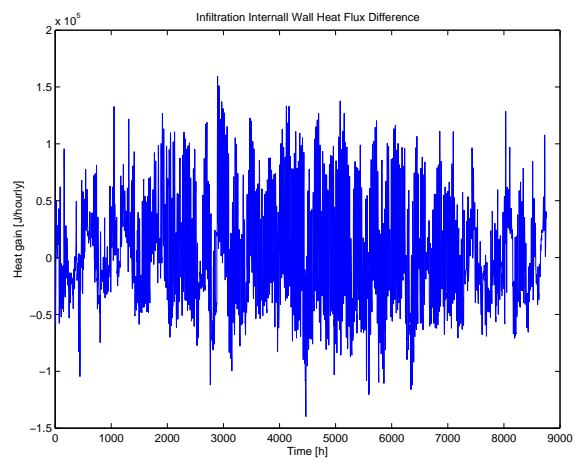


(b) Temperature difference

Figure 7.8: Infiltration internal wall temperature



(a) Matlab vs Ep heat flux path



(b) Heat flux difference

Figure 7.9: Infiltration internal wall heat flux

Windows

In this case, the Base model has been added with the windows and door contribution. In the Matlab-Simulink environment it consists of an additional resistive contribution between the indoor and outdoor environment. The envelope surface area is also diminished in order to consider the low mass surfaces.

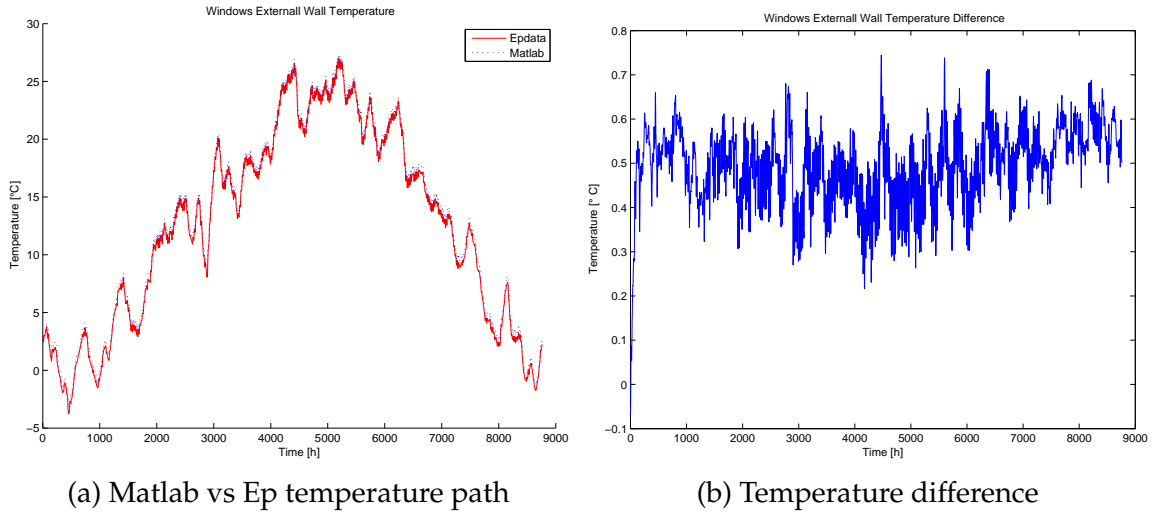


Figure 7.10: Windows external-wall temperature

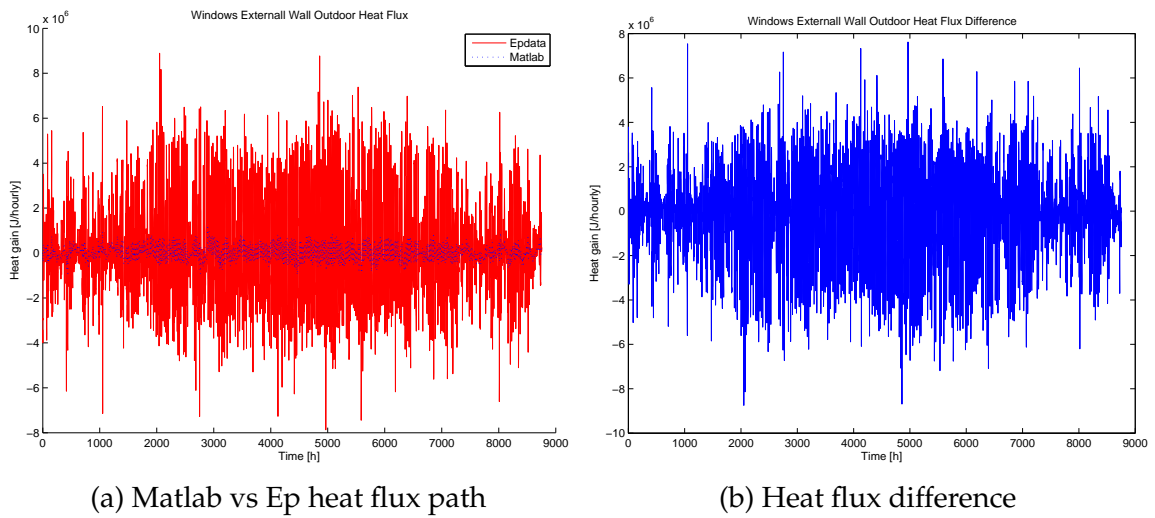
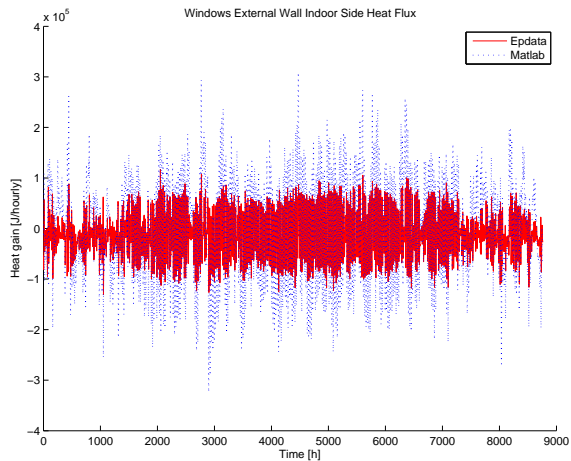
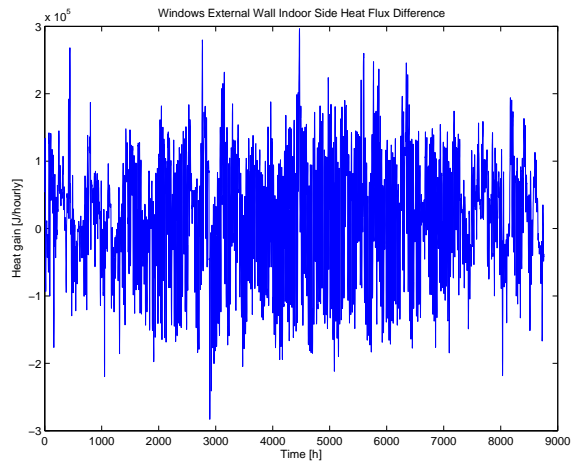


Figure 7.11: Windows external-wall outdoor side heat flux

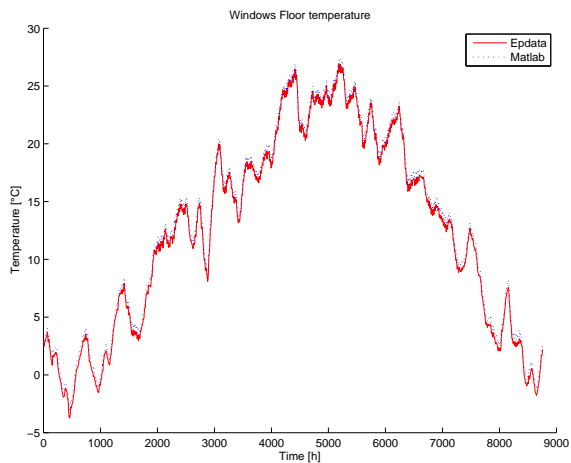


(a) Matlab vs Ep heat flux path

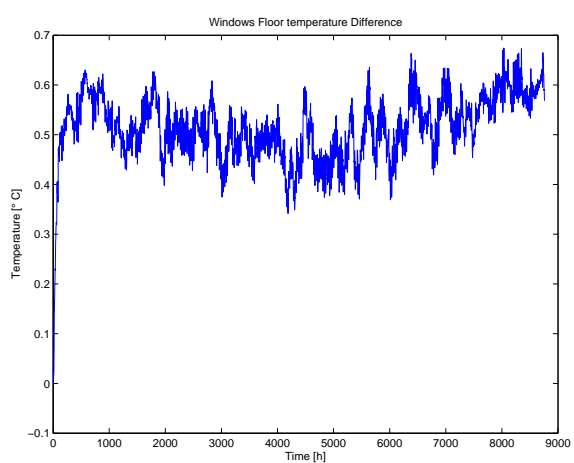


(b) Heat flux difference

Figure 7.12: Windows external-wall indoor side heat flux

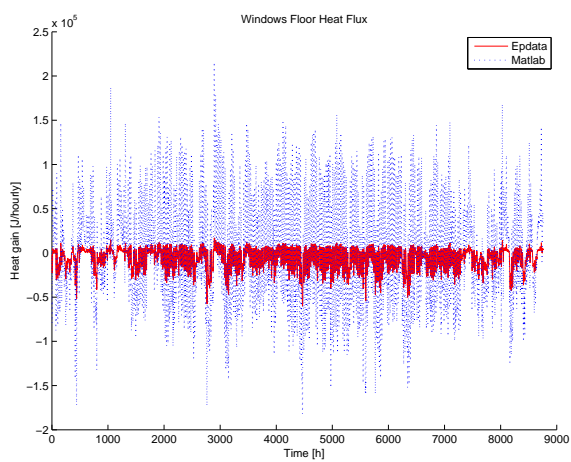


(a) Matlab vs Ep temperature path

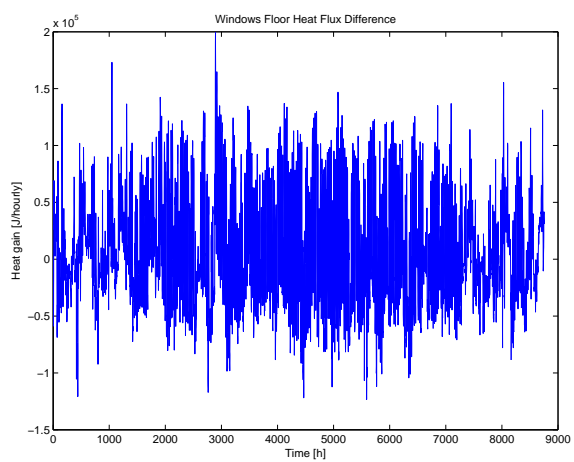


(b) Heat flux difference

Figure 7.13: Windows floor temperature

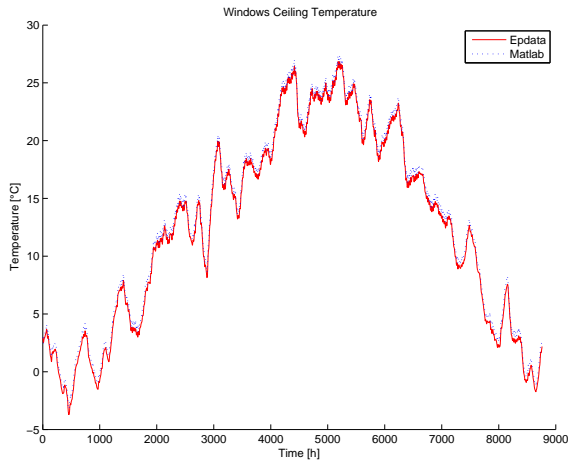


(a) Matlab vs Ep heat flux path

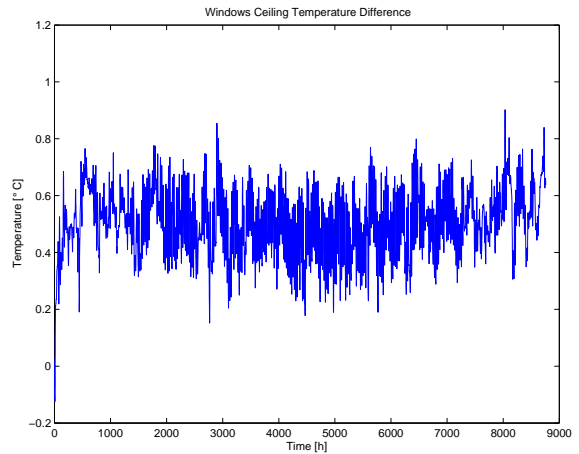


(b) Heat flux difference

Figure 7.14: Windows floor heat flux

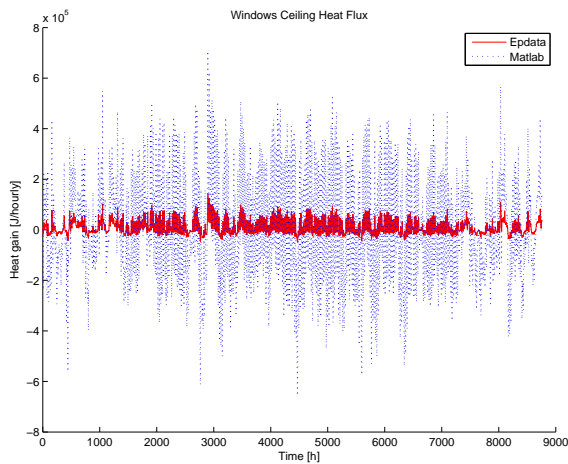


(a) Matlab vs Ep temperature path

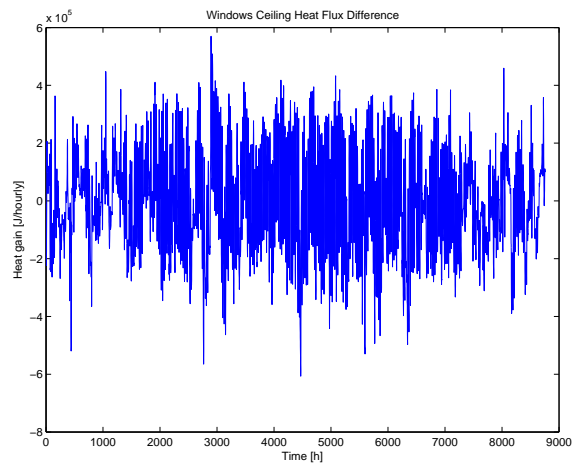


(b) Temperature difference

Figure 7.15: Windows ceiling temperature

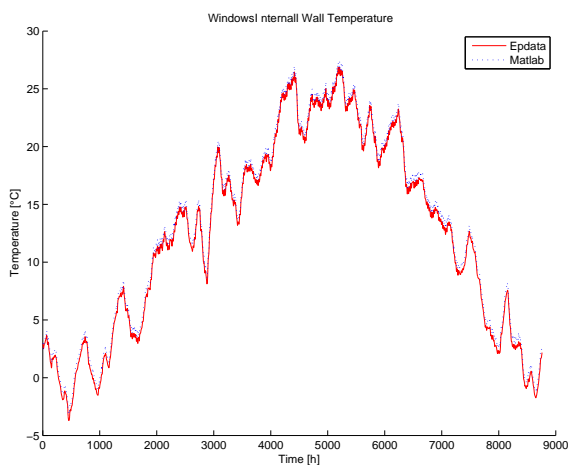


(a) Matlab vs Ep heat flux path

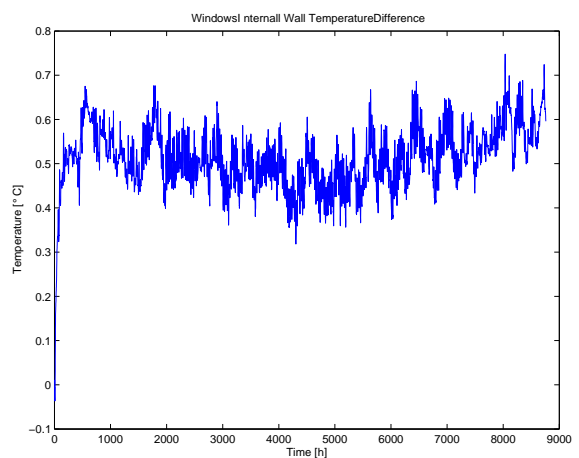


(b) Heat flux difference

Figure 7.16: Windows ceiling heat flux

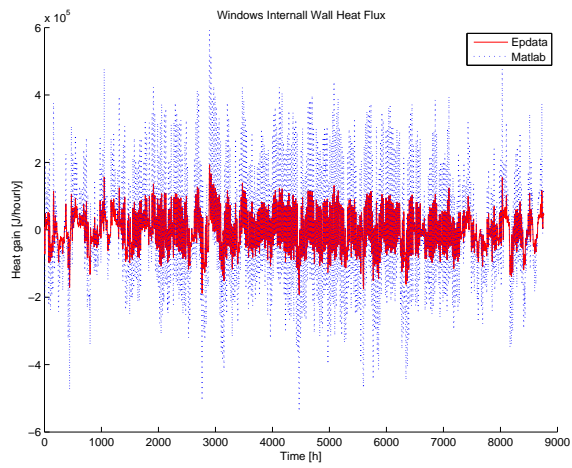


(a) Matlab vs Ep temperature path

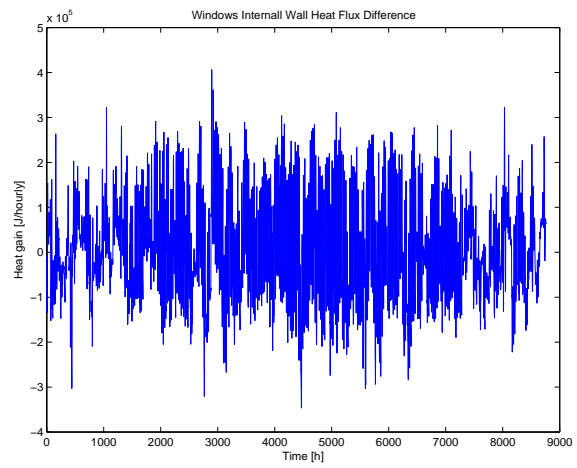


(b) Temperature difference

Figure 7.17: Windows internal wall temperature



(a) Matlab vs Ep heat flux path



(b) Heat flux difference

Figure 7.18: Windows internal wall heat flux

Furniture

The furniture contribution has been added to the Base case in this model, in order to check the furniture model.

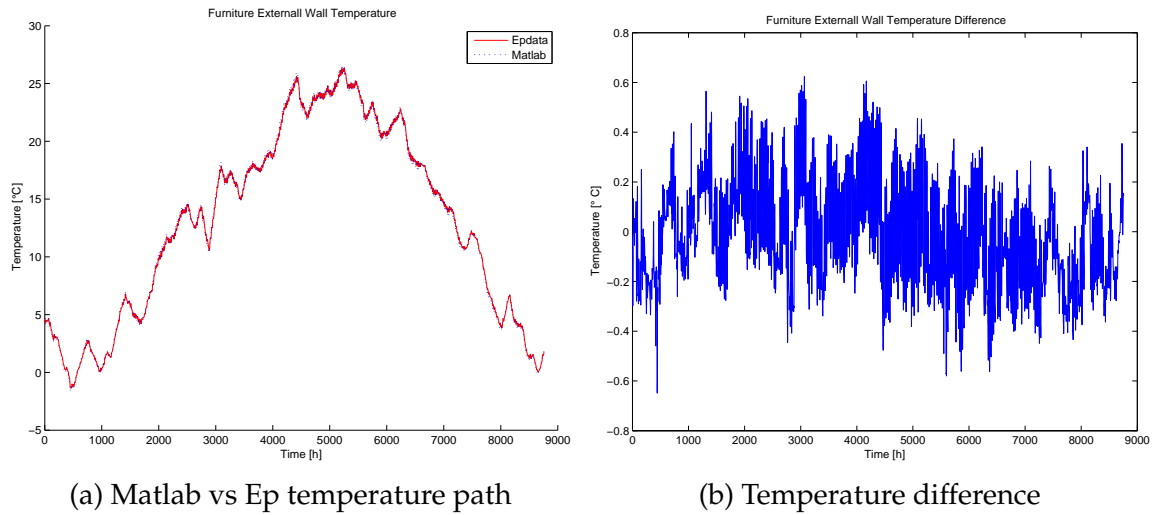


Figure 7.19: Furniture external-wall temperature

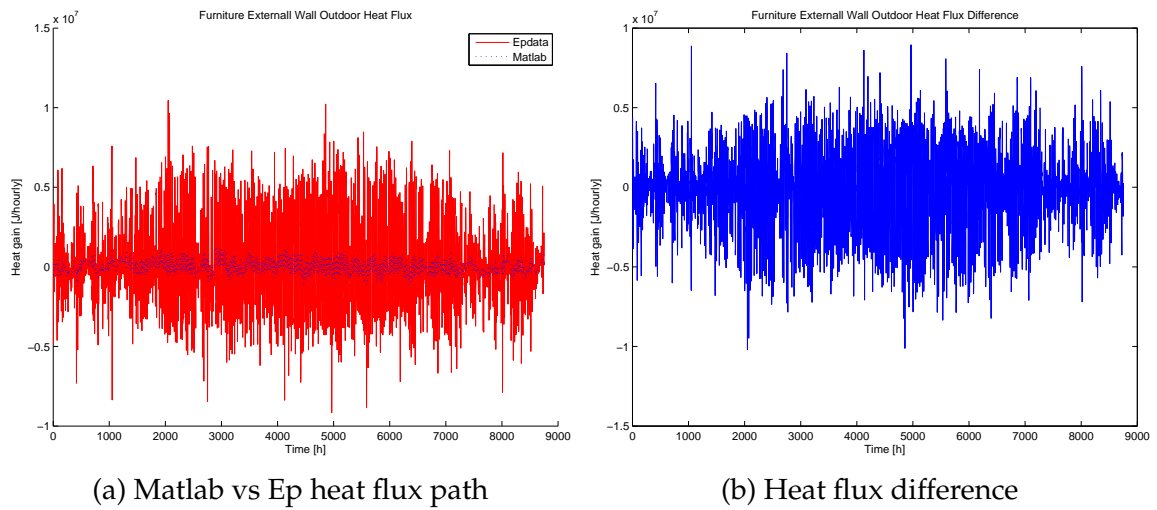
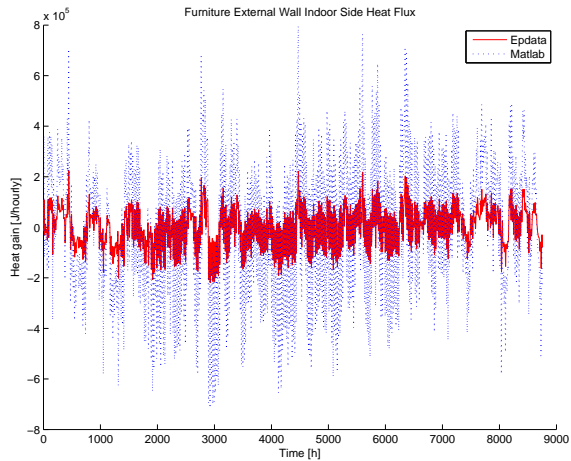
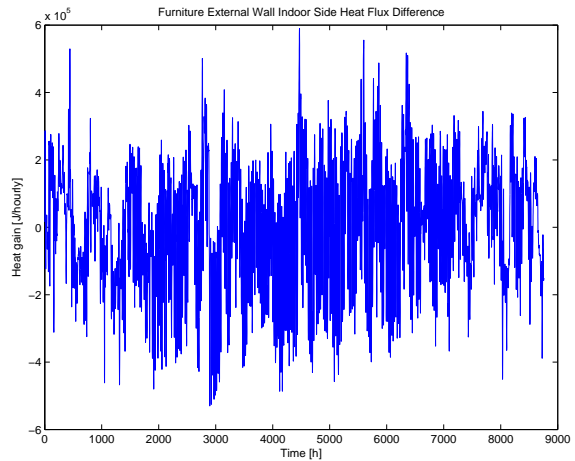


Figure 7.20: Furniture external-wall outdoor side heat flux

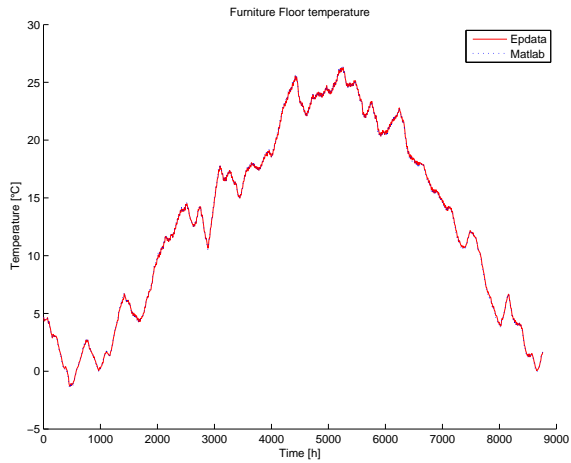


(a) Matlab vs Ep heat flux path

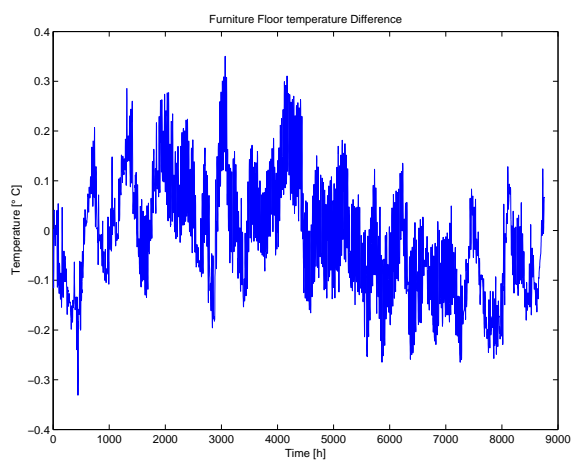


(b) Heat flux difference

Figure 7.21: Furniture external-wall indoor side heat flux

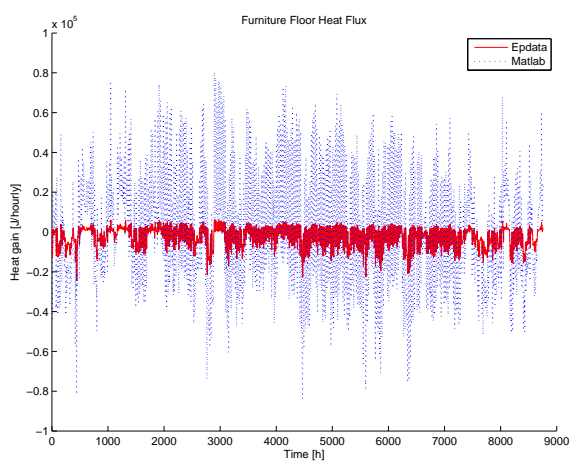


(a) Matlab vs Ep temperature path

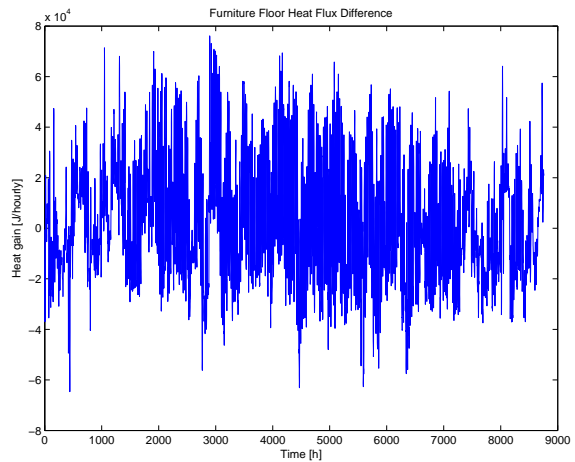


(b) Temperature difference

Figure 7.22: Furniture floor temperature

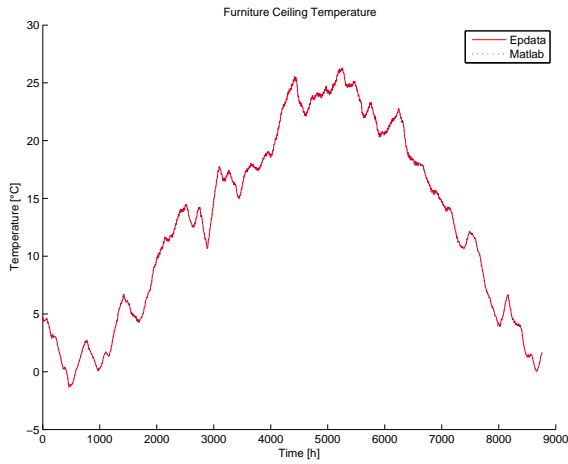


(a) Matlab vs Ep heat flux path

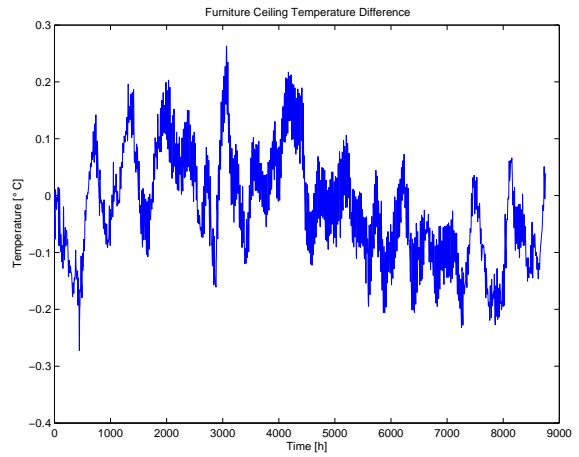


(b) Heat flux difference

Figure 7.23: Furniture floor heat flux

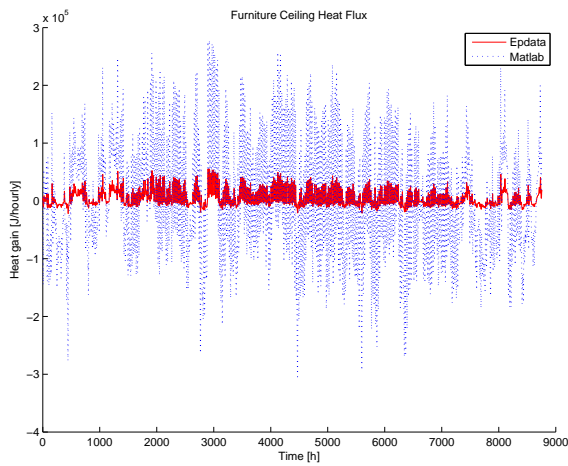


(a) Matlab vs Ep temperature path

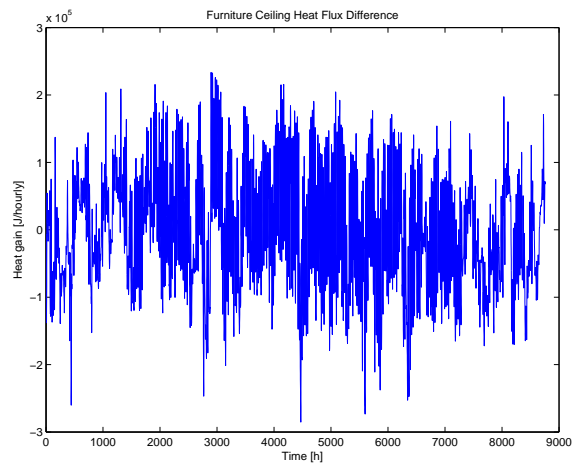


(b) Temperature difference

Figure 7.24: Furniture ceiling temperature

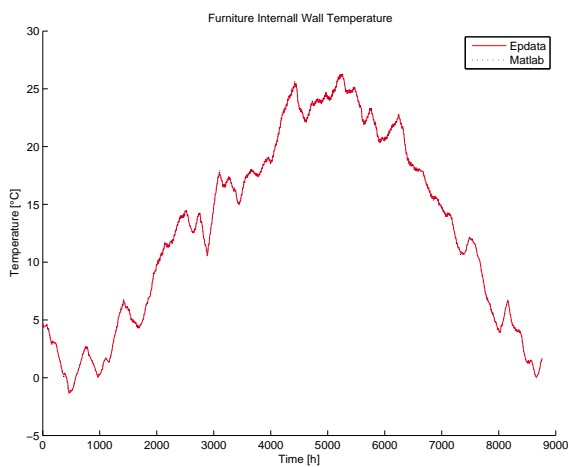


(a) Matlab vs Ep heat flux path

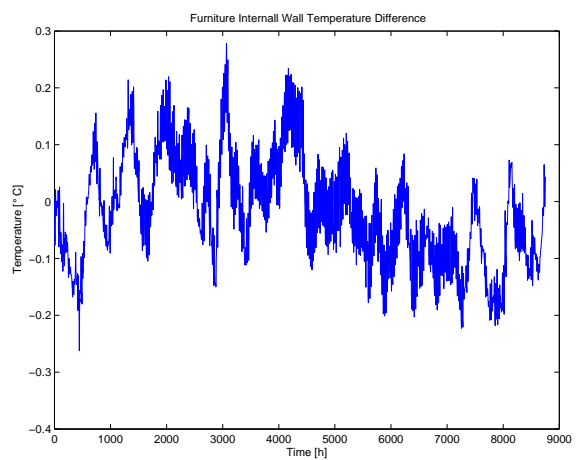


(b) Heat flux difference

Figure 7.25: Furniture ceiling heat flux

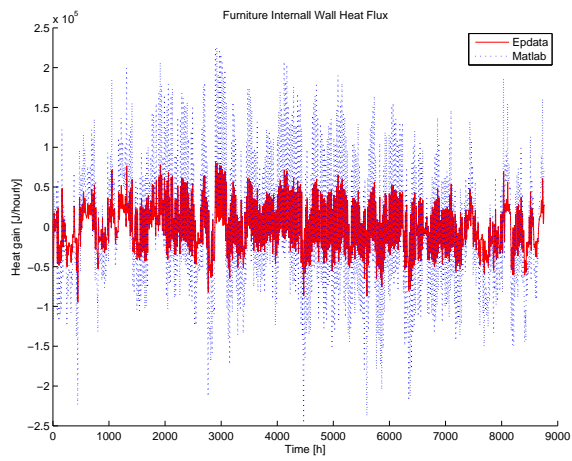


(a) Matlab vs Ep temperature path

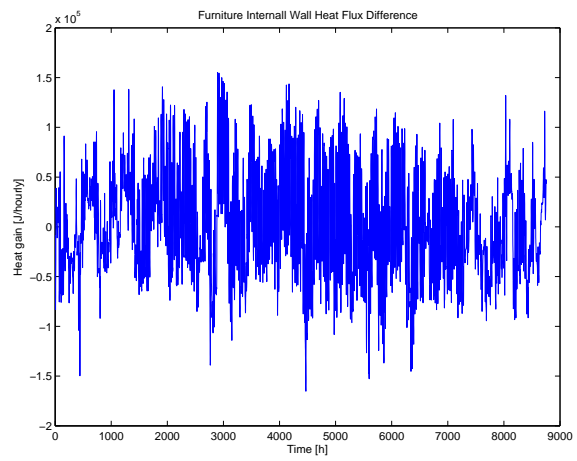


(b) Temperature difference

Figure 7.26: Furniture internal wall temperature



(a) Matlab vs Ep heat flux path



(b) Heat flux difference

Figure 7.27: Furniture internal wall heat flux

Sun

The sun effect has been added to the Base case effect in order to verify the model adopted for this contribution.

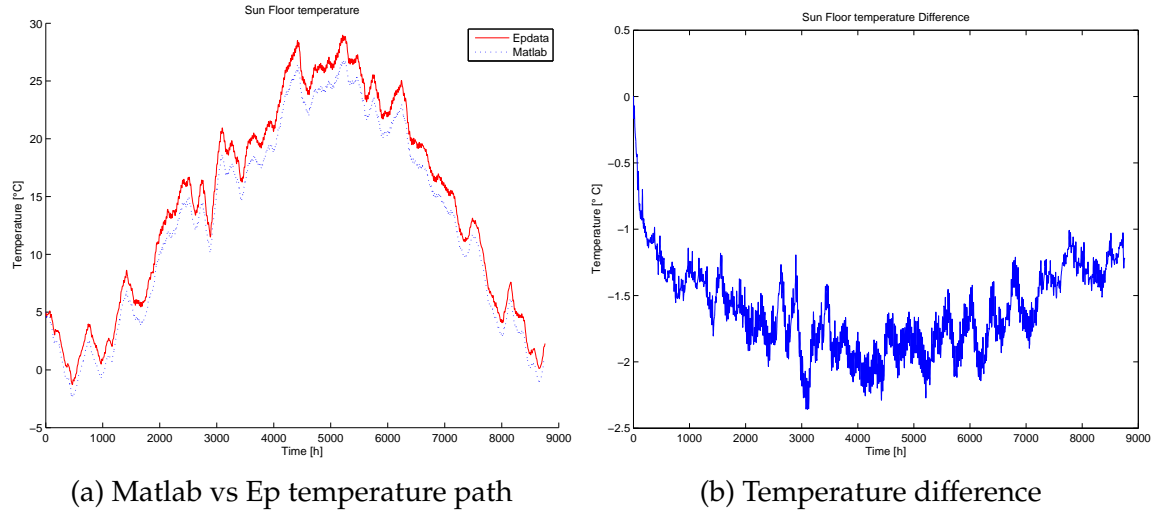


Figure 7.28: Floor temperature

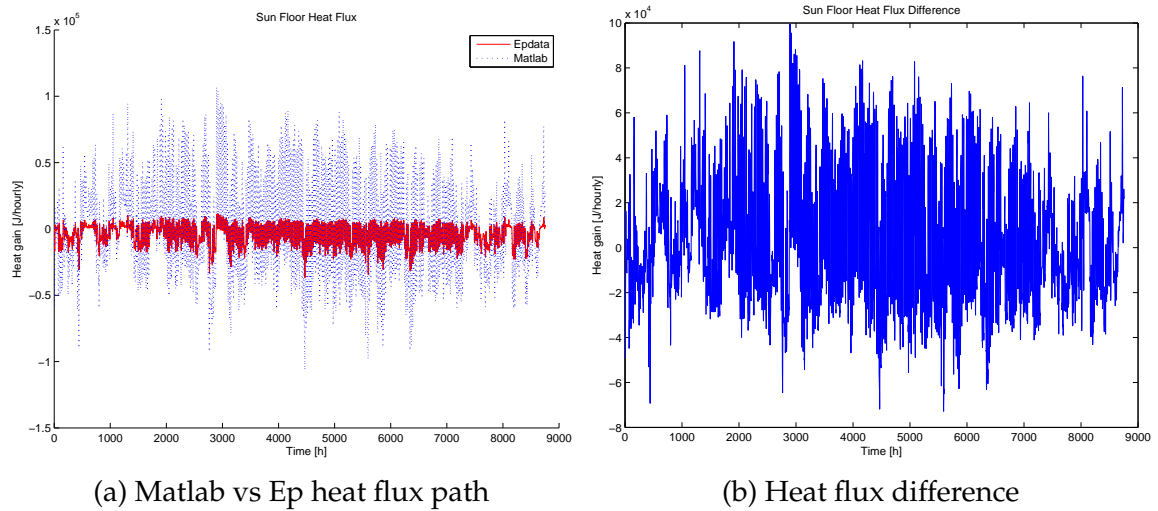
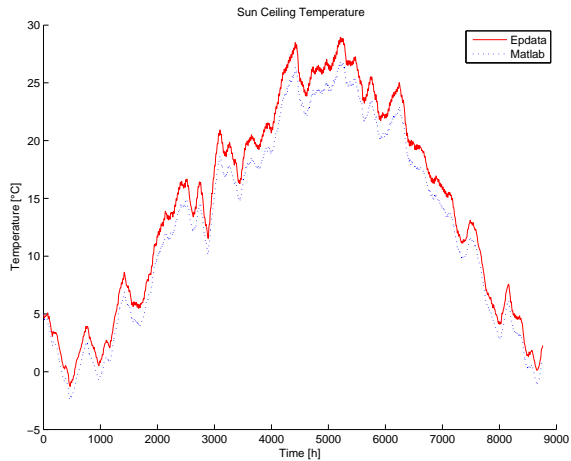
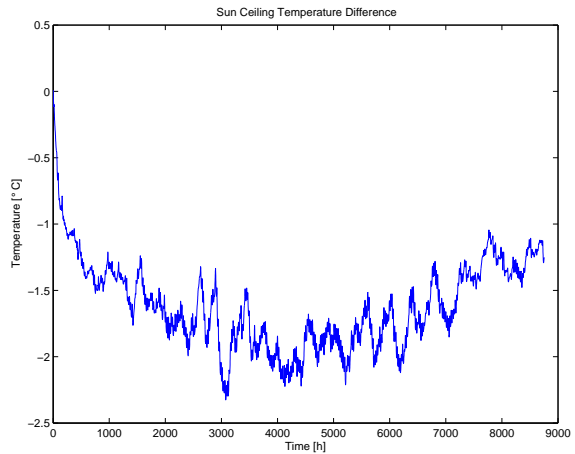


Figure 7.29: Sun floor heat flux

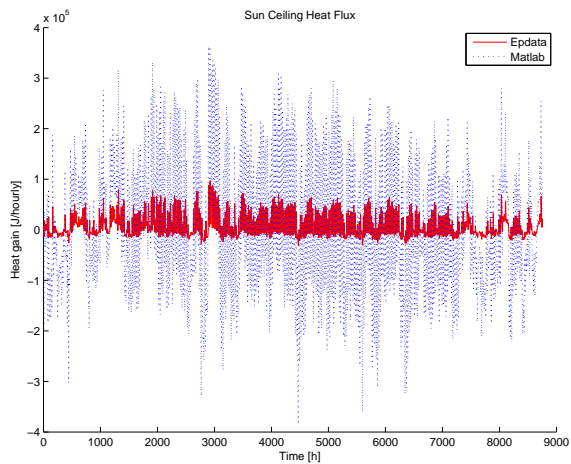


(a) Matlab vs Ep temperature path

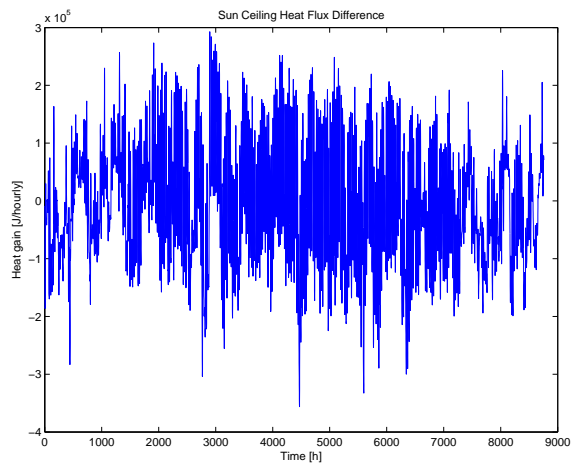


(b) Temperature difference

Figure 7.30: Ceiling temperature

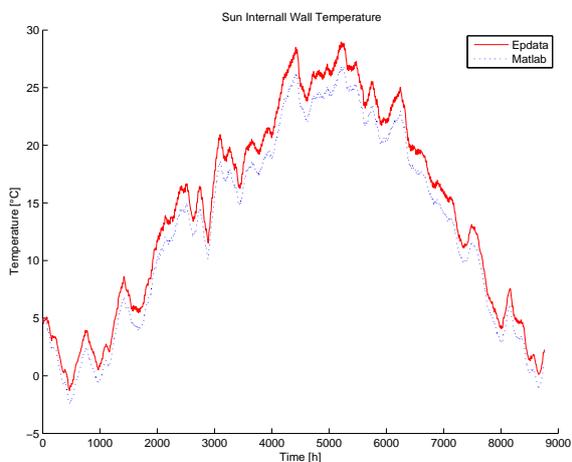


(a) Matlab vs Ep heat flux path

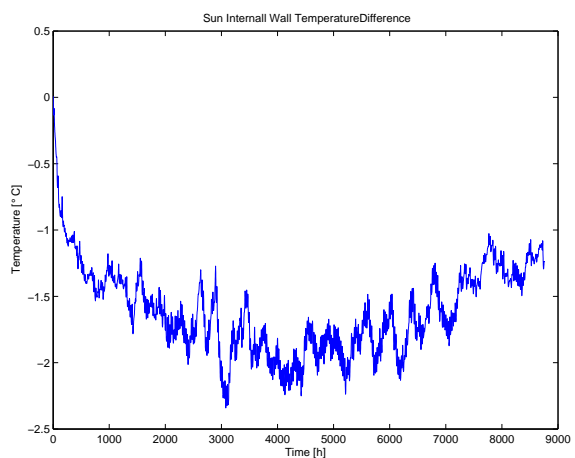


(b) Heat flux difference

Figure 7.31: Sun ceiling heat flux

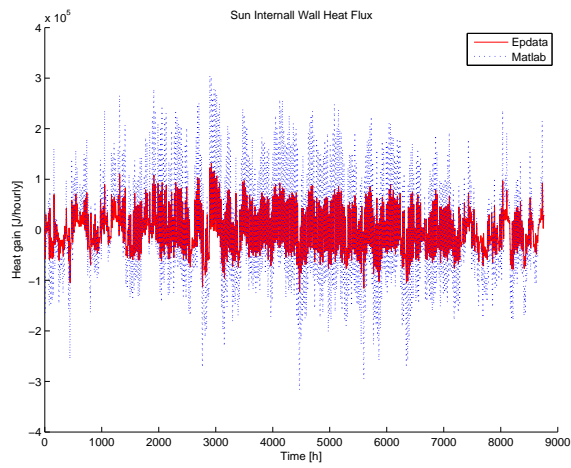


(a) Matlab vs Ep temperature path

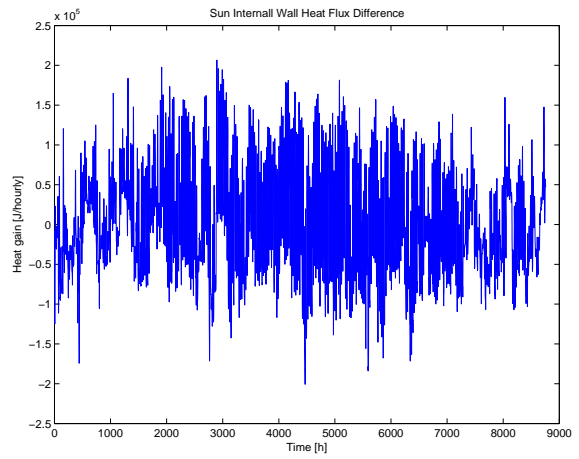


(b) Temperature difference

Figure 7.32: Sun internal wall temperature



(a) Matlab vs Ep heat flux path



(b) Heat flux difference

Figure 7.33: Sun internal wall heat flux

Bibliography

- [1] <http://www.makeitfrom.com/material-properties/Spruce-Pine-Fir-SPF-Softwood/>. Accessed: 2016-05-17.
- [2] http://www.engineeringtoolbox.com/air-specific-heat-capacity-d_705.html. Accessed: 2016-05-17.
- [3] Heat transfer. https://en.wikipedia.org/wiki/Heat_transfer.
- [4] Determinazione del fabbisogno di energia termica dell'edificio per la climatizzazione estiva ed invernale. Standard UNI/TS 11300:1, Ente Nazionale di Unificazione, May 2008. Revised 2010-07-22.
- [5] D. E. M. Bondy and J. Parvizi. Modeling, identification and control for heat dynamics of buildings using robust economic model predictive control, 2012.
- [6] Y.A. Çengel. *Heat transfer A practical Approach*. McGraw-Hill, 2002.
- [7] I. R. Doebber. Investigation of concrete wall systems for reducing heating and cooling requirements in single family residences. Master's thesis, Virginia Polytechnic Institute and State University, 2004.
- [8] F. Kreith, R. M. Manglik, and M.S. Bohn. *Principle of heat transfer*. Cengage Learning, 2011.
- [9] G. M. Masters. *Renewable and efficient electric power systems*. Wiley Interscience, 2004.
- [10] G. Masy. *Definition and Validation of a Simplified Multizone Dynamic Building Model Connected to Heating System and HVAC Unit*. Phd thesis, Université de Liège Faculté des Sciences Appliquées, 2008.
- [11] G. Morini. Energy and technical plant handout.
- [12] P. Palensky and D. Dietrich. Demand side management: Demand response, intelligent energy systems and smart loads. *IEEE Transaction on Industrial Informatics*, 7(3):381–388, 2011.
- [13] P. Raftery, E. Lee, T. Webster, T. Hoyt, and F. Bauman. Effects of furniture and contents on peak cooling load. *Energy and Buildings*, 85:445–457, 2014.
- [14] A. Tavlov. Dynamic optimization of power consumption. Master's thesis, DTU, 2008.

- [15] C.P. Underwood and F.W.H. Yik. *Modelling Methods for Energy in Buildings*. Blackwell Science, 2004.
- [16] H. Wolisz, T. M. Kull, R. Streblow, and D. Muller. The effect of furniture and floor covering upon dynamical thermal building simulatons. *Energy Procedia*, 77:2154–2159, 2015.
- [17] C. Yan, S. Wang, K. Shan, and Y. Lu. A simplified analytical model to evaluate the impact of the radiant heat on building cooling load. *Applied Thermal Engineering*, 77:30–41, 2015.
- [18] F. Fiorito Z. Zhao, G. Verbic. Model analysis of a residential builising for demand. *IEEE Eindhoven power tech*, 2015.